Molecular and cellular studies of the West Nile virus NS2B/NS3 protease

by

STEPHANIE ANNE CONDOTTA
B.Sc., Brock University, 2002
M.Sc., Brock University, 2005

A THESIS SUBMITTED IN PARTIAL FULFILLMENT OF
THE REQUIREMENT FOR THE DEGREE OF

DOCTOR OF PHILOSOPHY

in

THE FACULTY OF GRADUATE STUDIES
(Microbiology and Immunology)

THE UNIVERSITY OF BRITISH COLUMBIA
(Vancouver)

July 2010

Abstract

West Nile virus (WNV) is the most widely distributed arthropod-borne virus globally. It can cause a potentially fatal infection and has become a public health concern in North America since its introduction in 1999. Currently, there are no vaccines or treatments available for human WNV infections. As such, it is important to understand the virus life cycle, in order to develop effective therapeutics. The WNV protease heterocomplex, NS2B/NS3, is a prime target for antiviral therapy and has become the focus of much research. It is important to understand protease function first, in order to develop effective inhibitors. The overall goal of this thesis was to gain a better understanding into the function of the full-length NS2B/NS3 protease heterocomplex within the intracellular microenvironment. I hypothesized that there are critical residues essential for the interaction between NS2B and NS3 that affect protease activity and protein stability. The first aim of this project was to generate a cell-based fluorescent substrate assay to investigate the protease activity of the full-length NS2B/NS3 protease heterocomplex within the cell. My results demonstrate that the full-length NS2B/NS3 protease heterocomplex functions differently within the context of the cell, compared to what has been previously observed *in vitro* (Chapter 2). In the second aim, I investigated NS2B function on NS3 protease *cis*-cleavage and *trans*-cleavage activity. My results reveal an important dual role the NS2B protein plays in the proper function of the full-length NS2B/NS3 protease heterocomplex (Chapter 3). In the third aim, I utilized the information gathered to rationally design and test a serine protease inhibitor directed against the full-length NS2B/NS3 protease heterocomplex (Chapter 4). Taken together, my results highlight the importance of utilizing cell-based assays to assess protease activity, as this allows for the investigation of

NS2B/NS3 protease function in a more physiologically relevant environment. The results presented in this thesis further our understanding of the activity of the full-length WNV NS2B/NS3 protease heterocomplex within the context of the cell. The information gathered gives insight into the regulation of viral protease function that could be utilized in the rational drug design towards the WNV NS2B/NS3 protease heterocomplex.

Table of contents

List of tables

List of figures

List of abbreviations

↓	Scissile bond
α_1-PDX	Alpha$_1$-antitrypsin Portland
α_1-PIT	Alpha$_1$-antitrypsin Pittsburg
Ac	Acetyl
ADRP	Adipocyte differentiation-related protein
BBB	Blood brain barrier
BSA	Bovine serum albumin
C	Capsid
C	Cytosol fraction
CNS	Central nervous system
DC-SIGNR	Dendritic cell-specific intercellular adhesion molecule3 grabbing nonintegrin
DMEM	Dulbecco's modified Eagle's medium
DNV	Dengue virus
DsRed	*Discosoma sp.* red fluorescent protein
E	Envelope
EIP	Extrinsic incubation period
ER	Endoplasmic reticulum
GFP	Green fluorescent protein
gp	Glycoprotein
HCV	Hepatitis C virus
HEK 293A	Human embryonic kidney cells
HEK 293T	Derivative cell-line of HEK 293A cells

hel	Helicase
hf	His-tag and FLAG-tag
HIV	Human immunodeficiency virus
HTS	High-throughput-screening
Huh7	Human hepatocellular carcinoma cells
Huh7.5.1	Derivative cell-line of Huh7 cells
IFN	Interferon
IgM	Immunoglobulin M
IL-6	Interleukin-6
JEV	Japanese encephalitis virus
k_{cat}	Catalytic rate constant
k_{cat}/K_m	Specificity constant
kDa	Kilodaltons
K_i	Inhibition constant
K_m	Michaelis-Menten constant
M	Membrane
M	Membrane fraction
mRFP	Monomeric red fluorescent protein
NLS	Nuclear localization signal
NS	Nonstructural
ORF	Open reading frame
PBS	Phosphate-buffered saline
PBS-PI	PBS containing protease inhibitor

PBS-S	PBS containing saponin
PC	Proprotein convertase
Pn	Non-primed residues
Pn′	Primed residues
pNA	Para-nitroanilide
prM	Premembrane
pro	Protease
RCL	Reactive centre loop
RdRp	RNA dependent RNA polymerase
serpin	Serine protease inhibitor
sp	Signal peptide
TGN	*Trans*-Golgi network
TLR3	Toll-like receptor 3
Tm	Membrane-anchoring domain
TNF-α	Tumor necrosis factor alpha
WN	West Nile
WNF	West Nile fever
WNND	West Nile neuroinvasive disease
WNV	West Nile virus (in Chapter 2 refers to wild-type NS2B/NS3 active protease)
YFV	Yellow fever virus
ZPI	Z-dependent protease inhibitor

Acknowledgements

First, I would like to thank my supervisor Dr. François Jean for allowing me to pursue my PhD in his research group. You have allowed me to become a strong and independent scientist, capable of asking the correct scientific questions and knowing how to conduct proper scientific experiments. I have truly become a better person from this experience. Thank you for all of your support. This work was supported by a Canadian Institutes of Health Research operating grant MOP-84462 (to F. Jean).

I would like to thank my committee members, Dr. Mike Gold, Dr. Marc Horwitz and Dr. Martin Petric for all of your advice and wisdom over the years. Together, you have challenged me when I needed it and I have become a better scientist because of it. Thank you! I really appreciate all of your support throughout my PhD.

I would like to thank all past and present Jean Lab members. In particular, I would like to thank Martine Boutin for all of her tenaciousness in running the lab. I would also like to thank Dr. Morgan M. Martin for her determination. You inspired me to persevere and to get it done! I would like to thank Andrea Olmstead, Morgan Martin, Emma-Kate Loveday and Dr. Sandra Diederich for their friendship. Especially, Andrea, you made it possible to continue. Thank you for all of your encouragement. You can do it!

I would also like to thank all my family and friends back home. It has been very difficult to be away from all of you. Thank you for all of your love and support!

Lastly, I would like to thank my husband Dr. Martin J. Richer. I could not have done it without you. I love you. Thank you for your constant love and support and for always believing in me and making me laugh.

Milou you make me smile.

In addition, I would like to thank Dr. Michael Drebot (Public Health Agency of Canada) for the WNV sample. I would like to thank Dr. Charles Rice (The Rockefeller University) for the Huh7 cells, Dr. Francis Chisari (The Scripps Research Institute) for the Huh7.5.1 cells, Dr. Richard Leduc (Université de Sherbrooke) for the HEK 293A cells and Dr. Peter Cheung (British Columbia Centre for Excellence in HIV/AIDS) for the HEK 293T cells. I would like to thank Dr. Carl Hashimoto (Yale University) for the original Spn4A serpin plasmid. I would like to thank Dr. Jill Kelly and Dr. Martin J. Richer for proofreading and useful discussion of the manuscripts. I would also like to thank Reg Sidhu for technical assistance (Leica Microsystems).

Dedication

To my amazing husband Martin

You are my sunshine ❂

Co-authorship statement

Research design, data analysis and manuscript preparation for each chapter were completed by the author under the guidance of Dr. François Jean. The author performed all experiments presented within this thesis apart from the following exceptions:

Chapter 2: Martin Boutin cloned the full-length WNV NS2B/NS3 protease plasmid (pFLAG-NS2B/NS3-myc). Morgan Martin developed the original membrane-anchored red fluorescent protein substrate plasmid (pTm-CS-DsRed).

Chapter 3: Martin Boutin cloned the full-length WNV NS2B/NS3 protease plasmid (pFLAG-NS2B/NS3-myc). Morgan Martin developed the original membrane-anchored red fluorescent protein substrate plasmid (pTm-CS-DsRed).

Chapter 4: Martin Richer constructed the wild-type laboratory Spn4A serpin plasmid (psp-hf-Spn4A-HDEL). Hanah Tsao cloned the red fluorescent protein cytoplasmic Spn4A serpin plasmid (pmRFP-hf-Spn4A-HDEL). Christine Lai cloned the cytoplasmic Spn4A serpin plasmid (phf-Spn4A). Martin Boutin cloned the full-length WNV NS2B/NS3 protease plasmid (pFLAG-NS2B/NS3-myc). Morgan Martin developed the original membrane-anchored red fluorescent protein substrate plasmid (pTm-CS-DsRed).

Chapter 1

Introduction

1.1. Introduction

West Nile virus (WNV) was first reported in the Western Hemisphere in 1999 (1). It crossed the border into Canada in 2001 (2), and spread rapidly throughout North America. It has become a serious public health risk in North America, causing a potentially fatal infection. Currently, there are no prophylaxis or treatments available for human WNV infections. As such, extensive research has been undertaken to understand all aspects of the virus. In particular, understanding the virus life cycle is crucial for the rational design of novel therapeutics for this re-emerging global pathogen.

1.1.1. Discovery of West Nile virus

WNV was first isolated when Smithburn and colleagues conducted an epidemiological investigation within Africa in an attempt to isolate Yellow fever virus (YFV) from a presumably endemic zone extending from the West coast across central Africa and into Uganda. Blood was drawn from those that exhibited an illness suggestive of a YFV infection. Isolated serum was subsequently inoculated intracerebrally into mice and subinoculations were performed from the mice that became ill. In December 1937, blood was drawn from an African woman (aged 37 years) who had a fever (temperature 100.6°F) at Omogo, West Nile district in the Northern Province of Uganda. Serum was inoculated intracerebrally into ten mice, of which only one survived. Subinoculations were conducted and in its 53rd passage (September 15, 1939) no surviving mice had been reported since the first mouse passage. Subsequent experiments demonstrated pathogenesis in mice when inoculated intracerebrally, intranasally and intraperitoneally and slight pathogenesis following subcutaneous inoculation. Intracerebral inoculation into rhesus monkeys resulted

in fatal encephalitis. Neutralizing antibody reacted strongly to Japanese B encephalitis virus (JEV) suggesting relatedness between the two viruses. The lesions induced by the new virus were limited to the central nervous system but differed from those induced by other known neurotropic viruses. Taken together, the report described properties of a novel neurotropic virus isolated from the blood of a woman from the West Nile district in Uganda, which Smithburn and colleagues named West Nile virus (3).

1.1.2. Epidemiology

Little WNV activity was reported until the 1950s when epidemics were documented in Israel and Egypt (4, 5). Epidemiological investigations conducted in Egypt during the 1950s determined that virus transmission occurred primarily between a mosquito vector and a bird host with occasional infections occurring in humans and other animals (6). Serological surveys along the Egyptian Nile demonstrated that more than 60% of the human population had detectable WNV antibodies (7). WNV was isolated from the blood of children with acute febrile illness mainly between August and November suggesting that within endemic areas, WNV infections are typically acquired early in childhood and during the summer months. Within the endemic areas, the majority of patients demonstrated no clinical symptoms other than fever (6). A serological survey of horses conducted in 1959 demonstrated the presence of WNV antibodies in 54% of animals with one suspected fatal case confirmed by viral isolation from the brain (8).

In Israel, the first reported epidemic occurred in 1951-1952, with 52% of patients being children aged 6 years and under. The first cases of severe neurological symptoms were reported in 1957 and subsequently in 1962 (6). Throughout the years, several outbreaks have

been reported in France (1962-65), South Africa (1974, 1983-84) and sporadic cases have been reported in Russia, Romania, Spain and India (9). A large outbreak was reported in Europe (Bucharest in 1996) with more than 800 cases and in the Mediterranean basin outbreaks were reported in Algeria (1994), Morocco (1996), Tunisia (1997), Italy (1998), Isreal (1999-2000) and in France (2000) (6).

An outbreak of neurological disease of unknown etiology was reported in humans and birds in New York City in 1999 (1). This was confirmed to be caused by WNV and represents the first report of WNV in the Western Hemisphere (1). Following this single point of introduction into New York in 1999, WNV has spread throughout the continental United States, north into Canada and southward into the Caribbean Islands and Latin America (10). In total in North America, over the last ten years (1999-2009), there have been 34,179 positive human WNV cases; of these cases 1,199 have resulted in death (death rate of 3.5%) (11, 12). The North American outbreak represents the largest arthropod-borne meningoencephalitis outbreak recorded in the "New World" and has been the largest WNV meningoencephalitis outbreak ever seen worldwide (2). WNV is the most widely distributed arthropod-borne virus globally, occurring on all continents except Antarctica (13). It is important to understand all aspects of the virus in order to develop effective prevention and treatment strategies.

1.1.3. Molecular epidemiology

It remains currently unknown how WNV was originally introduced to the Western Hemisphere. Phylogenetic analysis has revealed that the New York 1999 (NY99) WNV strain (flamingo isolate) is closely related to an Israel 1998 WNV strain (goose isolate)

(99.8% nucleotide sequence similarity) suggesting that the NY99 WNV strain may have originated from the Middle East (Figure 1.1) (14). Additionally, phylogenetic analysis has revealed that WNV strains group into two major genetic lineages (1 and 2) (Figure 1.1) (14). Lineage 1 strains have a worldwide distribution ranging from North America, Middle East, Western Africa, Eastern Europe, India and Australia while lineage 2 strains are mostly limited to sub-Saharan Africa and Madagascar (15). Most lineage 1 strains have been isolated from epidemics where encephalitis and mortality occurred whereas lineage 2 strains are generally associated with asymptomatic or mild fever in humans (15). The original WNV 1937 Uganda strain is grouped within lineage 2 (15).

A difference in virulence between the lineage strains has been observed in a mouse model of neuroinvasion that correlated with genotype (16). Specifically, high neurovirulence was observed from lineage 1 strains whereas this phenotype was lacking in lineage 2 strains (16). Strains isolated from New York City in 1999 (lineage 1) were highly neuroinvasive (17). Sequence analysis has revealed that many of the WNV strains isolated from New York contain a N-linked glycosylation motif (NYS) at residue 154-156 of the envelope (E) protein (18). Shirato et al., (2004) demonstrated that mice infected with WNV containing a glycosylated E protein developed a lethal infection whereas mice infected with WNV that had a non-glycosylated E protein showed low mortality. Taken together, the results suggest that the glycosylation motif within the E protein is a molecular determinant of neuroinvasiveness in the New York WNV strains (18).

During the spread of WNV across North America a new dominant genotype emerged (referred to as WN02) and displaced the introductory WNV NY99 genotype. Sequence analysis has revealed that the majority of new isolates share a single amino acid substitution

of valine to alanine at residue 159 within the E protein (19, 20). Moudy et al., (2007) investigated whether there were any differences between the two genotypes that would explain why NY99 was displaced by WN02. *In vitro* analysis showed no detectable differences in replication or fitness within cell culture between WN02 and NY99. However, the extrinsic incubation period (EIP) of the WN02 genotype was up to 4 days shorter *in vivo* than the EIP of the NY99 genotype (EIP: the time between mosquito ingesting an infectious blood meal and transmission of the virus by that mosquito). Furthermore, virus titers were significantly higher in WN02-infected mosquitoes compared to NY99-infected mosquitoes indicating that WN02 replicates more efficiently *in vivo*. Taken together, the results demonstrated that there was a difference in viral replication efficiency within the mosquito vector between the two genotypes potentially allowing for WN02 to gain an advantage over NY99 (21). The suggested displacement model favours an increase in vectorial capacity of WN02. A decrease in EIP leads to an increase in WN02-infected mosquitoes that are able to infect the next naïve bird host at a subsequent blood meal (21). As a consequence, WN02-infected mosquitoes would be able to infect more birds than NY99-infected mosquitoes leading to a greater number of WN02-infected birds. As a result, there would be more WN02-infected birds present from which the next naïve mosquito vector could feed on. Since WN02 is more efficient at replicating within the mosquito vector, NY99 is out competed and as a consequence is displaced (21). The single point of introduction of WNV to New York in 1999 has given researchers a unique opportunity to study the WNV microevolution as it adapts to North America.

1.1.4. Transmission

The natural transmission of WNV involves an avian amplifying host and a mosquito vector that is maintained in a bird-mosquito-bird cycle (Figure 1.2) (22). WNV is transmitted primarily by *Culex* species mosquitoes (2). In North America, *Culex pipiens* and *Culex restuans* are the principal bird-biting mosquito vector (23). Other mosquito species are able to acquire blood meals from both birds and mammals thus acting as "bridge-vectors" transmitting WNV into incidental "dead-end" hosts such as humans and horses (Figure 1.2) (2, 24, 25). Viremia in these hosts does not reach levels that permit transmission back to mosquitoes (2). As the female mosquito feeds on an infected bird host, WNV enters the mosquito via the infected blood. It penetrates the mosquito midgut, replicates in tissues including the nervous system and salivary glands and produces a noncytopathic infection that persists for the life of the mosquito (26). Several mosquito species are able to survive through the winter, remaining dormant until they resurface in the spring and host-seek for a blood meal and subsequently infect the next host allowing for viral persistence within the population (27). Furthermore, the female mosquito is able to transmit WNV to her eggs and as a result the newly hatched pupa mature into infectious adult mosquitoes capable of transmitting WNV (28). In addition, a mosquito's metabolism and biology is greatly influenced by environmental conditions such as temperature (29). As a result, an increase in temperature affects the EIP, increasing the replication rate of the virus within the mosquito and consequently increasing the transmission rate (29).

An infected mosquito transmits WNV to susceptible birds, which serve as the major amplifying host. In particular, birds that are members of the *Corvidae* family (i.e. crows, blue jays, ravens) are highly susceptible (30). Komar et al., (2003) have demonstrated with

experimental infections of varying North American bird species that the highest viremia titers (10^{10} plaque-forming units/ml) were detected in crows. From the fatal crow cases, WNV was isolated from the brain, kidney, heart, spleen, liver, lung, intestine, esophagus, gonad, skin and eye (31). Due to their high mortality following WNV exposure, crows have been the primary bird species for dead bird surveillance programs (2).

WNV has an extremely large host and vector range and in North America it has been isolated in more than 60 different mosquito species and in over 300 bird species (32, 33). In addition to birds, WNV has been isolated in more than 30 species of nonavian vertebrate hosts, including humans, equines, rodents, reptiles, amphibians, felines, canines, bats and sea mammals (34). Non-mosquito modes of WNV transmission have also been reported (35) including transmission by organ transplantation, blood transfusion, breast milk, intrauterine (36) and occupational exposure (37-39). Since 2003, blood centers in the United States and Canada have been routinely screening for WNV in the blood supply (32). From 2003 to 2007, screening of blood supplies has identified 2,000 WNV positive blood donors (32, 40, 41).

1.1.5. Pathogenesis

As the infected mosquito acquires a blood meal it injects WNV intradermally through its infectious saliva. It is thought that WNV replicates at the site of inoculation in Langerhans dendritic cells (42). The infected cells migrate into the lymph nodes where WNV can enter into the bloodstream leading to primary viremia (43). Secondary viremia results from the dissemination of WNV and subsequent infection of peripheral tissues, such as the spleen and kidney (44). Virus can be detected in the blood one to two days post-

inoculation from the infected mosquito and viremia can persist for up to one week (45). By day seven post-infection, WNV is largely cleared from the blood coinciding with the appearance of IgM neutralizing antibodies (44, 45).

WNV can disseminate throughout the central nervous system (CNS) particularly in immunocomprised individuals and the elderly (44). In the CNS, WNV is able to infect neurons, glial cells, basal ganglia, brainstem and spinal cord (46). The precise mechanism by which WNV crosses the blood brain barrier (BBB) into the CNS remains poorly defined. Conflicting results have been observed during WNV infection within a mouse model (47, 48). Wang et al., (2004) demonstrated that mice deficient for Toll-like receptor 3 (TLR3) were more resistant to lethal WNV infection compared to wild-type mice. Wild-type mice had an increase in circulating inflammatory cytokines levels that coincided with an increase in BBB leakiness, suggesting a detrimental role of TLR3 (Figure 1.3) (47). Conversely, using the same TLR3 deficient mice, Daffis et al., (2008) demonstrated a protective role of TLR3. Wild-type mice were more resistant to lethal WNV infection compared to TLR3 deficient mice. TLR3 deficient mice had decreased survival rates and increased BBB permeability (48). The contribution of TLR3 in mediating the inflammatory response to WNV infection and virus entry into the CNS remains unclear.

1.1.6. Clinical features

The incubation period of a WNV infection in humans is three to 14 days and clinical symptoms range from a mild febrile illness to potentially fatal encephalitis (2). Approximately, 80% of human infections are asymptomatic, 20% develop West Nile fever (WNF) and less than 1% develop West Nile neuroinvasive disease (WNND) (45).

Individuals with a mild WNV infection frequently experience fever, headache and other nonspecific symptoms that last a few days. Common symptoms of WNF include abrupt onset of fever, headache, fatigue, nausea, vomiting, a rash on the trunk and extremities, muscle pain and weakness, neck pain or stiffness, chills, confusion and slurred speech that can last one month after onset (49-51). In addition, other nonneurological manifestations have been reported including hepatitis, pancreatitis and myocarditis (52).

WNND symptoms include meningitis, encephalitis, paralysis and poliomyelitis and extremely severe cases may result in mortality. Susceptibility to WNND is significantly increased in the elderly and immunocompromised individuals (45). Although, WNND is rarely reported in children, from 2002 to 2004 more than 1,000 WNV infections were reported in individuals aged 19 years or younger from which 30% of the cases were categorized as WNND (45). Most commonly reported symptoms in patients with WNND include high fever, confusion, delirium, trouble walking, tremors, blurry vision and numbness in limbs or body (45). Individuals with WNND have prolonged recovery times with symptoms lasting for over two months after onset. Generally, recovery occurs within four months of illness although some patients do not reach full recovery until one year after onset of symptoms (53). Physical and cognitive sequalae have also been reported and were found to be more prevalent one year after infection affecting daily living activities (53). WNV can cause a potentially fatal infection and has posed a serious health concern in North America since its introduction in 1999. Currently, there are no vaccines, antiviral therapies or treatments available for human WNV infections. Understanding the WNV life cycle is crucial in designing effective therapeutic strategies.

1.2. Virus biology

1.2.1. Classification

WNV is classified within the virus family *Flaviviridae* (from the Latin *flavus* or yellow referring to the prototype virus, YFV) (54). The *Flaviviridae* family is divided into three genera *flavivirus*, *pestivirus* and *hepacivirus* from which WNV is a member of the *flavivirus* genus (55). The *flavivirus* genus is composed of many arthropod-borne viruses (arboviruses) that are transmitted by either mosquitoes (mosquito-borne) or ticks (tick-borne); WNV is mosquito-borne (55). The mosquito-borne viruses are further subdivided into different antigenic serogroups according to serotype these include, Dengue virus (DNV) serogroup, JEV serogroup and YFV serogroup; WNV is a member of the JEV serogroup (55). Each serogroup is further divided into different virus species that is additionally grouped into different virus subtypes from which each subtype encompasses many genetically related virus strains. West Nile virus species is comprised of two subtypes, Kunjin virus and West Nile virus, which encompass various viral strains (29). Altogether, WNV is classified in the *Flaviviridae* family, genus *flavivirus*, mosquito-borne, member of the JEV serogroup, grouped into the West Nile virus species, West Nile virus subtype that is divided into two genetic lineages (1 and 2) (14).

1.2.2. Virion structure

WNV is a small (~50 nm diameter) virus particle that contains an icosahedral nucleocapsid surrounded by a lipid bilayer (56-59). The virus surface contains two viral proteins, envelope (E) protein and membrane (M) protein (Figure 1.4), and encased within the nucleocapsid is viral genomic RNA (55, 56). The E protein is the major viral surface

protein and the major antigenic determinant. It mediates binding and fusion during virus entry into host cells (56). The E protein is arranged in a head-to-tail homodimer conformation that lies parallel to the lipid bilayer on the virus surface (60).

The M protein is produced from the proteolytic processing of a premembrane (prM) precursor protein, which is mediated by the *trans*-Golgi network (TGN) host serine protease, furin, prior to virion release (Figure 1.4) (61). The prM precursor protects the E protein from fusing with intracellular membranes as the virion transits through the secretory pathway (Figure 1.5) (61). The immature prM-E virus particles are larger in size (~60 nm) compared to the mature M-E virions (~50 nm). The larger particle size is due to the prM-E heterodimer protruding from the virus surface resulting in a spiky appearance compared to the smooth outer surface observed in the M-E mature virion (Figure 1.5) (61, 62). Upon cleavage of the prM-E heterodimer by furin in the TGN, the E protein changes conformation lying parallel on the virus surface (63). However, the cleaved pr peptide remains associated to the E protein, preventing membrane fusion during virion release at the host cell surface (61). When the virion enters the extracellular milieu, the pr peptide dissociates from the E protein (Figure 1.5), allowing for membrane fusion to occur in the next replication cycle (61).

1.2.3. Replication cycle

WNV replication cycle is initiated when the E protein on the virus surface binds to receptors on the host cell surface (Figure 1.6). On the host cell surface, WNV utilizes the lectin DC-SIGNR (dendritic cell-specific intercellular adhesion molecule-3-grabbing nonintegrin) and possibly the integrin $\alpha_v\beta_3$ as receptors (64-67). The virion is internalized via clathrin-mediated endocytosis (68) and transported toward the endoplasmic reticulum

(ER) in lysosomal vesicles (Figure 1.6) (45). The low pH within the lysosome induces membrane fusion between the virus E protein and lysosomal membranes leading to the release of the viral nucleocapsid into the cytoplasm (68-71). The viral RNA genome is released from the nucleocapsid into the cytoplasm and is translated into a single polyprotein precursor (56). At the ER membrane, the polyprotein precursor is processed into individual components by both host and viral proteases (55, 56). Processing of the polyprotein results in the release of ten viral proteins that are involved in viral RNA genome replication, virus assembly or the subsequent release of viral progeny at the host cell surface (55). The viral RNA genome replicates via a double-stranded RNA intermediate within a replication complex (composed of several viral proteins) that is thought to be associated with the ER membrane (72). Assembly occurs in association with intracellular membranes and nascent virions transit through the secretory pathway where furin mediates the final cleavage event prior to virion release from the host cell surface (Figure 1.6) (55, 61).

1.2.4. Genome organization, protein translation and proteolytic processing

WNV contains a single-stranded positive-sense RNA genome of approximately 11,000 base pairs (54). Present at the 5′-terminus is a cap-like structure and the 3′-terminus ends with CU_{OH} thus lacking a polyadenylated tract (73, 74). The genome contains a single open reading frame (ORF) that is flanked with 5′- and 3′-noncoding regions (56).

Translation is cap-dependent and is initiated by ribosomal scanning (55). The viral RNA genome serves as mRNA, due to the positive polarity, and is translated immediately by the host ribosomal machinery upon release from the nucleocapsid (56). Translation from the ORF produces a single polyprotein precursor that is co- and post-translationally

processed by host and viral proteases (55). The polyprotein precursor is comprised of ten viral proteins, three of which are structural and seven that are nonstructural (NS) (Figure 1.7) (54). The three structural proteins, capsid (C), prM and E constitute the virus architecture (54-56). The seven NS proteins, NS1, NS2A, NS2B, NS3, NS4A, NS4B and NS5, are either involved in protease activity (NS2B, NS3) or participate in replication by forming the replication complex (NS1, NS2A, NS3, NS4A, NS4B, NS5), which facilitates polymerase activity by the viral RNA dependent RNA polymerase (RdRp) (NS5) (54-56).

The polyprotein precursor is arranged in the following order from N- to C-terminal: C-prM-E-NS1-NS2A-NS2B-NS3-NS4A-NS4B-NS5 (Figure 1.7) (54-58, 75, 76). Proteolytic processing of the polyprotein precursor is mediated by host proteases and the viral protease heterocomplex, NS2B/NS3 (77-80). Host proteases cleave at the protein junctions, C/prM, prM/E, E/NS1, whereas the viral protease is thought to cleave at the NS2A/NS2B, NS2B/NS3, NS3/NS4A, and NS4B/NS5 protein junctions (59, 61, 77, 78, 81). Viral genome replication cannot begin until all the proteins are cleaved and released from the polyprotein precursor (77). Inhibiting viral protease activity would in turn prevent viral genome replication making the NS2B/NS3 protease heterocomplex an attractive antiviral target for drug discovery. Gaining further understanding of NS2B/NS3 protease function is essential for the design of effective antiviral therapies.

1.2.5. Features of the NS2B/NS3 protease heterocomplex

The viral protease is comprised of two viral proteins NS2B and NS3 that are associated with each other to form a heterocomplex. NS3 is a large protein (~70 kDa) that contains two distinct enzymatic domains, a protease domain within the N-terminus (78, 82,

83) and a helicase/ATPase domain within the C-terminus (Figure 1.7) (84, 85). The helicase/ATPase domain is thought to participate in viral RNA genome replication in association with NS5 (RdRp) by unwinding the double-stranded RNA intermediates, facilitating NS5 polymerase activity (86).

The protease domain of NS3 is characteristic of serine proteases, containing the classic catalytic triad, hisitidine-aspartic acid-serine at amino acid residues 51, 75 and 135, respectively (Figure 1.7) (78, 82, 83). The protease mediates proteolytic processing of the polyprotein precursor at specific protein junctions by cleaving C-terminally at highly conserved dibasic residues followed by a small side-chain residue (59, 77, 78). Proteases catalyze the breakdown of proteins by hydrolyzing at a specific peptide bond, referred to as the scissile bond (↓) (87, 88). Amino acids that are N-terminal of the scissile bond are referred to as non-primed (Pn) residues and amino acids that are C-terminal of the scissile bond are referred to as primed (Pn′) residues (88). These residues determine the protease substrate specificity and typically include six Pn residues and four Pn′ residues, P6-P1↓P1′-P4′, constituting the substrate cleavage site sequence (87, 88).

In vitro studies, using a recombinant truncated form of the WNV protease, have demonstrated that the preferred substrate specificity of the WNV protease is KR↓GG (89, 90). However, commonly utilized in WNV *in vitro* protease assays are substrates that contain a chromogenic/fluorogenic moiety in the P1′ position as well as four or six Pn residues (91-93). This presents limitations into determining the contributions that the Pn′ residues have on protease specificity. Furthermore, optimal *in vitro* conditions for WNV protease activity occur at high pH and with the addition of glycerol and detergents, which are not physiologically representative (91-93).

NS2B is a small protein (~15 kDa) that facilitates the protease activity of NS3 (94-98). Hydrophobicity profiles of NS2B depict three regions, a central hydrophilic region (II) that is flanked by hydrophobic regions (I, III) (Figure 1.7). It is proposed that the hydrophobic regions of NS2B associate the protein to the ER membrane (55, 96, 97, 99, 100) and deletion studies of related flaviviruses have demonstrated that the central hydrophilic region of NS2B is sufficient to activate the protease domain of NS3 (94-98). *In vitro* studies have exploited this and utilize truncated forms of the NS2B and NS3 proteins incorporating the minimum amino acid residues required to elicit proteolytic activity (91-93).

Typically, the central hydrophilic region of NS2B (40 amino acids) is connected by a flexible glycine linker (G_4SG_4) to the protease domain of NS3 (NS3pro) generating the recombinant protein $NS2B_{40}$-G_4SG_4-NS3pro that can be bacterially expressed and purified for *in vitro* enzymatic studies (91-93). A crystal structure of the $NS2B_{40}$-G_4SG_4-NS3pro recombinant protein has been resolved illustrating that $NS2B_{40}$ wraps around NS3pro in a belt-like manner (Figure 1.8) (101-103). This suggests that NS2B may function as a cofactor to NS3, facilitating the arrangement of the catalytic triad into an active conformation (104). However, it has been argued that NS2B may instead function as a prodomain, needed only for the proper folding of NS3 and not the final proteolytic activity (105). The precise role NS2B has in the protease activity of NS3 remains debated and warrants further investigation.

It has been demonstrated *in vitro* with DNV that the addition of microsomal membranes enhances protease activity suggesting that membrane association may influence protease function (96). It has been proposed that NS3 is tethered to the ER membrane

through its interactions with NS2B and that NS2B associates to the ER membrane through its hydrophobic regions (55). Thus the interaction between NS2B and membranes may subsequently affect and/or regulate the proteolytic activity of NS3, factors that are not considered in conventional *in vitro* experimental conditions.

Utilizing the $NS2B_{40}$-G_4SG_4-NS3pro recombinant protein to assess WNV protease activity has been informative *in vitro* however, it does present with inherent limitations. The effect of membrane anchoring and influence of the intracellular microenvironment on protease activity are not considered. Additionally, the potential contribution that the other protein regions (i.e. NS2B hydrophobic regions and NS3 helicase domain) may have on the enzymatic properties of NS3 are not taken into account. In order to design an effective antiviral therapy it is imperative to study the full-length NS2B/NS3 protease heterocomplex within a physiologically relevant environment.

1.3. Antiviral strategies

1.3.1. Targets of inhibition

Currently, there are no vaccines or antiviral therapies available for human WNV infections, and as such research efforts have been focused on vaccine development and drug discovery. The primary prevention method is avoidance of the mosquito vector and the only treatment available is supportive care (2). Human vaccines are available for related flaviviruses such as YFV, JEV and tick-borne encephalitis virus (55). The prM and E proteins are highly antigenic and delivery of these antigens to elicit an immune response has been explored using chimeric viruses. Replacing the prM and E proteins of the YFV vaccine strain with WNV prM and E proteins has shown promise for vaccine development (106).

Immunization of animals has also been investigated using various strategies such as recombinant viral proteins, inactivated or attenuated virus or DNA plasmids expressing viral antigens (107-110). These approaches are promising, however, vaccine development is challenging and in the absence of prophylaxis the development of antiviral therapy becomes important, in order to reduce the morbidity and mortality associated with human WNV infections.

Several stages of the WNV replication cycle can be potentially targeted for antiviral therapies. One potential strategy is to block virus entry utilizing antibodies directed against the E protein, thereby inhibiting receptor binding and subsequent internalization of the virion into host cells (13, 111). Another potential therapeutic avenue would be to prevent viral RNA synthesis by targeting the RdRp activity of NS5 and the helicase activity of NS3 (111). A third approach is to inhibit virion maturation, by targeting the proteolytic activity of the host protease furin. Impeding this step would block the virion in an immature state, which is inefficient at membrane fusion and consequently reduce infectivity (61). Lastly, preventing the processing of the polyprotein precursor by targeting the proteolytic activity of the NS2B/NS3 protease heterocomplex is a very attractive strategy. Prohibiting the processing and release of the viral proteins from the polyprotein precursor would inhibit viral genome replication, thus reducing the number of virion progeny produced. A rationally designed inhibitor directed against the WNV NS2B/NS3 protease, is a promising therapeutic avenue towards the development of an antiviral agent (105, 112, 113). Viral protease inhibitors are currently used to treat HIV-1 infections (113) and Phase-III clinical trials are underway for the HCV viral protease inhibitors (114, 115) suggesting that targeting viral proteases represent a viable avenue for antiviral therapy.

1.3.2. Serine protease inhibitors

Protease inhibitors are rationally designed to mimic the protease's actual substrate. Utilizing knowledge of the protease's mechanism of action and substrate specificity, rational drug design aims at creating novel inhibitors that are specific for the target protease. The WNV NS2B/NS3 protease is a serine protease that has been shown *in vitro* to have a substrate specificity of KR↓GG (89, 90). Similarly, the host protease, furin, is a cellular serine protease with a substrate specificity of RX(R/K)R↓ (minimum cleavage sequence of RXXR↓) (116). Furin is a ubiquitously expressed serine protease, belonging to a family of enzymes called proprotein convertases (PC) (116). Several pathogens require processing by furin for cytotoxicity and for the generation of infectious virions (117-120). As such, furin has been targeted as a potential antiviral therapy (117, 118, 120). It has been demonstrated *in vitro* that the $NS2B_{40}$-G_4SG_4-NS3pro recombinant protein was able to cleave furin substrates, suggesting that furin inhibitors could act against the WNV NS2B/NS3 protease heterocomplex (105).

An endogenous serine protease inhibitor (serpin), Spn4A, was identified from *Drosophila melanogaster,* to be a potent inhibitor of furin (K_i = 13pM) (121). Classic serpin architecture comprises of nine α-helices (A-I), three β-sheets (A-C) and a reactive centre loop (RCL) that typically contains 20 amino acid residues (Figure 1.9) (122, 123). The RCL is flexible and contains a cleavage sequence that is complementary to the active site of the target protease (122). Serpins operate as a suicide substrate inhibitor (122). The RCL is recognized by the target protease as a substrate and proteolysis at the scissile bond begins (123). However, as the acyl-enzyme intermediate is formed the serpin undergoes a rapid and irreversible conformational change in which the RCL is incorporated into β-sheet A (122).

As a result, the protease becomes covalently linked to the P1 residue, translocated through to the bottom of the serpin and trapped in an inactive covalently linked conformation (Figure 1.9) (122, 123).

The RCL of Spn4A is comprised of the amino acid sequence AVRRKR↓AIMS, which contains the consensus cleavage sequence of furin (RX(R/K)R↓) (121). Since the WNV NS2B/NS3 protease, has a similar cleavage sequence to furin it is possible that Spn4A may have an inhibitory effect on the viral protease. Alternatively, altering residues within the RCL of Spn4A to residues that are preferred by the WNV protease may change the specificity of Spn4A allowing for the development of a selective inhibitor directed against the NS2B/NS3 protease. To this effect, it has been demonstrated with a related *Drosophila* serpin, Spn6, that altering specific residues within the RCL yielded a serpin with specific inhibitory properties towards the HCV viral protease (124). Based on this it would be feasible to alter the specificity of Spn4A from furin to the WNV NS2B/NS3 protease.

1.4. Project goal, hypothesis and aims

The overall goal of this project was to investigate the molecular and cellular characteristics of the full-length WNV viral protease heterocomplex, NS2B/NS3, within the intracellular microenvironment. I hypothesized that there are critical residues that are essential for the interaction between NS2B and NS3 that, in turn, affect protease activity and protein stability. The first aim of this project was to generate a cell-based fluorescent substrate assay to assess the protease activity of the full-length NS2B/NS3 protease heterocomplex within the intracellular microenvironment (Chapter 2). The second aim was to elucidate NS2B function on NS3 protease activity using the established cell-based

fluorescent substrate assay (Chapter 3). The third aim was to utilize the information gathered to rationally design a specific serine protease inhibitor directed against the full-length NS2B/NS3 protease heterocomplex (Chapter 4).

Figure 1.1. Phylogenetic tree of West Nile virus

Phylogenetic tree based on the E-glycoprotein nucleic acid sequence of West Nile virus (14). From Lanciotti, RS, JT Roehrig, V Deubel, J Smith, M Parker, et al., Origin of the West Nile virus responsible for an outbreak of encephalitis in the northeastern United States. Science 1999; 286: 2333. Reprinted with permission from AAAS.

Figure 1.1

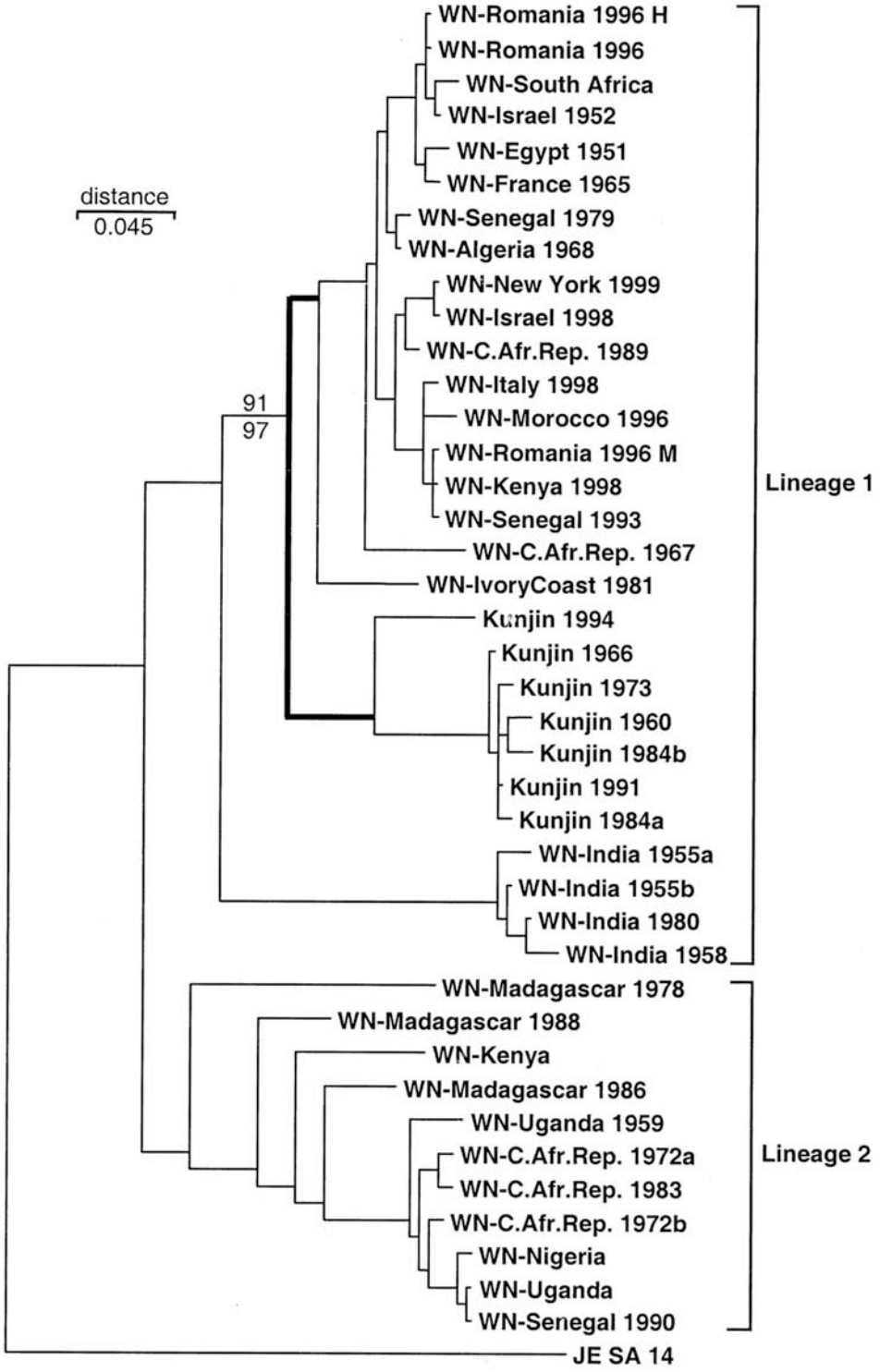
distance
0.045
91
97
WN-Romania 1996 H
WN-Romania 1996
WN-South Africa
WN-Israel 1952
WN-Egypt 1951
WN-France 1965
WN-Senegal 1979
WN-Algeria 1968
WN-New York 1999
WN-Israel 1998
WN-C.Afr.Rep. 1989
WN-Italy 1998
WN-Morocco 1996
WN-Romania 1996 M
WN-Kenya 1998
WN-Senegal 1993
WN-C.Afr.Rep. 1967
WN-IvoryCoast 1981
Kunjin 1994
Kunjin 1966
Kunjin 1973
Kunjin 1960
Kunjin 1984b
Kunjin 1991
Kunjin 1984a
WN-India 1955a
WN-India 1955b
WN-India 1980
WN-India 1958
Lineage 1
WN-Madagascar 1978
WN-Madagascar 1988
WN-Kenya
WN-Madagascar 1986
WN-Uganda 1959
WN-C.Afr.Rep. 1972a
WN-C.Afr.Rep. 1983
WN-C.Afr.Rep. 1972b
WN-Nigeria
WN-Uganda
WN-Senegal 1990
Lineage 2
JE SA 14

Figure 1.2

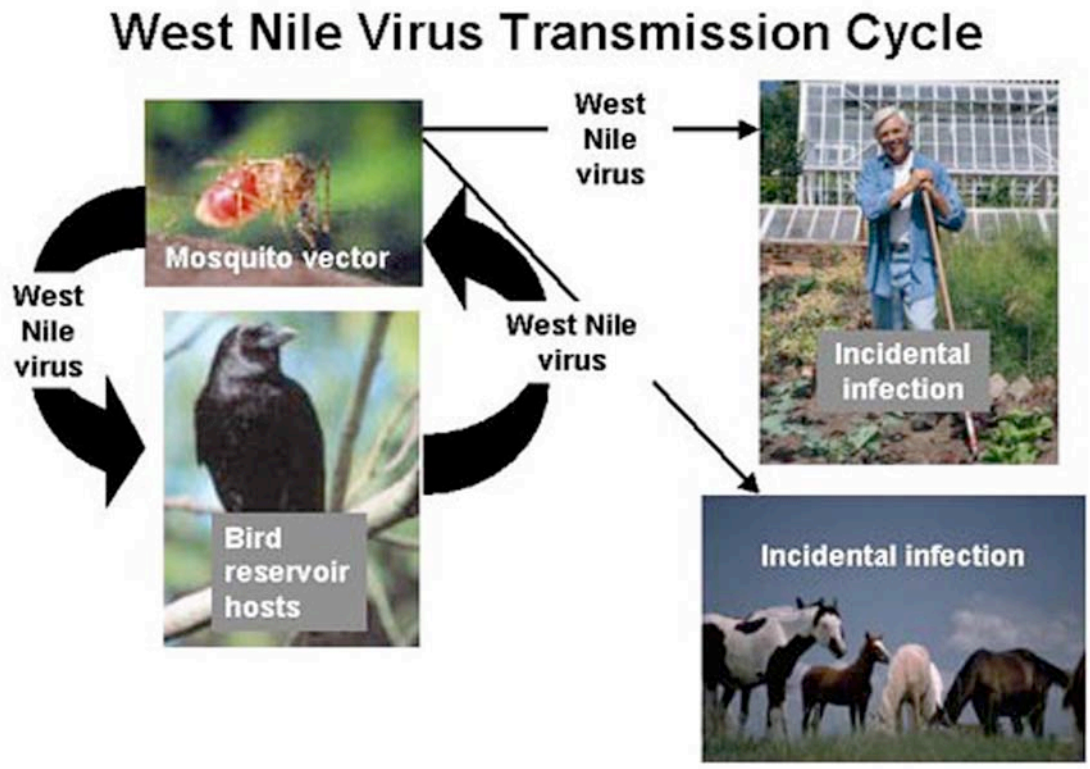

Figure 1.2. West Nile virus transmission cycle

West Nile virus transmission cycles between a mosquito vector and amplifying bird host. Mammals such as humans and horses are incidental dead-end hosts. Viremia in these hosts does not reach levels high enough to permit transmission back to the mosquito. Available at: www.cdc.gov/ncidod/dvbid/westnile/cycle.htm

Figure 1.3

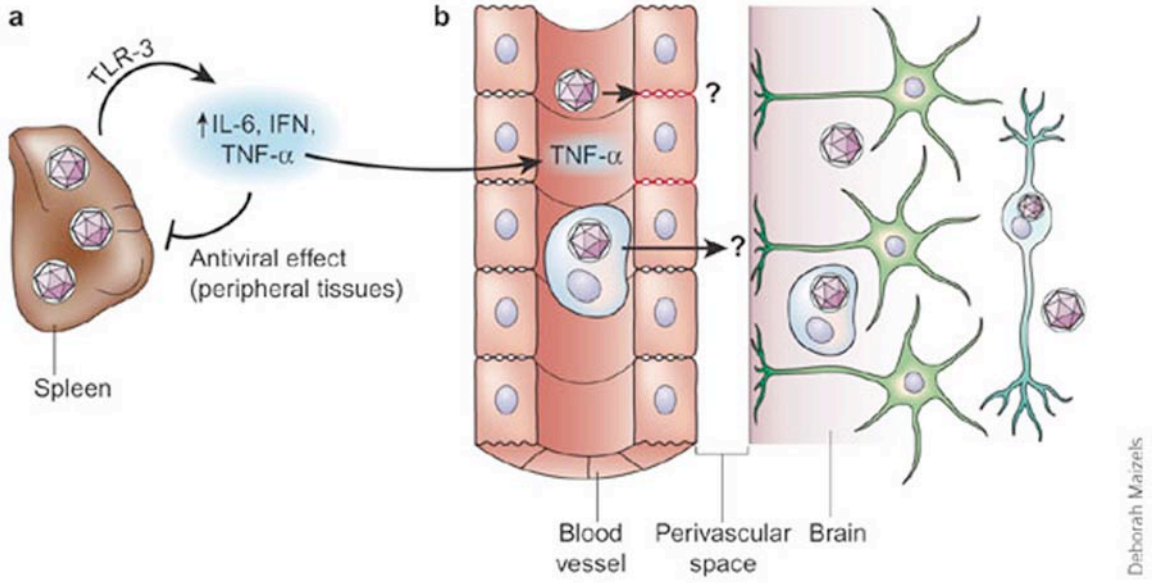

Figure 1.3. West Nile crossing

Infection of macrophages or dendritic cells by West Nile virus in peripheral lymphoid tissue induces TLR3-dependent secretion of antiviral and immunomodulatory cytokines such as IFN, IL-6 and TNF-α. These cytokines inhibit infection in peripheral tissues. TLR3-dependent induction of TNF-α, however, also facilitates West Nile virus penetration across the BBB. The exact mechanism of penetration remains unclear (125). Reprinted by permission from Macmillan Publishers Ltd: Nature Medicine, Diamond MS and RS Klein, West Nile virus: crossing the blood-brain barrier, copyright 2004.

Figure 1.4

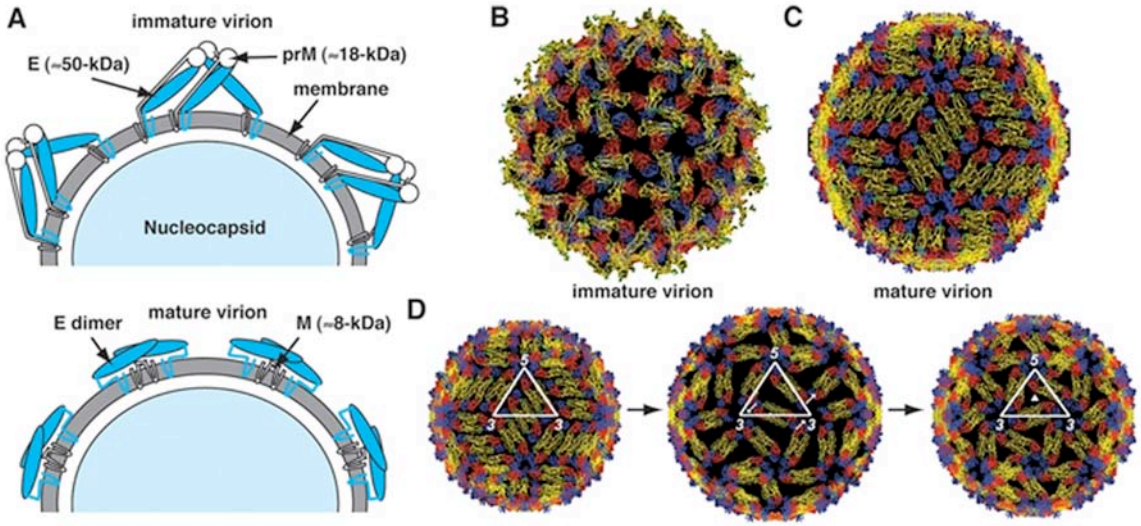

Figure 1.4. Structures of flavivirus particles

(A) Envelope proteins of mature and immature virions. (B) Cryo-electron microscopy reconstruction of immature Dengue virus 2 particles. (C) Cryo-electron microscopy of mature Dengue virus 2 particles. (D) Model of the low pH-induced fusogenic state (55). Reprinted with permission: Lindenbach, BD, H Thiel and CM Rice, Fields Virology 5th Edition, DM Knipe and PM Howley, Lippincott Williams & Wilkins, a Wolters Kluwer Business, 2007.

Figure 1.5

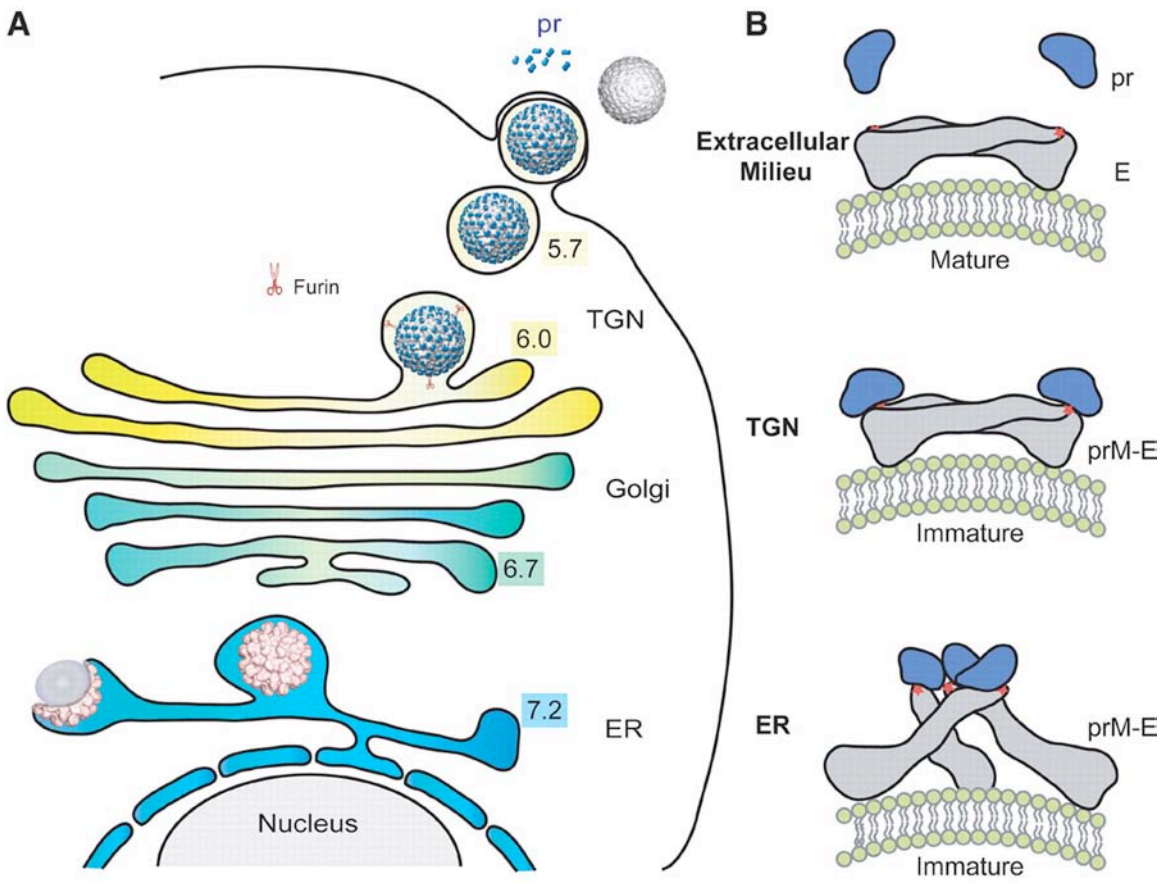

Figure 1.5. A model of the flavivirus maturation pathway

(A) The conformational changes of the virus particles in the secretory pathway. Immature particles bud into the ER and are transported through the TGN where acidification induces a conformational change of the virion. Furin cleavage takes place in the TGN and pr remains associated until the virion is released to the extracellular milieu. (B) Configuration of the glycoproteins on the surface of the virion during maturation (61). From Yu I, W Zhang, HA Holdaway, L Li, VA Kostyuchenko, et al., Structure of the immature Dengue virus at low pH primes proteolytic maturation. Science 2008; 319: 1834. Reprinted with permission from AAAS.

Figure 1.6. Flavivirus life cycle

Virions attach to the surface of a host cell and subsequently enter the cell by receptor-mediated endocytosis. Acidification of the endosomal vesicle triggers conformational changes in the virion, fusion of the viral and cell membranes, and particle disassembly. Once the genome is released into the cytoplasm, the positive-sense RNA is translated into a single polyprotein that is processed co- and post-translationally by viral and host proteases. Genome replication occurs on intracellular membranes. Virus assembly occurs on the surface of the ER when the structural proteins and newly synthesized RNA buds into the lumen of the ER. The resultant immature particles are transported through the TGN. The immature virions are cleaved by furin, resulting in mature particles (65). Reprinted by permission from Macmillan Publishers Ltd: Nature Reviews Microbiology, Mukhopadhyay S, RJ Kuhn and MG Rossmann, A structural perspective of the flavivirus life cycle, copyright 2005.

Figure 1.6

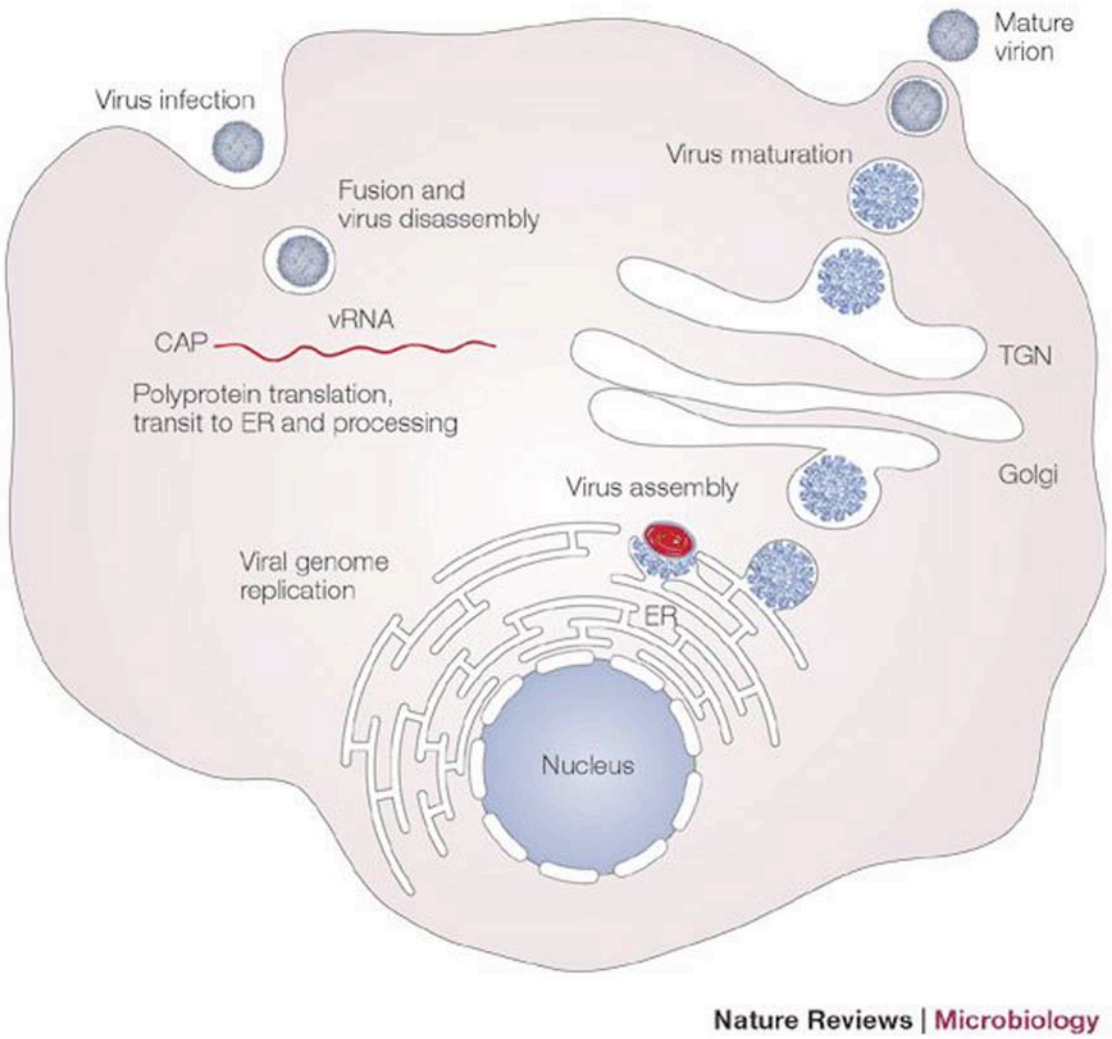
Mature virion
Virus infection
Virus maturation
Fusion and virus disassembly
vRNA
CAP
Polyprotein translation, transit to ER and processing
TGN
Golgi
Virus assembly
Viral genome replication
ER
Nucleus
Nature Reviews | Microbiology

Figure 1.7

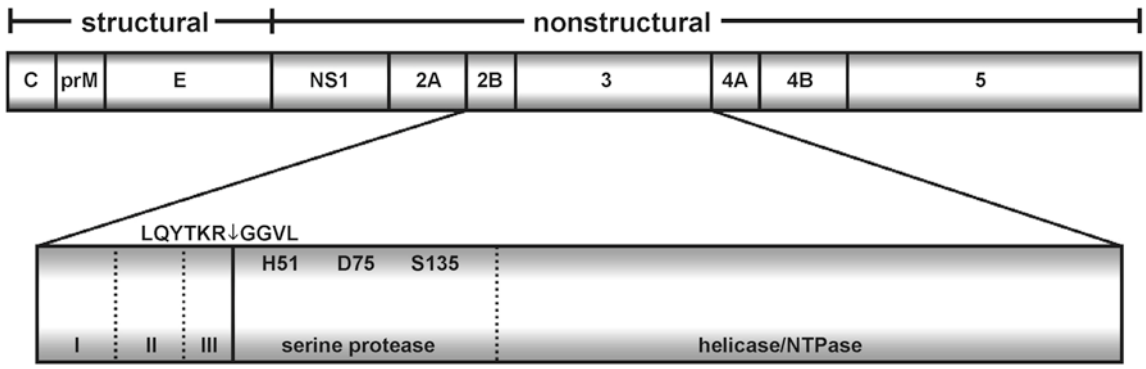

Figure 1.7. West Nile virus polyprotein precursor

The polyprotein precursor is comprised of three structural proteins (capsid (C), premembrane (prM), envelope (E)) and seven nonstructural (NS) proteins (NS1, NS2A, NS2B, NS3, NS4A, NS4B, NS5). The polyprotein precursor is arranged in the following order from N- to C-terminal: C-prM-E-NS1-NS2A-NS2B-NS3-NS4A-NS4B-NS5. The viral protease heterocomplex, NS2B/NS3, is depicted as the enlarged section. The NS2B/NS3 protein junction site sequence (LQYTKR↓GGVL) is indicated. NS2B, 15 kDa protein, is comprised of three regions (separated by dotted lines), N-terminus hydrophobic region (I), central hydrophilic region (II) and a C-terminus hydrophobic region (III). NS3, 70 kDa protein, is composed of two enzymatic domains (separated by dotted lines). Within the N-terminus of NS3 is a serine protease (catalytic triad indicated, H51, D75, S135) and encoded within the C-terminus is a helicase/NTPase domain.

Figure 1.8

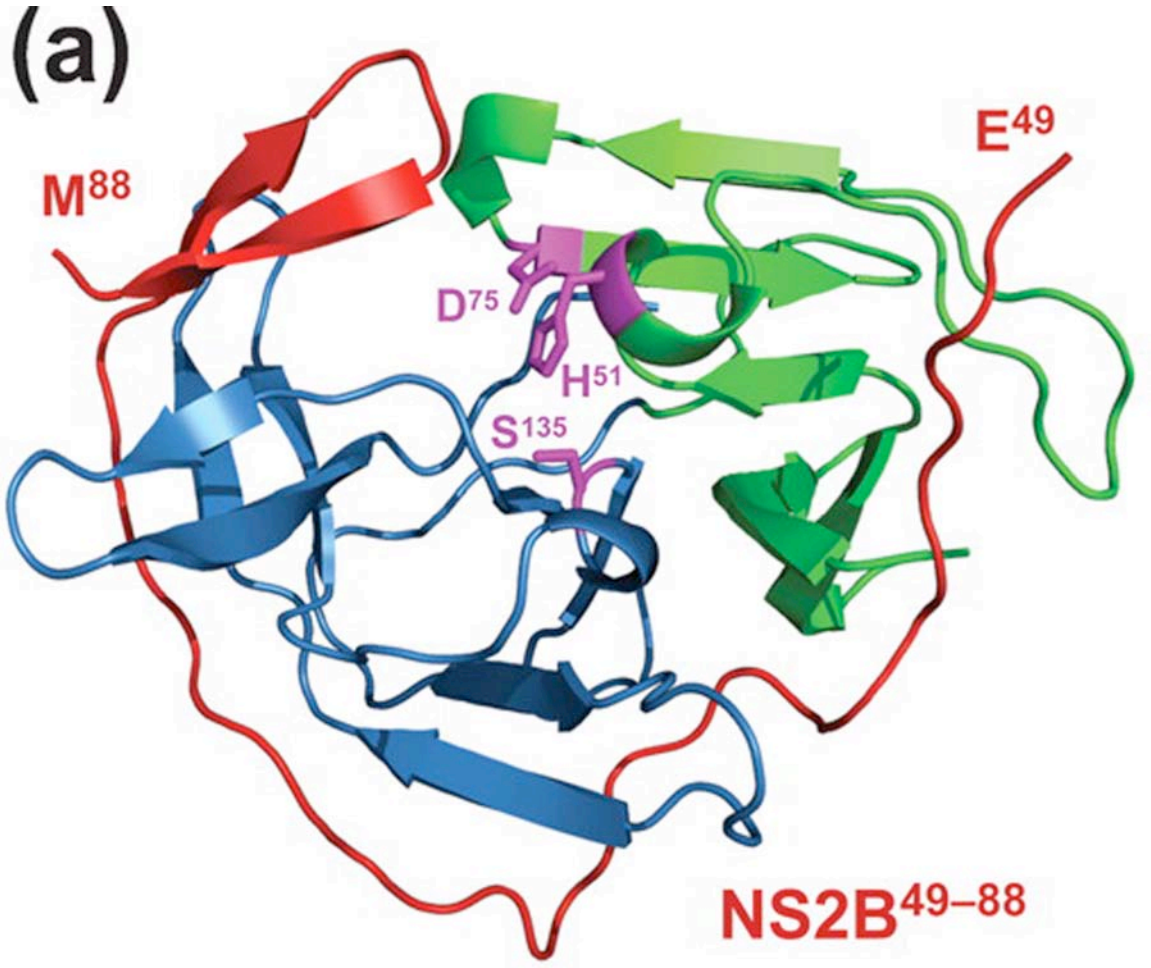

Figure 1.8. Structure of the West Nile virus NS2B$_{40}$-G$_4$SG$_4$-NS3pro

The structure of the NS2B$_{40}$-G$_4$SG$_4$-NS3pro is depicted in ribbon form with the NS3 N-terminal β-barrel coloured in green and the C-terminal β-barrel in blue. The central domain of NS2B is shown in red with the catalytic triad residues in stick form in magenta (103). Adapted from Chappell, KJ, MJ Stoermer, DP Fairlie, PR Youg. Mutagenesis of the West Nile virus NS2B cofactor domain reveals two regions essential for protease activity. J Gen Virol 2008; 89: 1010. Reprinted with permission from the Society for General Microbiology.

Figure 1.9. Formation of the complex

Ribbon depiction of the native α_1-antitrypsin (serpin) with trypsin (protease) aligned above it (left) and the complex with the full insertion of the cleaved reactive center loop (RCL) into the β-sheet A (right). Red, α_1-antitrypsin β-sheet A; yellow, RCL; green ball and stick, P1 (122). Reprinted by permission from Macmillan Publishers Ltd: Nature, Huntington JA, RJ Read and RW Carrell, Structure of a serpin-protease complex shows inhibition by deformation, copyright 2000.

Figure 1.9

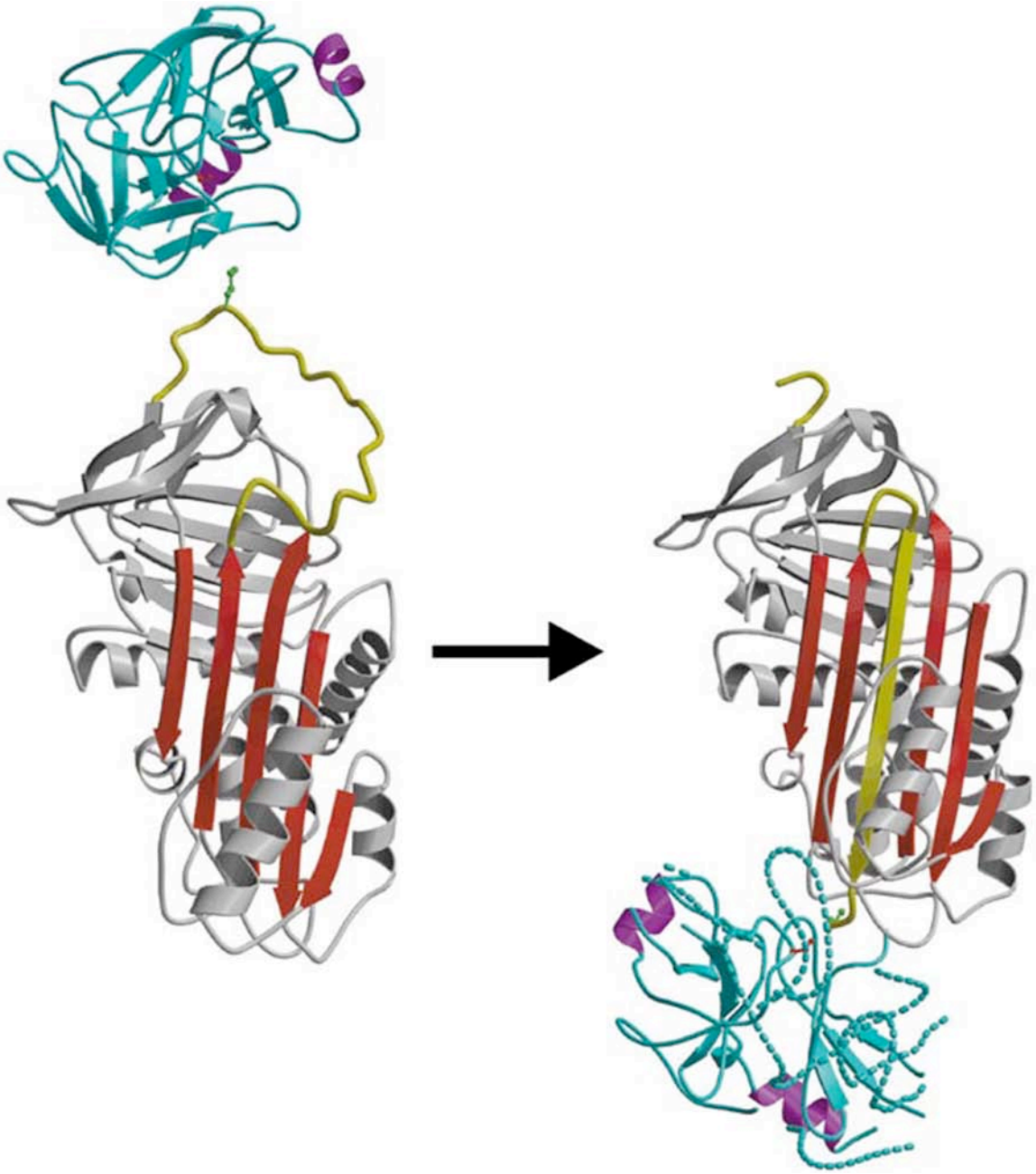

1.5. References

1. (CDC), C. o. D. C. a. P. 1999. Outbreak of West Nile-like viral encephalitis--New York, 1999. *MMWR Morb Mortal Wkly Rep* 48:845-849.
2. Drebot, M. A., R. Lindsay, I. K. Barker, P. A. Buck, M. Fearon, F. Hunter, P. Sockett, and H. Artsob. 2003. West Nile virus surveillance and diagnostics: A Canadian perspective. *Can J Infect Dis* 14:105-114.
3. Smithburn, K. C., T. P. Hughes, A. W. Burke, and J. H. Paul. 1940. A neurotropic virus isolated from the blood of a native of Uganda. *Am J Trop Med Hyg* 20:471-492.
4. Bernkopf, H., S. Levine, and R. Nerson. 1953. Isolation of West Nile virus in Israel. *J Infect Dis* 93:207-218.
5. Melnick, J. L., J. R. Paul, J. T. Riordan, V. H. Barnett, N. Goldblum, and E. Zabin. 1951. Isolation from human sera in Egypt of a virus apparently identical to West Nile virus. *Proc Soc Exp Biol Med* 77:661-665.
6. Murgue, B., S. Murri, H. Triki, V. Deubel, and H. G. Zeller. 2001. West Nile in the Mediterranean basin: 1950-2000. *Ann N Y Acad Sci* 951:117-126.
7. Hurlbut, H. S., F. Rizk, R. M. Taylor, and T. H. Work. 1956. A study of the ecology of West Nile virus in Egypt. *Am J Trop Med Hyg* 5:579-620.
8. Schmidt, J. R., and H. K. Elmansoury. 1963. Natural and Experimental Infection of Egyptian Equines with West Nile Virus. *Ann Trop Med Parasitol* 57:415-427.
9. Hubalek, Z., and J. Halouzka. 1999. West Nile fever--a reemerging mosquito-borne viral disease in Europe. *Emerg Infect Dis* 5:643-650.

10. Dauphin, G., S. Zientara, H. Zeller, and B. Murgue. 2004. West Nile: worldwide current situation in animals and humans. *Comp Immunol Microbiol Infect Dis* 27:343-355.

11. (CDC), C. o. D. C. a. P. West Nile Virus: Statistics, Surveillance, and Control. Available at: http://www.cdc.gov/ncidod/dvbid/westnile/surv&controlCaseCount09_detailed.htm (Last modified: April 13, 2010).

12. (PHAC), P. H. A. o. C. West Nile Virus Monitor. Available at: http://www.phac-aspc.gc.ca/wnv-vwn/mon-hmnsurv-archive-eng.php (Last modified: June 26, 2009).

13. Kramer, L. D., L. M. Styer, and G. D. Ebel. 2008. A global perspective on the epidemiology of West Nile virus. *Annu Rev Entomol* 53:61-81.

14. Lanciotti, R. S., J. T. Roehrig, V. Deubel, J. Smith, M. Parker, K. Steele, B. Crise, K. E. Volpe, M. B. Crabtree, J. H. Scherret, R. A. Hall, J. S. MacKenzie, C. B. Cropp, B. Panigrahy, E. Ostlund, B. Schmitt, M. Malkinson, C. Banet, J. Weissman, N. Komar, H. M. Savage, W. Stone, T. McNamara, and D. J. Gubler. 1999. Origin of the West Nile virus responsible for an outbreak of encephalitis in the northeastern United States. *Science* 286:2333-2337.

15. Lanciotti, R. S., G. D. Ebel, V. Deubel, A. J. Kerst, S. Murri, R. Meyer, M. Bowen, N. McKinney, W. E. Morrill, M. B. Crabtree, L. D. Kramer, and J. T. Roehrig. 2002. Complete genome sequences and phylogenetic analysis of West Nile virus strains isolated from the United States, Europe, and the Middle East. *Virology* 298:96-105.

16. Beasley, D. W., L. Li, M. T. Suderman, and A. D. Barrett. 2001. West Nile virus strains differ in mouse neurovirulence and binding to mouse or human brain membrane receptor preparations. *Ann N Y Acad Sci* 951:332-335.

17. Beasley, D. W., M. C. Whiteman, S. Zhang, C. Y. Huang, B. S. Schneider, D. R. Smith, G. D. Gromowski, S. Higgs, R. M. Kinney, and A. D. Barrett. 2005. Envelope protein glycosylation status influences mouse neuroinvasion phenotype of genetic lineage 1 West Nile virus strains. *J Virol* 79:8339-8347.

18. Shirato, K., H. Miyoshi, A. Goto, Y. Ako, T. Ueki, H. Kariwa, and I. Takashima. 2004. Viral envelope protein glycosylation is a molecular determinant of the neuroinvasiveness of the New York strain of West Nile virus. *J Gen Virol* 85:3637-3645.

19. Ebel, G. D., J. Carricaburu, D. Young, K. A. Bernard, and L. D. Kramer. 2004. Genetic and phenotypic variation of West Nile virus in New York, 2000-2003. *Am J Trop Med Hyg* 71:493-500.

20. Davis, C. T., G. D. Ebel, R. S. Lanciotti, A. C. Brault, H. Guzman, M. Siirin, A. Lambert, R. E. Parsons, D. W. Beasley, R. J. Novak, D. Elizondo-Quiroga, E. N. Green, D. S. Young, L. M. Stark, M. A. Drebot, H. Artsob, R. B. Tesh, L. D. Kramer, and A. D. Barrett. 2005. Phylogenetic analysis of North American West Nile virus isolates, 2001-2004: evidence for the emergence of a dominant genotype. *Virology* 342:252-265.

21. Moudy, R. M., M. A. Meola, L. L. Morin, G. D. Ebel, and L. D. Kramer. 2007. A newly emergent genotype of West Nile virus is transmitted earlier and more efficiently by Culex mosquitoes. *Am J Trop Med Hyg* 77:365-370.

22. Campbell, G. L., A. A. Marfin, R. S. Lanciotti, and D. J. Gubler. 2002. West Nile virus. *Lancet Infect Dis* 2:519-529.

23. Condotta, S. A., F. F. Hunter, and M. J. Bidochka. 2004. West Nile virus infection rates in pooled and individual mosquito samples. *Vector Borne Zoonotic Dis* 4:198-203.

24. Turell, M. J., M. R. Sardelis, D. J. Dohm, and M. L. O'Guinn. 2001. Potential North American vectors of West Nile virus. *Ann N Y Acad Sci* 951:317-324.

25. White, D. J., L. D. Kramer, P. B. Backenson, G. Lukacik, G. Johnson, J. A. Oliver, J. J. Howard, R. G. Means, M. Eidson, I. Gotham, V. Kulasekera, and S. Campbell. 2001. Mosquito surveillance and polymerase chain reaction detection of West Nile virus, New York State. *Emerg Infect Dis* 7:643-649.

26. Girard, Y. A., V. Popov, J. Wen, V. Han, and S. Higgs. 2005. Ultrastructural study of West Nile virus pathogenesis in Culex pipiens quinquefasciatus (Diptera: Culicidae). *J Med Entomol* 42:429-444.

27. Nasci, R. S., H. M. Savage, D. J. White, J. R. Miller, B. C. Cropp, M. S. Godsey, A. J. Kerst, P. Bennett, K. Gottfried, and R. S. Lanciotti. 2001. West Nile virus in overwintering Culex mosquitoes, New York City, 2000. *Emerg Infect Dis* 7:742-744.

28. Miller, B. R., R. S. Nasci, M. S. Godsey, H. M. Savage, J. J. Lutwama, R. S. Lanciotti, and C. J. Peters. 2000. First field evidence for natural vertical transmission of West Nile virus in Culex univittatus complex mosquitoes from Rift Valley province, Kenya. *Am J Trop Med Hyg* 62:240-246.

29. Gubler, D. J., G. Kuno, and L. Markoff. 2007. Flaviviruses. In *Fields Virology*, 5 ed. D. M. Knipe, and P. M. Howley, eds. Lippincott William and Wilkins, Philadelphia. 1153-1252.

30. Eidson, M., L. Kramer, W. Stone, Y. Hagiwara, and K. Schmit. 2001. Dead bird surveillance as an early warning system for West Nile virus. *Emerg Infect Dis* 7:631-635.

31. Komar, N., S. Langevin, S. Hinten, N. Nemeth, E. Edwards, D. Hettler, B. Davis, R. Bowen, and M. Bunning. 2003. Experimental infection of North American birds with the New York 1999 strain of West Nile virus. *Emerg Infect Dis* 9:311-322.

32. Petersen, L. R. 2009. Global Epidemiology of West Nile Virus. In *West Nile Encephalitis Virus Infection*. M. S. Diamond, ed. Springer, New York. 1-23.

33. (CDC), C. o. D. C. a. P. West Nile Virus: Vertebrate Ecology. Available at: http://www.cdc.gov/ncidod/dvbid/westnile/birdspecies.htm (Last modified: April 28, 2009).

34. Komar, N. 2003. West Nile virus: epidemiology and ecology in North America. *Adv Virus Res* 61:185-234.

35. (CDC), C. o. D. C. a. P. 2002. Provisional surveillance summary of the West Nile virus epidemic--United States, January-November 2002. *MMWR Morb Mortal Wkly Rep* 51:1129-1133.

36. Hayes, E. B., and D. R. O'Leary. 2004. West Nile virus infection: a pediatric perspective. *Pediatrics* 113:1375-1381.

37. (CDC), C. o. D. C. a. P. 2003. West Nile virus infection among turkey breeder farm workers--Wisconsin, 2002. *MMWR Morb Mortal Wkly Rep* 52:1017-1019.

38. Nir, Y., A. Beemer, and R. A. Goldwasser. 1965. West Nile Virus infection in mice following exposure to a viral aerosol. *Br J Exp Pathol* 46:443-449.

39. (CDC), C. o. D. C. a. P. 2002. Laboratory-acquired West Nile virus infections--United States, 2002. *MMWR Morb Mortal Wkly Rep* 51:1133-1135.

40. Busch, M. P., S. Caglioti, E. F. Robertson, J. D. McAuley, L. H. Tobler, H. Kamel, J. M. Linnen, V. Shyamala, P. Tomasulo, and S. H. Kleinman. 2005. Screening the blood supply for West Nile virus RNA by nucleic acid amplification testing. *N Engl J Med* 353:460-467.

41. Stramer, S. L., C. T. Fang, G. A. Foster, A. G. Wagner, J. P. Brodsky, and R. Y. Dodd. 2005. West Nile virus among blood donors in the United States, 2003 and 2004. *N Engl J Med* 353:451-459.

42. Chambers, T. J., and M. S. Diamond. 2003. Pathogenesis of flavivirus encephalitis. *Adv Virus Res* 60:273-342.

43. Johnston, L. J., G. M. Halliday, and N. J. King. 2000. Langerhans cells migrate to local lymph nodes following cutaneous infection with an arbovirus. *J Invest Dermatol* 114:560-568.

44. Samuel, M. A., and M. S. Diamond. 2006. Pathogenesis of West Nile Virus infection: a balance between virulence, innate and adaptive immunity, and viral evasion. *J Virol* 80:9349-9360.

45. Davis, L. E., R. DeBiasi, D. E. Goade, K. Y. Haaland, J. A. Harrington, J. B. Harnar, S. A. Pergam, M. K. King, B. K. DeMasters, and K. L. Tyler. 2006. West Nile virus neuroinvasive disease. *Ann Neurol* 60:286-300.

46. Guarner, J., W. J. Shieh, S. Hunter, C. D. Paddock, T. Morken, G. L. Campbell, A. A. Marfin, and S. R. Zaki. 2004. Clinicopathologic study and laboratory diagnosis of 23 cases with West Nile virus encephalomyelitis. *Hum Pathol* 35:983-990.

47. Wang, T., T. Town, L. Alexopoulou, J. F. Anderson, E. Fikrig, and R. A. Flavell. 2004. Toll-like receptor 3 mediates West Nile virus entry into the brain causing lethal encephalitis. *Nat Med* 10:1366-1373.

48. Daffis, S., M. A. Samuel, M. S. Suthar, M. Gale, Jr., and M. S. Diamond. 2008. Toll-like receptor 3 has a protective role against West Nile virus infection. *J Virol* 82:10349-10358.

49. Nash, D., F. Mostashari, A. Fine, J. Miller, D. O'Leary, K. Murray, A. Huang, A. Rosenberg, A. Greenberg, M. Sherman, S. Wong, and M. Layton. 2001. The outbreak of West Nile virus infection in the New York City area in 1999. *N Engl J Med* 344:1807-1814.

50. Petersen, L. R., and A. A. Marfin. 2002. West Nile virus: a primer for the clinician. *Ann Intern Med* 137:173-179.

51. Kumar, D., G. V. Prasad, J. Zaltzman, G. A. Levy, and A. Humar. 2004. Community-acquired West Nile virus infection in solid-organ transplant recipients. *Transplantation* 77:399-402.

52. Hayes, E. B., N. Komar, R. S. Nasci, S. P. Montgomery, D. R. O'Leary, and G. L. Campbell. 2005. Epidemiology and transmission dynamics of West Nile virus disease. *Emerg Infect Dis* 11:1167-1173.

53. Klee, A. L., B. Maidin, B. Edwin, I. Poshni, F. Mostashari, A. Fine, M. Layton, and D. Nash. 2004. Long-term prognosis for clinical West Nile virus infection. *Emerg Infect Dis* 10:1405-1411.

54. Chambers, T. J., C. S. Hahn, R. Galler, and C. M. Rice. 1990. Flavivirus genome organization, expression, and replication. *Annu Rev Microbiol* 44:649-688.

55. Lindenbach, B. D., H. Thiel, and C. M. Rice. 2007. Flaviviridae: The viruses and their replication. In *Fields Virology*, 5 ed. D. M. Knipe, and P. M. Howley, eds. Lippincott William and Wilkins, Philadelphia. 1101-1152.

56. Brinton, M. A. 2002. The molecular biology of West Nile Virus: a new invader of the western hemisphere. *Annu Rev Microbiol* 56:371-402.

57. Castle, E., T. Nowak, U. Leidner, and G. Wengler. 1985. Sequence analysis of the viral core protein and the membrane-associated proteins V1 and NV2 of the flavivirus West Nile virus and of the genome sequence for these proteins. *Virology* 145:227-236.

58. Castle, E., U. Leidner, T. Nowak, and G. Wengler. 1986. Primary structure of the West Nile flavivirus genome region coding for all nonstructural proteins. *Virology* 149:10-26.

59. Yamshchikov, V. F., and R. W. Compans. 1993. Regulation of the late events in flavivirus protein processing and maturation. *Virology* 192:38-51.

60. Rey, F. A., F. X. Heinz, C. Mandl, C. Kunz, and S. C. Harrison. 1995. The envelope glycoprotein from tick-borne encephalitis virus at 2 A resolution. *Nature* 375:291-298.

61. Yu, I. M., W. Zhang, H. A. Holdaway, L. Li, V. A. Kostyuchenko, P. R. Chipman, R. J. Kuhn, M. G. Rossmann, and J. Chen. 2008. Structure of the immature dengue virus at low pH primes proteolytic maturation. *Science* 319:1834-1837.

62. Zhang, Y., J. Corver, P. R. Chipman, W. Zhang, S. V. Pletnev, D. Sedlak, T. S. Baker, J. H. Strauss, R. J. Kuhn, and M. G. Rossmann. 2003. Structures of immature flavivirus particles. *Embo J* 22:2604-2613.

63. Zhang, W., P. R. Chipman, J. Corver, P. R. Johnson, Y. Zhang, S. Mukhopadhyay, T. S. Baker, J. H. Strauss, M. G. Rossmann, and R. J. Kuhn. 2003. Visualization of membrane protein domains by cryo-electron microscopy of dengue virus. *Nat Struct Biol* 10:907-912.

64. Davis, C. W., H. Y. Nguyen, S. L. Hanna, M. D. Sanchez, R. W. Doms, and T. C. Pierson. 2006. West Nile virus discriminates between DC-SIGN and DC-SIGNR for cellular attachment and infection. *J Virol* 80:1290-1301.

65. Mukhopadhyay, S., R. J. Kuhn, and M. G. Rossmann. 2005. A structural perspective of the flavivirus life cycle. *Nat Rev Microbiol* 3:13-22.

66. Chu, J. J., and M. L. Ng. 2004. Interaction of West Nile virus with alpha v beta 3 integrin mediates virus entry into cells. *J Biol Chem* 279:54533-54541.

67. Lee, J. W., J. J. Chu, and M. L. Ng. 2006. Quantifying the specific binding between West Nile virus envelope domain III protein and the cellular receptor alphaVbeta3 integrin. *J Biol Chem* 281:1352-1360.

68. Chu, J. J., and M. L. Ng. 2004. Infectious entry of West Nile virus occurs through a clathrin-mediated endocytic pathway. *J Virol* 78:10543-10555.

69. Gollins, S. W., and J. S. Porterfield. 1985. Flavivirus infection enhancement in macrophages: an electron microscopic study of viral cellular entry. *J Gen Virol* 66 (Pt 9):1969-1982.

70. Gollins, S. W., and J. S. Porterfield. 1986. The uncoating and infectivity of the flavivirus West Nile on interaction with cells: effects of pH and ammonium chloride. *J Gen Virol* 67 (Pt 9):1941-1950.

71. Heinz, F. X., and S. L. Allison. 2000. Structures and mechanisms in flavivirus fusion. *Adv Virus Res* 55:231-269.

72. Uchil, P. D., and V. Satchidanandam. 2003. Architecture of the flaviviral replication complex. Protease, nuclease, and detergents reveal encasement within double-layered membrane compartments. *J Biol Chem* 278:24388-24398.

73. Brinton, M. A., A. V. Fernandez, and J. H. Dispoto. 1986. The 3'-nucleotides of flavivirus genomic RNA form a conserved secondary structure. *Virology* 153:113-121.

74. Wengler, G. 1981. Terminal sequences of the genome and replicative-from RNA of the flavivirus West Nile virus: absence of poly(A) and possible role in RNA replication. *Virology* 113:544-555.

75. Rice, C. M., E. M. Lenches, S. R. Eddy, S. J. Shin, R. L. Sheets, and J. H. Strauss. 1985. Nucleotide sequence of yellow fever virus: implications for flavivirus gene expression and evolution. *Science* 229:726-733.

76. Castle, E., and G. Wengler. 1987. Nucleotide sequence of the 5'-terminal untranslated part of the genome of the flavivirus West Nile virus. *Arch Virol* 92:309-313.

77. Chambers, T. J., R. C. Weir, A. Grakoui, D. W. McCourt, J. F. Bazan, R. J. Fletterick, and C. M. Rice. 1990. Evidence that the N-terminal domain of nonstructural protein NS3 from yellow fever virus is a serine protease responsible for site-specific cleavages in the viral polyprotein. *Proc Natl Acad Sci U S A* 87:8898-8902.

78. Wengler, G., G. Czaya, P. M. Farber, and J. H. Hegemann. 1991. In vitro synthesis of West Nile virus proteins indicates that the amino-terminal segment of the NS3 protein contains the active centre of the protease which cleaves the viral polyprotein after multiple basic amino acids. *J Gen Virol* 72 (Pt 4):851-858.

79. Cahour, A., B. Falgout, and C. J. Lai. 1992. Cleavage of the dengue virus polyprotein at the NS3/NS4A and NS4B/NS5 junctions is mediated by viral protease NS2B-NS3, whereas NS4A/NS4B may be processed by a cellular protease. *J Virol* 66:1535-1542.

80. Amberg, S. M., A. Nestorowicz, D. W. McCourt, and C. M. Rice. 1994. NS2B-3 proteinase-mediated processing in the yellow fever virus structural region: in vitro and in vivo studies. *J Virol* 68:3794-3802.

81. Falgout, B., and L. Markoff. 1995. Evidence that flavivirus NS1-NS2A cleavage is mediated by a membrane-bound host protease in the endoplasmic reticulum. *J Virol* 69:7232-7243.

82. Bazan, J. F., and R. J. Fletterick. 1989. Detection of a trypsin-like serine protease domain in flaviviruses and pestiviruses. *Virology* 171:637-639.

83. Gorbalenya, A. E., A. P. Donchenko, E. V. Koonin, and V. M. Blinov. 1989. N-terminal domains of putative helicases of flavi- and pestiviruses may be serine proteases. *Nucleic Acids Res* 17:3889-3897.

84. Gorbalenya, A. E., E. V. Koonin, A. P. Donchenko, and V. M. Blinov. 1989. Two related superfamilies of putative helicases involved in replication, recombination, repair and expression of DNA and RNA genomes. *Nucleic Acids Res* 17:4713-4730.

85. Wengler, G. 1991. The carboxy-terminal part of the NS 3 protein of the West Nile flavivirus can be isolated as a soluble protein after proteolytic cleavage and represents an RNA-stimulated NTPase. *Virology* 184:707-715.

86. Chernov, A. V., S. A. Shiryaev, A. E. Aleshin, B. I. Ratnikov, J. W. Smith, R. C. Liddington, and A. Y. Strongin. 2008. The two-component NS2B-NS3 proteinase represses DNA unwinding activity of the West Nile virus NS3 helicase. *J Biol Chem* 283:17270-17278.

87. Turk, B. 2006. Targeting proteases: successes, failures and future prospects. *Nat Rev Drug Discov* 5:785-799.

88. Schechter, I., and A. Berger. 1967. On the size of the active site in proteases. I. Papain. *Biochem Biophys Res Commun* 27:157-162.

89. Shiryaev, S. A., I. A. Kozlov, B. I. Ratnikov, J. W. Smith, M. Lebl, and A. Y. Strongin. 2007. Cleavage preference distinguishes the two-component NS2B-NS3 serine proteinases of Dengue and West Nile viruses. *Biochem J* 401:743-752.

90. Shiryaev, S. A., B. I. Ratnikov, A. E. Aleshin, I. A. Kozlov, N. A. Nelson, M. Lebl, J. W. Smith, R. C. Liddington, and A. Y. Strongin. 2007. Switching the substrate

specificity of the two-component NS2B-NS3 flavivirus proteinase by structure-based mutagenesis. *J Virol* 81:4501-4509.

91. Nall, T. A., K. J. Chappell, M. J. Stoermer, N. X. Fang, J. D. Tyndall, P. R. Young, and D. P. Fairlie. 2004. Enzymatic characterization and homology model of a catalytically active recombinant West Nile virus NS3 protease. *J Biol Chem* 279:48535-48542.

92. Chappell, K. J., T. A. Nall, M. J. Stoermer, N. X. Fang, J. D. Tyndall, D. P. Fairlie, and P. R. Young. 2005. Site-directed mutagenesis and kinetic studies of the West Nile Virus NS3 protease identify key enzyme-substrate interactions. *J Biol Chem* 280:2896-2903.

93. Shiryaev, S. A., A. E. Aleshin, B. I. Ratnikov, J. W. Smith, R. C. Liddington, and A. Y. Strongin. 2007. Expression and purification of a two-component flaviviral proteinase resistant to autocleavage at the NS2B-NS3 junction region. *Protein Expr Purif* 52:334-339.

94. Chambers, T. J., A. Grakoui, and C. M. Rice. 1991. Processing of the yellow fever virus nonstructural polyprotein: a catalytically active NS3 proteinase domain and NS2B are required for cleavages at dibasic sites. *J Virol* 65:6042-6050.

95. Chambers, T. J., A. Nestorowicz, S. M. Amberg, and C. M. Rice. 1993. Mutagenesis of the yellow fever virus NS2B protein: effects on proteolytic processing, NS2B-NS3 complex formation, and viral replication. *J Virol* 67:6797-6807.

96. Clum, S., K. E. Ebner, and R. Padmanabhan. 1997. Cotranslational membrane insertion of the serine proteinase precursor NS2B-NS3(Pro) of dengue virus type 2 is

required for efficient in vitro processing and is mediated through the hydrophobic regions of NS2B. *J Biol Chem* 272:30715-30723.

97. Brinkworth, R. I., D. P. Fairlie, D. Leung, and P. R. Young. 1999. Homology model of the dengue 2 virus NS3 protease: putative interactions with both substrate and NS2B cofactor. *J Gen Virol* 80 (Pt 5):1167-1177.

98. Yusof, R., S. Clum, M. Wetzel, H. M. Murthy, and R. Padmanabhan. 2000. Purified NS2B/NS3 serine protease of dengue virus type 2 exhibits cofactor NS2B dependence for cleavage of substrates with dibasic amino acids in vitro. *J Biol Chem* 275:9963-9969.

99. Wengler, G., T. Nowak, and E. Castle. 1990. Description of a procedure which allows isolation of viral nonstructural proteins from BHK vertebrate cells infected with the West Nile flavivirus in a state which allows their direct chemical characterization. *Virology* 177:795-801.

100. Yamshchikov, V. F., D. W. Trent, and R. W. Compans. 1997. Upregulation of signalase processing and induction of prM-E secretion by the flavivirus NS2B-NS3 protease: roles of protease components. *J Virol* 71:4364-4371.

101. Erbel, P., N. Schiering, A. D'Arcy, M. Renatus, M. Kroemer, S. P. Lim, Z. Yin, T. H. Keller, S. G. Vasudevan, and U. Hommel. 2006. Structural basis for the activation of flaviviral NS3 proteases from dengue and West Nile virus. *Nat Struct Mol Biol* 13:372-373.

102. Bera, A. K., R. J. Kuhn, and J. L. Smith. 2007. Functional characterization of cis and trans activity of the Flavivirus NS2B-NS3 protease. *J Biol Chem* 282:12883-12892.

103. Chappell, K. J., M. J. Stoermer, D. P. Fairlie, and P. R. Young. 2008. Mutagenesis of the West Nile virus NS2B cofactor domain reveals two regions essential for protease activity. *J Gen Virol* 89:1010-1014.

104. Chappell, K. J., M. J. Stoermer, D. P. Fairlie, and P. R. Young. 2007. Generation and characterization of proteolytically active and highly stable truncated and full-length recombinant West Nile virus NS3. *Protein Expr Purif* 53:87-96.

105. Shiryaev, S. A., B. I. Ratnikov, A. V. Chekanov, S. Sikora, D. V. Rozanov, A. Godzik, J. Wang, J. W. Smith, Z. Huang, I. Lindberg, M. A. Samuel, M. S. Diamond, and A. Y. Strongin. 2006. Cleavage targets and the D-arginine-based inhibitors of the West Nile virus NS3 processing proteinase. *Biochem J* 393:503-511.

106. Arroyo, J., C. Miller, J. Catalan, G. A. Myers, M. S. Ratterree, D. W. Trent, and T. P. Monath. 2004. ChimeriVax-West Nile virus live-attenuated vaccine: preclinical evaluation of safety, immunogenicity, and efficacy. *J Virol* 78:12497-12507.

107. Davis, B. S., G. J. Chang, B. Cropp, J. T. Roehrig, D. A. Martin, C. J. Mitchell, R. Bowen, and M. L. Bunning. 2001. West Nile virus recombinant DNA vaccine protects mouse and horse from virus challenge and expresses in vitro a noninfectious recombinant antigen that can be used in enzyme-linked immunosorbent assays. *J Virol* 75:4040-4047.

108. Ng, T., D. Hathaway, N. Jennings, D. Champ, Y. W. Chiang, and H. J. Chu. 2003. Equine vaccine for West Nile virus. *Dev Biol (Basel)* 114:221-227.

109. Minke, J. M., L. Siger, K. Karaca, L. Austgen, P. Gordy, R. Bowen, R. W. Renshaw, S. Loosmore, J. C. Audonnet, and B. Nordgren. 2004. Recombinant canarypoxvirus

vaccine carrying the prM/E genes of West Nile virus protects horses against a West Nile virus-mosquito challenge. *Arch Virol Suppl*:221-230.

110. Hall, R. A., D. J. Nisbet, K. B. Pham, A. T. Pyke, G. A. Smith, and A. A. Khromykh. 2003. DNA vaccine coding for the full-length infectious Kunjin virus RNA protects mice against the New York strain of West Nile virus. *Proc Natl Acad Sci U S A* 100:10460-10464.

111. Geiss, B. J., H. Stahla, A. M. Hannah, H. H. Gari, and S. M. Keenan. 2009. Focus on flaviviruses: current and future drug targets. *Future Med Chem* 1:327.

112. Chappell, K. J., M. J. Stoermer, D. P. Fairlie, and P. R. Young. 2008. West Nile Virus NS2B/NS3 protease as an antiviral target. *Curr Med Chem* 15:2771-2784.

113. Anderson, J., C. Schiffer, S. K. Lee, and R. Swanstrom. 2009. Viral protease inhibitors. *Handb Exp Pharmacol*:85-110.

114. Merck. Merck February Combined Pipeline. Available at: http://www.merck.com/research/pipeline/home.html (Last modified: March 1, 2010).

115. Vertex. Development Pipeline. Available at: http://www.vrtx.com/current-projects.html (Last modified: February 22, 2010).

116. Thomas, G. 2002. Furin at the cutting edge: from protein traffic to embryogenesis and disease. *Nat Rev Mol Cell Biol* 3:753-766.

117. Anderson, E. D., L. Thomas, J. S. Hayflick, and G. Thomas. 1993. Inhibition of HIV-1 gp160-dependent membrane fusion by a furin-directed alpha 1-antitrypsin variant. *J Biol Chem* 268:24887-24891.

118. Watanabe, M., A. Hirano, S. Stenglein, J. Nelson, G. Thomas, and T. C. Wong. 1995. Engineered serine protease inhibitor prevents furin-catalyzed activation of the

fusion glycoprotein and production of infectious measles virus. *J Virol* 69:3206-3210.

119. Jean, F., K. Stella, L. Thomas, G. Liu, Y. Xiang, A. J. Reason, and G. Thomas. 1998. alpha1-Antitrypsin Portland, a bioengineered serpin highly selective for furin: application as an antipathogenic agent. *Proc Natl Acad Sci U S A* 95:7293-7298.

120. Jean, F., L. Thomas, S. S. Molloy, G. Liu, M. A. Jarvis, J. A. Nelson, and G. Thomas. 2000. A protein-based therapeutic for human cytomegalovirus infection. *Proc Natl Acad Sci U S A* 97:2864-2869.

121. Richer, M. J., C. A. Keays, J. Waterhouse, J. Minhas, C. Hashimoto, and F. Jean. 2004. The Spn4 gene of Drosophila encodes a potent furin-directed secretory pathway serpin. *Proc Natl Acad Sci U S A* 101:10560-10565.

122. Huntington, J. A., R. J. Read, and R. W. Carrell. 2000. Structure of a serpin-protease complex shows inhibition by deformation. *Nature* 407:923-926.

123. Gettins, P. G. 2002. Serpin structure, mechanism, and function. *Chem Rev* 102:4751-4804.

124. Richer, M. J., L. Juliano, C. Hashimoto, and F. Jean. 2004. Serpin mechanism of hepatitis C virus nonstructural 3 (NS3) protease inhibition: induced fit as a mechanism for narrow specificity. *J Biol Chem* 279:10222-10227.

125. Diamond, M. S., and R. S. Klein. 2004. West Nile virus: crossing the blood-brain barrier. *Nat Med* 10:1294-1295.

Chapter 2

Detection and in-cell selectivity profiling of the full-length West Nile virus NS2B/NS3 serine protease using membrane-anchored fluorescent substrates[1]

[1] **A version of this chapter has been published:** Condotta, SA, MM Martin, M Boutin, F Jean. (2010) Detection and in-cell selectivity profiling of the full-length West Nile virus NS2B/NS3 serine protease using membrane-anchored fluorescent substrates. Biol Chem. 391:549-559 (cover illustration).

2.1. Introduction

West Nile virus (WNV) (family *Flaviviridae,* genus *flavivirus*) can cause a potentially fatal infection and has posed a serious health concern in North America since its introduction in 1999 (1). WNV is a zoonotic pathogen that is maintained in an enzootic cycle involving a mosquito vector and an amplifying bird host. Mammals such as humans and horses are incidental dead-end hosts, as viral titers do not reach levels that permit transmission back to mosquitoes (2). Although WNV is a serious public health problem, no antiviral therapies or vaccines are currently available. Understanding the virus life cycle is essential for the design of an effective therapy.

WNV is a small (~50 nm) enveloped virus with a single-stranded plus sense RNA genome (3-6). Upon uncoating, the viral genomic RNA is translated into a single polyprotein precursor composed of ten viral proteins (7). The structural proteins (capsid (C), premembrane (prM), and envelope (E)) are located at the N-terminal and the nonstructural (NS) proteins are located at the C-terminal in the following order: 5′-UTR-C-prM-E-NS1-NS2A-NS2B-NS3-NS4A-NS4B-NS5-UTR-3′ (3, 4, 7-9). Within the *flavivirus* genus, *in vitro* studies suggest that host proteases and the viral protease heterocomplex, NS2B/NS3 protease, cleave within the polyprotein precursor at specific sites (10-13). The NS2B/NS3 protease recognizes and cleaves C-terminally to highly conserved dibasic residues followed by a small side-chain residue, at protein junctions NS2A/NS2B, NS2B/NS3, NS3/NS4A, and NS4B/NS5 (5, 10, 11). The remaining viral proteins are released following cleavage by host proteases (12, 14, 15). These proteolytic processing events are essential for the virus life cycle (10), making the NS2B/NS3 protease an attractive antiviral target.

The NS2B/NS3 protease is composed of two viral proteins: NS2B and NS3. The

complex molecular interplay between the viral cofactor NS2B and the NS3 bi-functional enzyme [protease (NS3pro) and helicase (NS3hel): NS3pro-hel] have been a major challenge in studying these induced-fit viral proteases (16-18). N-terminal of NS3 is a 180-amino-acid serine protease domain (NS3pro), which contains the classic catalytic triad of serine proteases, histidine-aspartic acid-serine, at residues 51, 75, and 135, respectively (11, 19, 20); and C-terminal is a helicase/ATPase domain (NS3hel) (21, 22).

Many studies have shown that the viral protein NS2B is required for NS3 protease activity (23-27). Hydrophobicity profiles of NS2B illustrate a central hydrophilic region flanked by hydrophobic regions, which are thought to associate NS2B to the endoplasmic reticulum (ER) membrane (6, 23, 26, 28, 29). Deletion studies have demonstrated that 40 amino acids from the central hydrophilic region of NS2B are sufficient for the proteolytic activity of the protease domain of NS3 (23-27).

In vitro studies have exploited this and have investigated protease activity using truncated bacterial-expressed recombinant forms of the NS2B and NS3 proteins (30-32). The 40-amino-acid hydrophilic domain of NS2B ($NS2B_{40}$) is linked with a glycine-serine linker to the protease domain of NS3 (NS3pro), generating a recombinant $NS2B_{40}$-G_4SG_4-NS3pro protein (30-32). As a consequence, the flanking N- and C-terminal hydrophobic domains of NS2B and the helicase/ATPase domain of NS3 are omitted, therefore artificially producing the viral protease complex. In addition, these assays use synthetic chromogenic and fluorescent peptidyl-substrates with four or six amino-acid peptides containing a chromogenic or fluorogenic group at the P1′ position (33), which presents serious limitations for probing the contributions of residues at the C-terminus of the scissile peptide bond to the enzyme specificity (17)**.** Furthermore, optimal conditions for detecting protease

activity *in vitro* occur at alkaline pH and with the addition of glycerol and detergents (30-32).

Although *in vitro* assays have been very informative and have helped elucidate some of the important residues of NS2B and NS3 involved in NS2B/NS3 intrinsic enzymatic properties, these studies remain limited. Assays using recombinant truncated forms of NS2B and NS3 do not take into account the potential contributions of other nonstructural protein domains (e.g., NS3hel, NS2B N-terminal domain, and NS2B C-terminal domain) to the enzymatic properties of NS3pro. Furthermore, the complexity of the intracellular environment including the effects of membrane anchoring on protease activity is not considered.

To this effect, it has been shown *in vitro* that the addition of microsomal membranes enhances the efficiency of cleavage by the WNV NS2B/NS3 protease (11, 34) and by the related Dengue virus, suggesting that membrane association affects protease activity (26). Importantly, flaviviral NS2B/NS3pro-hel molecules are localized with the virus-induced membrane-bound replication complexes in the host cytoplasm (6, 35, 36), making the studies of these serine proteases *in cellulo* extremely challenging.

To address these issues, we developed a cell-based *trans*-cleavage assay for the detection of full-length WNV NS2B/NS3pro-hel endoproteolytic activity using ER membrane-anchored red-shifted fluorescent substrates. The substrates consist of an ER membrane-anchoring domain, a protease-specific cleavage sequence, and a DsRed fluorescent reporter group. When the protease cleaves the specific sequence, the DsRed reporter group is released, changing its localization in the cell from membrane-bound punctate perinuclear to diffuse cytoplasmic. This change in protein location can be

monitored by fluorescent microscopy, and cleavage products can be detected and quantified with Western blot analysis. We examined the WNV NS2B/NS3 cleavage activities against our internally consistent set of ER membrane-anchored red-shifted fluorescent substrates encoding for the proprotein cleavage sequences that correspond to the protein junctions NS2A/NS2B, NS2B/NS3, NS3/NS4A, and NS4B/NS5 within the WNV polyprotein precursor. In-cell selectivity profiling of the NS2B/NS3 serine protease demonstrated that only the NS4B/NS5 protein junction sequence is significantly cleaved compared to controls under our experimental conditions. Interestingly, as opposed to what has been reported *in vitro* (30), all other WNV proprotein junction sequences tested *in cellulo* were not significantly cleaved in *trans* by NS2B/NS3pro-hel as compared to controls.

Our data demonstrate the robustness of our *trans*-cleavage fluorescence-based assay to capture single-cell imaging of membrane-associated WNV NS2B/NS3 endoproteolytic activity. Importantly, our work reveals that within the intracellular environment of host cells, the WNV NS2B/NS3 heterocomplex serine protease presents an unexpected substrate selectivity underlying the importance of developing membrane-targeted activity-based probes to study these complex induced-fit viral proteases associated with the ER-anchored replication complexes during flavivirus infection.

2.2. Results

2.2.1. Development of novel membrane-anchored red-shifted fluorescent protein substrates to detect WNV NS2B/NS3 endoproteolytic activity in human cells

One of the major goals of this study was to generate a cell-based *trans*-cleavage assay for monitoring the endoproteolytic activity of the WNV NS2B/NS3pro-hel. We cloned

the full-length WNV NS2B/NS3 polyprotein into the pFLAG-myc-CMV™-20 epitope mammalian expression vector (Figure 2.1A). N-terminal of NS3 contains the classic catalytic triad of serine proteases, histidine-aspartic acid-serine, located within the protease domain at residues 51, 75, and 135, respectively (11, 19, 37). We used site-directed mutagenesis to mutate residue serine 135 to alanine (S135A) (Figure 2.1A). No autocatalytic cleavage products were detected in the S135A mutant compared to wild-type, indicating that this mutation rendered the NS2B/NS3 protease catalytically inactive (data not shown), which is consistent with previous reports (31, 38).

The membrane-bound fluorescent substrates consist of a fluorescent reporter group, DsRed, tethered to the ER membrane by a membrane-anchoring domain (Tm) (Tm is the hepatitis C virus (HCV) NS5A N-terminal amphipathic α-helix amino acid residues 1-34 (18)). Between Tm and DsRed is a cleavage sequence comprised of 10 amino acids corresponding to P6-P1↓P1′-P4′ residues (Figure 2.1B). In order for cleavage to occur, there is a critical requirement for co-localization of both the substrate and protease within the cell (18). That is, the substrate cannot be cleaved unless the protease encounters the substrate at the ER-membrane allowing the initial protease-substrate complex and subsequent endoproteolytic cleavage of the substrate, resulting in the release of the enzymatic reaction product from the ER-membrane. Intact fluorescent substrate is localized perinuclear, observed as a punctate pattern of DsRed at the ER membrane, whereas the cleaved fluorescent reaction product displays a diffuse cytoplasmic DsRed pattern (Figure 2.1C) that can be monitored with fluorescent microscopy in intact cells.

The parent substrate plasmid (pTm-DSSTPS↓SGSW-DsRed) was generated previously for the NS3/NS4A heterocomplex serine protease of HCV (18). The NS3

protease of HCV has a preferred cleavage sequence of (D/E)XXXX(C/T)↓(S/A) (16, 39) whereas the NS3 protease of WNV has a cleavage sequence preference of (K/R)R↓GG (40). We modified the P2P1↓P1′ residues with three sequential rounds of site-directed mutagenesis to generate the substrate pTm-DSST**KR↓G**GSW-DsRed (Figure 2.1B; KRG).

With the recent demonstration by Hinson et al., (2009) that the N-terminal amphipathic α-helices of viperin and HCV NS5A (Tm) that are responsible for the ER localization of both cellular and viral protein in host cells are also necessary and sufficient to localize both proteins to lipid droplets, we investigated the subcellular localization of the KRG membrane-anchored fluorescent substrate within intact cells using markers for ER membrane (anti-calnexin antibody) and lipid droplets (anti-ADRP antibody) (Figure 2.2) (41). Using confocal microscopy, we demonstrated a high degree of colocalization between the KRG substrate and the ER endogenous membrane marker calnexin in Huh7 cells (Figure 2.2; KRG-calnexin-merge) when compared to the relative colocalization of KRG and the lipid droplets endogenous marker ADRP (Figure 2.2; KRG-ADRP-merge).

We tested for *trans*-cleavage of the KRG substrate by double-transfecting active WNV protease or inactive S135A protease and monitoring cleavage with fluorescent microscopy. A diffuse cytoplasmic DsRed protein pattern was only observed upon transfection of active WNV protease (Figure 2.3; WNV-DsRed) whereas a perinuclear punctate DsRed pattern was observed with inactive S135A protease (Figure 2.3; S135A-DsRed) and in substrate-only controls (Figure 2.3; Substrate only-DsRed). Protease expression was confirmed in the active WNV protease and inactive S135A protease samples with immunofluorescent microscopy (Figure 2.3; myc panel). These results demonstrate that our membrane-anchored cell-based fluorescent substrate assay can be used to monitor the

endoproteolytic activity of the WNV NS2B/NS3pro-hel in intact cells. To our knowledge, this is the first experimental evidence demonstrating that the WNV NS2B/NS3 protease is active at the ER membrane using intact cells.

2.2.2. In-cell substrate selectivity of WNV NS2B/NS3 protease

Building from our KRG proof-of-concept study, our next goal was to use our cellular assay to test a series of membrane-anchored fluorescent substrates engineered to present the cleavage sequences of the WNV NS polyprotein precursor that was proposed to be proteolytically cleaved by the NS3 protease. *In vitro* studies suggest that the flaviviral protease cleaves the C-terminal side of dibasic residues at protein junctions NS2A/NS2B, NS2B/NS3, NS3/NS4A, and NS4B/NS5. The P6-P1↓P1′-P4′ amino-acid residues found at these protein junctions are DPNRKR↓GWPA, LQYTKR↓GGVL, FASGKR↓SQIG, and KPGLKR↓GGAK, respectively (Figure 2.1B).

We wanted to evaluate the relative *trans*-cleavage endoproteolytic activity of WNV NS2B/NS3pro-hel when tested using an internally consistent set of membrane-anchored substrates. We modified the cleavage sequence of the KRG substrate with several rounds of site-directed mutagenesis to generate substrates containing the P6-P1↓P1′-P4′ amino-acid residues found at these protein junctions (Figure 2.1B; 2A/2B, 2B/3, 3/4A, 4B/5). We then double-transfected substrates with active WNV protease or inactive S135A protease and monitored cleavage with fluorescent microscopy. A diffuse cytoplasmic DsRed protein pattern was only observed with active WNV protease transfected with the 4B/5 substrate (Figure 2.4; WNV-4B/5). All the other protein junction substrates transfected with active WNV protease, as well as substrates transfected with inactive S135A protease and in

substrate-only controls, illustrated a perinuclear punctate DsRed pattern (Figure 2.4). Protease expression was confirmed with immunofluorescent microscopy in active WNV protease and inactive S135A protease samples (data not shown). The results demonstrate that only the NS4B/NS5 protein junction site can be endoproteolytically cleaved efficiently in *trans* by the WNV NS2B/NS3pro-hel under our experimental conditions.

We next examined substrate cleavage with Western blot analysis and observed that the intact substrate migrated at 34 kDa (Figure 2.5A; white arrow) and the DsRed-containing cleavage product migrated at 29 kDa (Figure 2.5A; WNV-black arrow). A faint cleavage band was observed in substrate-only controls and in inactive S135A protease samples (Figure 2.5; thin black arrow). In the active WNV protease samples, the 4B/5 substrate was processed efficiently compared to the other protein junction site substrates tested with 2A/2B substrate being processed the least. Processing of the KRG substrate was comparable to the 4B/5 substrate (Figure 2.5A; WNV).

We subsequently quantified and calculated the percent of substrate cleaved from the Western blots by dividing the lower cleavage band signal by the total signal (uncleaved + cleaved) (Figure 2.5B) (Table 2.1). In the active WNV protease samples, the 4B/5 substrate had a higher percent of cleavage compared to the other substrates tested (2A/2B = 5.0 ± 0.9%; 2B/3 = 16.0 ± 4.3%; 3/4A = 7.5 ± 1.3%; 4B/5 = 34.5 ± 9.3%) (Figure 2.5B; WNV-black bars) with significant differences ($p<0.05$) between 4B/5 compared to 2A/2B and 3/4A substrates as well as between controls (S135A = 7.0 ± 0.7%; substrate-only = 8.2 ± 1.9%) (Figure 2.5B; S135A-grey bar, substrate only-white bar). The other protein junction site substrates tested (2A/2B, 2B/3, and 3/4A) were not significant above inactive S135A protease or substrate-only controls (Figure 2.5B) (Table 2.1). Interestingly, a trend of a

lower percent of substrate cleaved was observed in the inactive S135A protease samples (Figure 2.5B; S135A-grey bars) compared to the substrate-only samples (Figure 2.5B; substrate-only-white bars), suggesting that the inactive WNV S135A protease forms an initial enzyme–substrate complex that could protect the membrane-anchored substrates from being cleaved by host protease(s) (Table 2.1).

In the KRG substrate, significant differences were observed between the active WNV protease compared to the inactive S135A protease and substrate-only samples (WNV = 33.5 ± 8.3%; S135A = 7.7 ± 1.2%; substrate-only = 11.2 ± 0.8%) ($p<0.05$). In the active WNV protease samples, no significant differences were observed between the KRG and 4B/5 substrates. The substrates KRG, 4B/5, and 2B/3 all contain the KR↓GG sequence (Figure 2.1B); however, the 2B/3 substrate was poorly processed compared to the other two (Figure 2.5B) (Table 2.1), suggesting that the other residues present in the cleavage sequences tested have an effect on WNV NS2B/NS3 protease substrate selectivity and/or cleavage efficiency.

2.3. Discussion

In this study, we report novel membrane-anchored fluorescent substrates for detecting the endoproteolytic activity of the full-length WNV NS2B/NS3pro-hel intracellularly. Our results demonstrate that the substrate that corresponds to the NS4B/NS5 junction site was cleaved in *trans* whereas the remaining substrates that correspond to the NS2A/NS2B, NS2B/NS3, and NS3/NS4A proprotein junction sites were poorly processed in *trans* under our experimental conditions. To our knowledge, this is the first demonstration that the WNV NS2B/NS3pro-hel is an active endoproteolytic enzyme at the ER membrane

and the first study reporting the in-cell selectivity profiling of the membrane-anchored flaviviral protease.

Processing of the polyprotein precursor by the NS2B/NS3 protease is essential in the flavivirus life cycle (10), and as such, it has been one of the prime antiviral targets for WNV therapy. Typically, *in vitro* substrate assays are used to assess WNV NS2B/NS3 protease activity using the truncated bacterial-expressed recombinant form of the protease, $NS2B_{40}$-G_4SG_4-NS3pro (30-32, 38, 40, 42-48). Nall et al., (2004) investigated the enzymatic characterization of the WNV recombinant $NS2B_{40}$-G_4SG_4-NS3pro protease *in vitro*. The substrates synthesized were chromogenic hexapeptidyl substrates composed of the P6-P1 residues corresponding to the protein junctions NS2A/NS2B (Ac-DPNRKR-*p*NA), NS2B/NS3 (Ac-LQYTKR-*p*NA), NS3/NS4A (Ac-FASGKR-*p*NA), and NS4B/NS5 (Ac-KPGLKR-*p*NA). The authors ranked the relative substrate processing efficiency based on performance constants (k_{cat}/K_m: $M^{-1}s^{-1}$) as NS3/NS4A (4222 ± 313) > NS4B/NS5 (1827 ± 124) ≥ NS2A/NS2B (1756 ± 96) ≥ NS2B/NS3 (1233 ± 86 units) with NS3/NS4A being cleaved the best and NS2B/NS3 cleaved the least (30).

Shiryaev et al., (2007) examined the substrate recognition pattern of the WNV recombinant protease $NS2B_{40}$-G_4SG_4-NS3pro *in vitro*. They used fluorescent-biotin tagged octapeptidyl substrates composed of the P4-P1↓P1′-P4′ residues spanning several potential cleavage sites within the WNV polyprotein precursor. They demonstrated that the protease was able to cleave substrates corresponding to the NS2B/NS3, NS4B/NS5, and NS2A/NS2B junction sites; however, no cleavage was detected with the NS3/NS4A peptidyl substrate (relative cleavage efficiencies of 73%, 73%, 64%, 0%, respectively) (40).

On the contrary, our results using decapeptidyl subtrates demonstrate that in the

context of the host cell, the 4B/5 substrate is the only membrane-anchored red-shifted fluorescent protein substrate efficiently cleaved in *trans* by WNV NS2B/NS3pro-hel under our experimental conditions (Table 2.1). Interestingly, similar results were demonstrated in a cellular expression system of the related Yellow Fever virus (YFV) (24). Chambers et al., (1991) demonstrated via a vaccinia virus-T7 expression system of YFV that the NS4B/NS5 junction site was efficiently cleaved in *trans* whereas the NS2A/NS2B and NS3/NS4A junctions were inefficiently cleaved. They suggested that perhaps *cis*-cleavage is preferred at these junction sites (24). Taken together, the results suggest that the membrane microenvironment and/or the other nonstructural protein domains not examined *in vitro* (e.g., NS3hel, NS2B N-terminal domain, and NS2B C-terminal domain) contribute to the flaviviral NS3pro enzymatic properties in host cells.

Alternatively, the experimental conditions used to perform the enzymatic tests *in vitro* such as high pH, the addition of glycerol, and detergents - not used in our cell-based *trans*-cleavage assay - could also explain in part the apparent discrepancy between these results obtained using *in vitro* and *in cellulo* enzymatic assays. For example, Ezgimen et al., (2009) recently showed that varying detergents have an effect on the protease activity of WNV. They demonstrated *in vitro* that nonionic detergents such as Triton X-100, Tween, and NP-40 enhanced WNV protease activity 2 to 2.5-fold, ultimately making these detergents unsuitable for drug discovery (49).

Another important difference in the experimental design developed in our *in cellulo* study by contrast to *in vitro* studies is the engineering of an internally consistent set of membrane-anchored fluorescent protein substrates encompassing the amino-acid residues from P6-P1$\downarrow$P1′-P4′ around the scissile peptide bond of the WNV nonstructural polyprotein

precursor cleavage sites. In general, *in vitro* enzymatic tests are performed using tetrapeptidyl or hexapeptidyl substrates based on the NS2B/NS3 protein junction site (32, 35, 40, 42-45). The tetra- and hexa-peptidyl substrates contain a chromogenic or fluorogenic group in the P1′ position; as a consequence, the influence of the residues in the Pn′ position of the cleavage site is not taken into account. Our results obtained using decapeptidyl substrate sequences demonstrated that despite the fact that both the NS2B/NS3 and NS4B/NS5 protein junction sites have the KR↓GG (P2-P1↓P1′-P2′) primary sequence, the 4B/5 substrate was cleaved more efficiently compared to the 2B/3 substrate (Table 2.1). This strongly suggests that the other residues located within the P6-P1↓P1′-P4′ positions around the scissile peptide bond of the substrates have an effect on *trans*-cleavage and that the WNV NS2B/NS3 protease has broader substrate requirements than previously appreciated. The P6-P1↓P1′-P4′ amino-acid residues found at the NS2B/NS3 and NS4B/NS5 junction sites are LQYTKR↓GGVL and KPGLKR↓GGAK, respectively, with differences in amino-acid properties occurring at P6, P5, P3, and P4′, suggesting that these residues affect the enzyme-substrate molecular interactions perhaps favoring the NS4B/NS5 protein junction site to be cleaved in *trans*. Interestingly, It has been reported that mutations of certain residues at the YFV proprotein junction sites affect cleavage efficiency and flaviviral polyprotein processing (50). Furthermore, Chambers et al., (1995) showed that varying substitutions at the P4-P1′ residues of the NS2B/NS3 junction site of the YFV polyprotein precursor reduced or enhanced cleavage efficiency, suggesting that the wild-type residues are not optimal for cleavage by the flaviviral protease (51). In this regard, one might argue that the lack of apparent *trans*-cleavage of the other membrane-anchored fluorescent protein substrates tested in our study may be temporal. Our enzymatic assays were performed at 24

h post-transfection; perhaps this time point may be too early for *trans*-cleavage event to occur efficiently at the other flaviviral proprotein junction sites examined in this study. Taken together, these results underline the importance of the amino-acid residues present at the proprotein cleavage sites for the NS2B/NS3 site-specific mediated cleavage events of the viral polyprotein precursor and the resultant intracellular viral protein molarity of the nonstructural flavivirus endoproteolyic products during WNV replication.

Replication of the flaviviral genome takes place within a membrane-associated replication complex that is composed of the viral protein NS5 (the RNA-dependent RNA polymerase) and the helicase/ATPase domain of NS3 (36). The viral proteins NS1, NS2A, and NS4A are thought to be involved in the replication complex although their exact function is still unclear (36). Using the full-length NS2B and NS3 proteins allows us to study the WNV NS2B/NS3 protease with all protein domains considered, allowing for the proper folding and subcellular localization and the effects of membrane anchoring to be taken into account.

NS3, mostly a hydrophilic protein, is predicted to be associated to the ER membrane through its interaction with NS2B, and NS2B is thought to be membrane-associated via its hydrophobic domains (Figure 2.1C) (6, 11). Clum et al., (1997) examined the effects of membranes on the viral protease of the related Dengue virus. They demonstrated that the addition of microsomal membranes *in vitro* enhanced the activity of the protease. They concluded that the membrane association of the NS2B protein might influence the activity of the NS3 protease (26). In this study, we observed a difference in substrate selectivity compared to *in vitro* conditions, which may be attributed in part to the intracellular microenvironment, such as the interplay of membranes on the proper folding and/or function

of the WNV NS2B/NS3 heterocomplex serine protease.

In conclusion, we report a novel series of internally consistent sets of ER membrane-anchored red-shifted fluorescent substrates to examine the membrane-associated WNV NS2B/NS3 endoproteolytic activity in host cells. The results of our in-cell selectivity profiling of the full-length WNV NS2B/NS3 serine protease reveal that the viral protease behaves differently within the complex intracellular environment of the host cell compared to *in vitro* conditions, emphasizing the need for cell-based assays for studying flaviviral induced-fit proteases, such as the one described in this report. This assay is an invaluable tool that will significantly advance our understanding of WNV protease biology and allow for the biochemical characterization of the full-length NS2B/NS3pro-hel heterocomplex serine protease in a more physiologically relevant environment. Furthermore, the information obtained will be useful for the rational design of specific flaviviral NS2B/NS3 protease inhibitors that in turn can be validated in our novel cell-based assay.

2.4. Material and methods

2.4.1. Construction of plasmids expressing WNV full-length NS2B/NS3pro-hel

Total RNA was extracted from a WNV bird sample (a kind gift from Dr. Michael A. Drebot, National Microbiology Laboratory, Public Health Agency of Canada) with an RNeasy Kit (Qiagen, Mississauga, ON, CA). cDNA was made and the full-length NS2B/NS3pro-hel was cloned into pFLAG-myc-CMV™-20 Expression Vector (Sigma, St-Louis, MO, USA) using the EcoRI and XbaI restriction sites (Forward primer: 5'-CGCGAATTCAGGATGGCCCGCAACT-3'; Reverse primer: 5'-CCTCTAGAACGTTTTCCCGAGGC-3'; EcoRI and XbaI restriction sites underlined,

respectively). Wild-type NS2B/NS3pro-hel was indicated as active WNV protease (Figure 2.1A). An alanine mutation was generated with site-directed mutagenesis (Stratagene, La Jolla, CA, USA) within the N-terminal serine protease domain of NS3 at the catalytic triad residue serine 135 (S135A) (11, 19, 31). Mutation was confirmed by automated sequencing (UBC DNA Sequencing Laboratory, Vancouver, BC, CA). The S135A mutant was indicated as inactive S135A protease (Figure 2.1A).

2.4.2. Construction of substrate plasmids expressing WNV nonstructural polyprotein precursor cleavage sites

The parent substrate plasmid contained an ER membrane-anchoring domain (Tm) (N-terminal amphipathic α-helix of HCV NS5A protein amino acid residues 1-34), a protease-specific cleavage sequence that includes the P6-P1↓P1′-P4′ residues (33), and a fluorescent reporter group (DsRed-Express, referred to as "DsRed"), as has been reported previously (18). pTm-DSSTPS↓SGSW-DsRed was sequentially mutated with site-directed mutagenesis (Stratagene) to generate the substrate plasmid, pTm- DSST**KR↓G**GSW-DsRed (designated: KRG) (Figure 2.1B). The KRG substrate plasmid was sequentially mutated with site-directed mutagenesis (Stratagene) to generate substrate plasmids containing cleavage sequences corresponding to the protein junctions that are cleaved by the WNV NS2B/NS3 protease within the polyprotein precursor: NS2A/NS2B (pTm-DPNRKR↓GWPA-DsRed), NS2B/NS3 (pTm-LQYTKR↓GGVL-DsRed), NS3/NS4A (pTm-FASGKR↓SQIG-DsRed), and NS4B/NS5 (pTm-KPGLKR↓GGAK-DsRed) (Figure 2.1B). All mutations were confirmed by sequencing (UBC DNA Sequencing Laboratory).

2.4.3. Cell culture

Human hepatocellular carcinoma cells (Huh7 cells) were grown in complete Dulbecco's modified Eagle's medium [DMEM cat no. 11965-092, Gibco, Invitrogen (Burlington, ON, CA)] supplemented with heat-inactivated 10% v/v fetal bovine serum (Invitrogen), 50 units/ml penicillin, 50 μg/ml streptomycin, and 100 μM non-essential amino acids (Invitrogen). Cells were grown at 37ºC in the presence of 5% CO_2.

2.4.4. Fluorescence and immunofluorescence microscopy

Huh7 cells were seeded in 24-well plates on top of a glass coverslip at 20 000 cells/well and grown for 2 d until approximately 60% confluent. Huh7 cells were double-transfected with 1.0 μg of active WNV protease plasmid and 1.0 μg of each substrate plasmid using *Trans*IT-LT1 transfection reagent (Mirus Bio, Madison, WI, USA). Controls included double-transfection of Huh7 cells with 1.0 μg of inactive S135A protease and 1.0 μg of each substrate plasmid or single-transfection with 1.0 μg of substrate plasmid. All processing steps were done at room temperature unless otherwise noted. 24 h post-transfection, cells were washed two times with 0.5 ml PBS and fixed in 3.8% v/v formaldehyde (Fischer Scientific, Pittsburg, PA, USA) in PBS (30 min). Cells were rinsed two times with 0.5 ml PBS. For immunofluorescent microscopy, cells were permeabilized in 0.5 ml PBS containing 0.05% w/v saponin (PBS-S) (Sigma-Aldrich Corp., St-Louis, MO, USA) (30 min). Cells were blocked in 0.2 ml of PBS-S containing 3% w/v bovine serum albumin (BSA) (Sigma-Aldrich Corp.) (30 min). For the lipid droplet marker, primary anti-ADRP (adipocyte differentiation-related protein) monoclonal antibody was added directly to cells (ready to use, Progen, Heidelberg, Germany) (60 min). The other primary and all

secondary antibodies were diluted in PBS-S containing 3% BSA. For the ER membrane marker, primary anti-calnexin polyclonal antibody was added to cells (1:100, Sigma-Aldrich Corp) (60 min). For protease detection, cells were probed with primary anti-myc monoclonal antibody (1:100, Stratagene) (60 min). Cells were then washed six times with 0.5 ml PBS-S. Cells were probed with secondary Alexa Fluor-488-conjugated donkey anti-mouse monoclonal antibody or Alexa Fluor-488-conjugated donkey anti-rabbit polyclonal antibody (1:100, Molecular Probes, Invitrogen) (60 min). Cells were washed three times with 0.5 ml PBS-S, then three times with 0.5 ml PBS. Nuclei were stained using 0.5 ml Hoechst stain (Invitrogen) (5 μg/ml, 15 min). Cells were washed three times with 0.5 ml PBS, then two times with 0.5 ml HPLC water (Sigma). Coverslips were removed from 24-well plates and air-dried. Coverslips were mounted with mounting solution containing 2.5% w/v DABCO (1,4-Diazabicyclo[2.2.2]octane, Sigma-Aldrich Corp.) in 1:10 buffered glycerol and sealed with clear nail polish. Images were acquired using either a Leica TCS-SP5 confocal microscope (Leica Microsystems) or an Olympus Fluoview FV1000 laser scanning confocal microscope (Olympus Corporation).

2.4.5. Transfections and Western blotting

Six well plates were seeded with Huh7 cells at 200 000 cells/well and grown for 3 d until approximately 80% confluent. Huh7 cells were double-transfected with 2.5 μg of active WNV protease plasmid and 2.5 μg of each substrate plasmid using *Trans*IT-LT1 Transfection Reagent (Mirus Bio). Controls included double-transfection of Huh7 cells with 2.5 μg of inactive S135A protease and 2.5 μg of each substrate plasmid or single-transfection with 2.5 μg of substrate plasmid. 24 h post-transfection, cells were placed on ice

and washed with 3 ml of phosphate-buffered saline containing 1x protease inhibitor cocktail (PBS-PI) [EDTA-free Complete Protease Inhibitor, Roche (Laval, QC, CA)]. Cells were harvested by scraping in 0.5 ml PBS-PI, pelleted (16 110 *g*, 1 min, 4°C), then frozen (-86°C) for Western blot analysis. Cell pellets were re-suspended in 0.2 ml hypotonic lysis buffer (20 mM Tris pH 7.4, 10 mM $MgCl_2$, 10 mM $CaCl_2$) containing 1x protease inhibitor cocktail (Roche). Cells were placed on ice and vortexed every 5 min for a total of 15 min. Fifteen microliters of sample was removed, added to 15 μL of 2x SDS-PAGE sample buffer (0.1 M Tris pH 6.8, 20% v/v glycerol, 4% w/v SDS, 0.002% w/v bromophenol blue, 0.7 M 2-mercaptoethanol), and boiled (10 min, 95°C). Twenty microliters of sample was resolved on a 12% SDS-polyacrylamide gel (110 V, 90 min) and transferred to a nitrocellulose membrane (25 V, 60 min) using a semi-dry electrophoretic transfer system (Bio-Rad Laboratories, Mississauga, ON, CA). Membranes were rinsed three times in PBS and blocked with Odyssey Blocking Buffer (LI-COR Biosciences, Lincoln, NE, USA) (60 min). The membranes were probed according to Odyssey Infrared Imaging System Western blot analysis protocol (LI-COR Biosciences).

Primary and secondary antibodies were diluted in Odyssey Blocking Buffer (LI-COR Biosciences) containing 0.1% v/v Tween-20 (Sigma-Aldrich Corp.). Membranes were probed with primary anti-DsRed polyclonal antibody (1:1 000, Clontech Laboratories, Mountain View, CA, USA) (60 min). Membranes were washed six times with PBS containing 0.1% v/v Tween-20. Membranes were probed with secondary IRDye 680-conjugated goat anti-rabbit polyclonal antibody (1:10 000, LI-COR Biosciences) (30 min). Membranes were washed six times with PBS containing 0.1% v/v Tween-20, then imaged using an Odyssey Infrared Imaging System (LI-COR Biosciences).

2.4.6. Quantification and statistical analysis

Analysis and quantification of integrated band intensity were performed using the Odyssey Infrared Imaging System application software version 2.1.12 (LI-COR Biosciences). The percent of substrate cleaved was calculated by dividing the cleaved signal by the total signal (cleaved plus uncleaved), thereby normalizing the readout for each sample. Averages were calculated from four independent experiments run in duplicate. GraphPad Prism (GraphPad Software, Inc., La Jolla, CA, USA) was used for graphical representation and statistical analysis. P values were obtained for two-tailed, unpaired, student's *t*-test, and significance was noted when $p<0.05$.

Figure 2.1. Cell-based *trans*-cleavage assay for the detection of the full-length WNV NS2B/NS3pro-hel endoproteolytic activity

(A) Schematic of WNV protease plasmids. The full-length NS2B/NS3 was cloned into the pFLAG-myc-CMV™-20 Expression Vector. Serine 135 within the catalytic triad of NS3 was mutated to alanine. Wild-type NS2B/NS3 protease is referred to as active WNV protease and the S135A mutant is referred to as inactive S135A protease. (B) Schematic of substrate plasmids. Each substrate plasmid contains the ER membrane-anchoring domain (Tm), a specific cleavage sequence (CS) that includes the P6-P1↓P1′-P4′ residues and a fluorescent reporter group (DsRed). The KRG substrate was generated from the pTm-DSSTPS↓SGSW-DsRed plasmid reported previously (18). The WNV junction site substrate plasmids were generated from the KRG substrate plasmid and correspond to the protein junction sites NS2A/NS2B (2A/2B), NS2B/NS3 (2B/3), NS3/4A (3/4A), and NS4B/NS5 (4B/5). (C) Schematic representation of the membrane-anchored cell-based fluorescent substrate assay. Protein topology is depicted respective to the ER membrane. The WNV NS2B/NS3 protease associates with the ER membrane through the hydrophobic domains of NS2B. Intact substrate produces a perinuclear punctate DsRed protein pattern at the ER membrane. Upon cleavage sequencing processing, DsRed is released from the ER membrane, resulting in a diffuse cytoplasmic DsRed protein pattern. Change in protein location can be monitored with fluorescent microscopy.

Figure 2.1

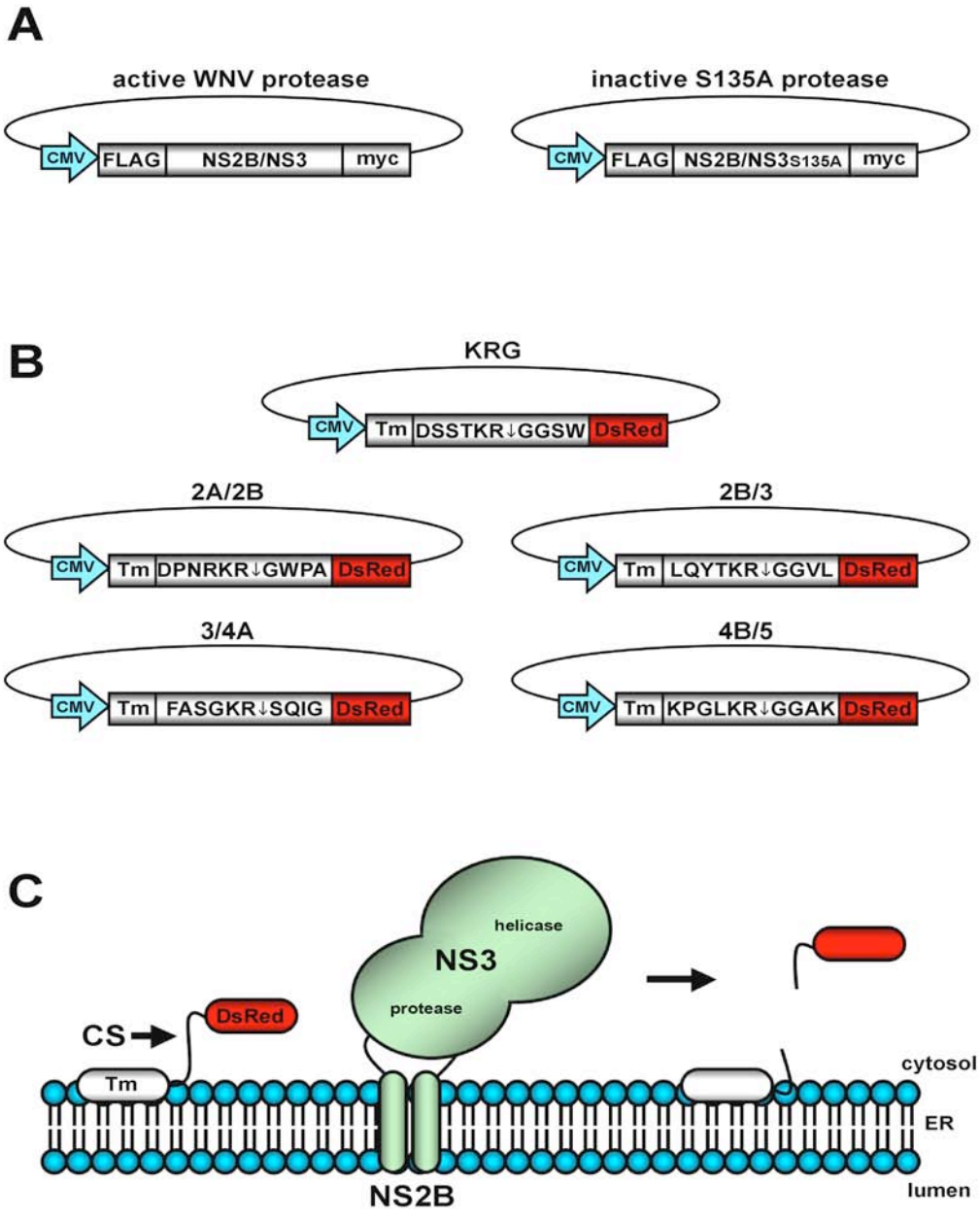
A
active WNV protease
CMV
FLAG
NS2B/NS3
myc
inactive S135A protease
CMV
FLAG
NS2B/NS3S135A
myc
B
KRG
CMV
Tm
DSSTKR↓GGSW
DsRed
2A/2B
CMV
Tm
DPNRKR↓GWPA
DsRed
2B/3
CMV
Tm
LQYTKR↓GGVL
DsRed
3/4A
CMV
Tm
FASGKR↓SQIG
DsRed
4B/5
CMV
Tm
KPGLKR↓GGAK
DsRed
C
helicase
NS3
protease
CS
DsRed
Tm
cytosol
ER
lumen
NS2B

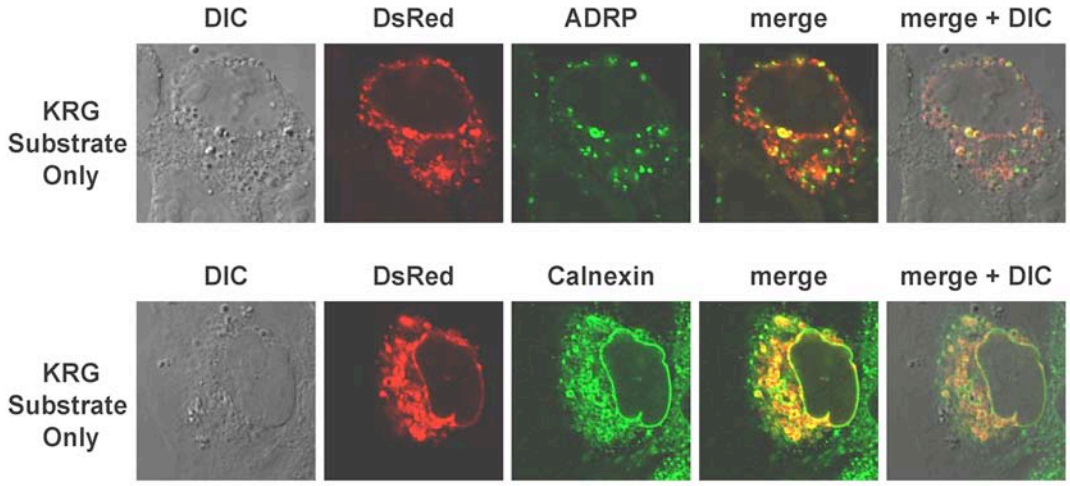

Figure 2.2. Localization of KRG substrate

Huh7 cells were transfected with the KRG substrate and fixed 24 h post-transfection. Cells were probed with either a lipid droplet maker (anti-ADRP monoclonal antibody) or an ER membrane marker (anti-calnexin polyclonal antibody). The KRG substrate DsRed protein pattern was observed using the DsRed signal. Shown is KRG substrate with lipid droplet marker ADRP (top row) and KRG substrate with ER membrane marker calnexin (bottom row). DIC (differential interference contrast) was acquired at time of imaging (first column-DIC); the KRG substrate DsRed protein pattern (second column-DsRed) (shown in red); lipid droplet and ER membrane marker (third column-ADRP or -calnexin, respectively) (shown in green); merged DsRed and lipid droplet or ER membrane marker (fourth column-merge); merged DsRed, lipid droplet, or ER membrane marker and DIC (last column-merge + DIC). Cells were imaged using a Leica TCS-SP5 confocal microscrope (Leica Microsystems).

Figure 2.3

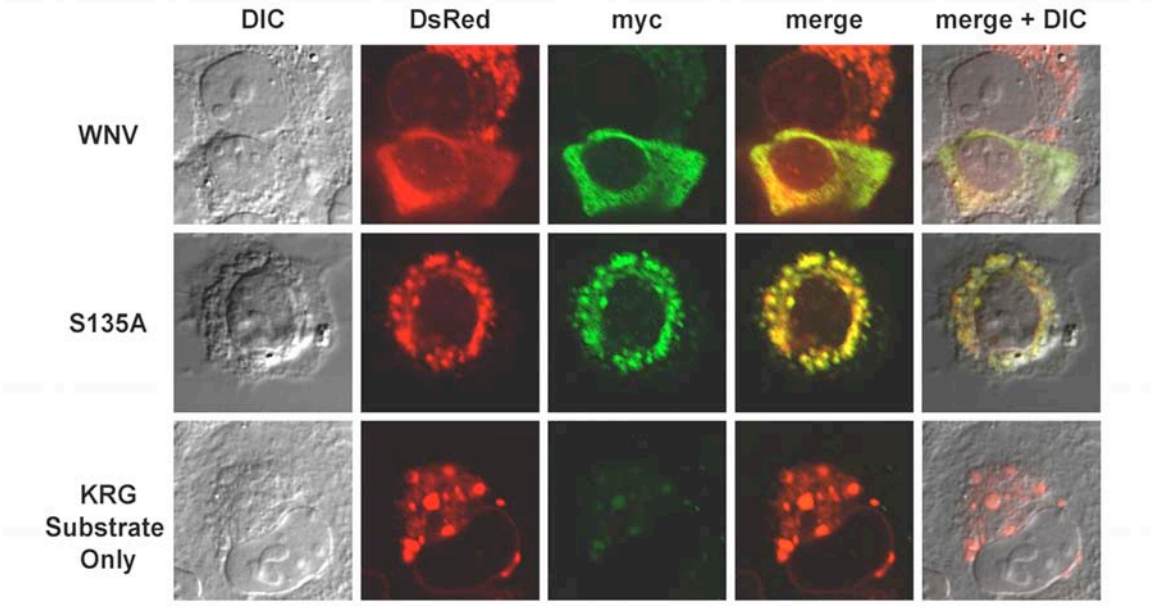

Figure 2.3. Proof-of-concept: active WNV protease is able to cleave substrate at the ER membrane

Huh7 cells were double-transfected with KRG substrate and either active WNV protease or with inactive S135A protease, or singly-transfected with KRG substrate. 24 h post-transfection, cells were fixed and protease was probed for with anti-myc monoclonal antibody. Processing of the substrate cleavage sequence by the NS2B/NS3 protease was monitored using the DsRed signal. Shown are active WNV protease with KRG substrate (top row), inactive S135A protease with KRG substrate (middle row), and KRG substrate-only control (bottom row). DIC (differential interference contrast) was acquired at time of imaging (first column-DIC). Processing of substrate cleavage sequence (second column-DsRed) (shown in red); protease probe (third column-myc) (shown in green); merged DsRed and myc signal (fourth column-merge); merged DsRed, myc, and DIC (last column-merge + DIC). Cells were imaged with a Leica TCS-SP5 confocal microscope (Leica Microsystems).

Figure 2.4. *Trans*-cleavage of fluorescent substrates containing WNV protein junction site sequences

Huh7 cells were double-transfected with WNV junction site substrates and either active WNV protease or with inactive S135A protease, or singly with substrate. 24 h post-transfection, cells were fixed and processing of the substrate cleavage sequence was monitored with the DsRed signal (shown in red). Shown are active WNV protease with substrate (top row-WNV), inactive S135A protease with substrate (middle row-S135A), and substrate-only controls (bottom row-substrate-only). Substrates correspond to the WNV protein junction sites NS2A/NS2B (first column-2A/2B), NS2B/NS3 (second column-2B/3), NS3/4A (third column-3/4A), and the NS4B/NS5 (fourth column-4B/5). Nuclei were visualized with Hoechst staining (shown in blue). Cells were imaged with an Olympus Fluoview scanning confocal microscope (Olympus Corporation).

Figure 2.4

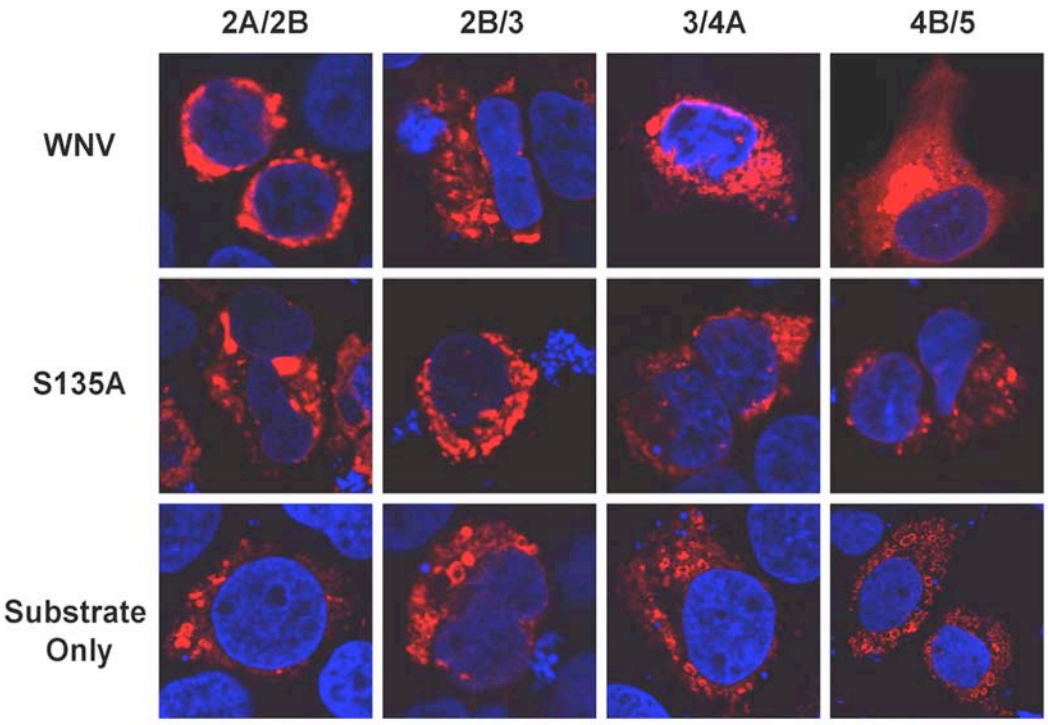

Figure 2.5. In-cell substrate selectivity profiling of WNV NS2B/NS3 protease

(A) *Trans*-cleavage of fluorescent substrates detected by Western blot analysis. Huh7 cells were double-transfected with active WNV protease and each substrate, or with inactive S135A protease and each substrate, or singly-transfected with substrate only. 24 h post-transfection, cells were harvested and whole cell lysates were probed by Western blotting using the anti-DsRed polyclonal antibody. Intact substrate was detected at 34 kDa (white arrow), and cleaved substrate was detected at 29 kDa (black arrow). Shown are active WNV protease with substrate (top row), inactive S135A protease with substrate (middle row), and substrate-only controls (bottom row). Substrates correspond to the KRG substrate (first column-KRG) and the WNV protein junction sites NS2A/NS2B (second column-2A/2B), NS2B/NS3 (third column-2B/3), NS3/4A (fourth column-3/4A), and the NS4B/NS5 (last column-4B/5). (B) Quantification of Western blot analysis. Depicted are percent of substrate cleaved (y-axis). Substrates correspond to the KRG substrate and the WNV protein junction site substrates, 2A/2B, 2B/3, 3/4A, and 4B/5 (x-axis). Active WNV protease samples (black bars), inactive S135A protease samples (grey bars), and substrate-only samples (white bars). Results shown are the average of four independent experiments run in duplicate. Significance was noted in samples having differences in substrates with active WNV protease compared to substrate with inactive S135A protease and substrate-only controls (*$p<0.05$).

Figure 2.5

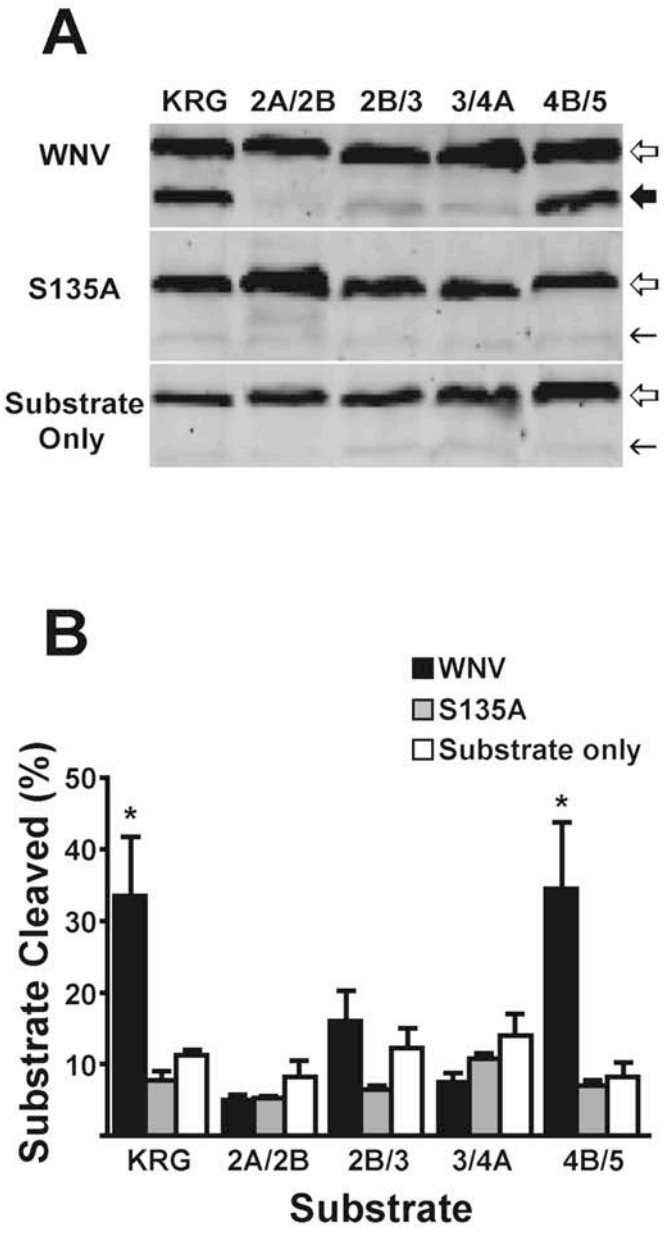
A
KRG
2A/2B
2B/3
3/4A
4B/5
WNV
S135A
Substrate Only
B
WNV
S135A
Substrate only
Substrate Cleaved (%)
50
40
30
20
10
*
*
KRG
2A/2B
2B/3
3/4A
4B/5
Substrate

Table 2.1

Protease	Substrate				
	KRG	2A/2B	2B/3	3/4A	4B/5
WNV	33.5 ± 8.3*	5.0 ± 0.9	16.0 ± 4.3	7.5 ± 1.3	34.5 ± 9.3*
S135A	7.7 ± 1.2	5.2 ± 0.2	6.5 ± 0.6	10.7 ± 0.7	7.0 ± 0.7
Substrate-only	11.2 ± 0.8	8.2 ± 2.2	12.2 ± 2.6	14.0 ± 2.9	8.2 ± 1.9

Table 2.1. Percent of substrate cleaved

Listed are the percent of substrate cleaved as quantified from Western blotting (Figure 2.5). Percentages were calculated from the average of four independent duplicate experiments. Significance was noted in samples having differences in substrates with active WNV protease compared to substrate with inactive S135A protease and substrate-only controls (*$p<0.05$). Statistical analysis was performed with a two-tailed, unpaired, student's *t*-test.

2.5. References

1. (CDC), C. o. D. C. a. P. 1999. Outbreak of West Nile-like viral encephalitis--New York, 1999. *MMWR Morb Mortal Wkly Rep* 48:845-849.
2. Drebot, M. A., R. Lindsay, I. K. Barker, P. A. Buck, M. Fearon, F. Hunter, P. Sockett, and H. Artsob. 2003. West Nile virus surveillance and diagnostics: A Canadian perspective. *Can J Infect Dis* 14:105-114.
3. Castle, E., T. Nowak, U. Leidner, and G. Wengler. 1985. Sequence analysis of the viral core protein and the membrane-associated proteins V1 and NV2 of the flavivirus West Nile virus and of the genome sequence for these proteins. *Virology* 145:227-236.
4. Castle, E., U. Leidner, T. Nowak, and G. Wengler. 1986. Primary structure of the West Nile flavivirus genome region coding for all nonstructural proteins. *Virology* 149:10-26.
5. Yamshchikov, V. F., and R. W. Compans. 1993. Regulation of the late events in flavivirus protein processing and maturation. *Virology* 192:38-51.
6. Lindenbach, B. D., H. Thiel, and C. M. Rice. 2007. Flaviviridae: The viruses and their replication. In *Fields Virology*, 5 ed. D. M. Knipe, and P. M. Howley, eds. Lippincott William and Wilkins, Philadelphia.
7. Brinton, M. A. 2002. The molecular biology of West Nile Virus: a new invader of the western hemisphere. *Annu Rev Microbiol* 56:371-402.
8. Castle, E., and G. Wengler. 1987. Nucleotide sequence of the 5'-terminal untranslated part of the genome of the flavivirus West Nile virus. *Arch Virol* 92:309-313.

9. Rice, C. M., E. M. Lenches, S. R. Eddy, S. J. Shin, R. L. Sheets, and J. H. Strauss. 1985. Nucleotide sequence of yellow fever virus: implications for flavivirus gene expression and evolution. *Science* 229:726-733.

10. Chambers, T. J., R. C. Weir, A. Grakoui, D. W. McCourt, J. F. Bazan, R. J. Fletterick, and C. M. Rice. 1990. Evidence that the N-terminal domain of nonstructural protein NS3 from yellow fever virus is a serine protease responsible for site-specific cleavages in the viral polyprotein. *Proc Natl Acad Sci U S A* 87:8898-8902.

11. Wengler, G., G. Czaya, P. M. Farber, and J. H. Hegemann. 1991. In vitro synthesis of West Nile virus proteins indicates that the amino-terminal segment of the NS3 protein contains the active centre of the protease which cleaves the viral polyprotein after multiple basic amino acids. *J Gen Virol* 72 (Pt 4):851-858.

12. Cahour, A., B. Falgout, and C. J. Lai. 1992. Cleavage of the dengue virus polyprotein at the NS3/NS4A and NS4B/NS5 junctions is mediated by viral protease NS2B-NS3, whereas NS4A/NS4B may be processed by a cellular protease. *J Virol* 66:1535-1542.

13. Amberg, S. M., A. Nestorowicz, D. W. McCourt, and C. M. Rice. 1994. NS2B-3 proteinase-mediated processing in the yellow fever virus structural region: in vitro and in vivo studies. *J Virol* 68:3794-3802.

14. Falgout, B., and L. Markoff. 1995. Evidence that flavivirus NS1-NS2A cleavage is mediated by a membrane-bound host protease in the endoplasmic reticulum. *J Virol* 69:7232-7243.

15. Yu, I. M., W. Zhang, H. A. Holdaway, L. Li, V. A. Kostyuchenko, P. R. Chipman,

R. J. Kuhn, M. G. Rossmann, and J. Chen. 2008. Structure of the immature dengue virus at low pH primes proteolytic maturation. *Science* 319:1834-1837.

16. Richer, M. J., L. Juliano, C. Hashimoto, and F. Jean. 2004. Serpin mechanism of hepatitis C virus nonstructural 3 (NS3) protease inhibition: induced fit as a mechanism for narrow specificity. *J Biol Chem* 279:10222-10227.

17. Hamill, P., and F. Jean. 2005. Enzymatic characterization of membrane-associated hepatitis C virus NS3-4A heterocomplex serine protease activity expressed in human cells. *Biochemistry* 44:6586-6596.

18. Martin, M. M., and F. Jean. 2006. Single-cell resolution imaging of membrane-anchored hepatitis C virus NS3/4A protease activity. *Biol Chem* 387:1075-1080.

19. Bazan, J. F., and R. J. Fletterick. 1989. Detection of a trypsin-like serine protease domain in flaviviruses and pestiviruses. *Virology* 171:637-639.

20. Gorbalenya, A. E., A. P. Donchenko, E. V. Koonin, and V. M. Blinov. 1989. N-terminal domains of putative helicases of flavi- and pestiviruses may be serine proteases. *Nucleic Acids Res* 17:3889-3897.

21. Gorbalenya, A. E., E. V. Koonin, A. P. Donchenko, and V. M. Blinov. 1989. Two related superfamilies of putative helicases involved in replication, recombination, repair and expression of DNA and RNA genomes. *Nucleic Acids Res* 17:4713-4730.

22. Wengler, G. 1991. The carboxy-terminal part of the NS 3 protein of the West Nile flavivirus can be isolated as a soluble protein after proteolytic cleavage and represents an RNA-stimulated NTPase. *Virology* 184:707-715.

23. Brinkworth, R. I., D. P. Fairlie, D. Leung, and P. R. Young. 1999. Homology model of the dengue 2 virus NS3 protease: putative interactions with both substrate and

NS2B cofactor. *J Gen Virol* 80 (Pt 5):1167-1177.

24. Chambers, T. J., A. Grakoui, and C. M. Rice. 1991. Processing of the yellow fever virus nonstructural polyprotein: a catalytically active NS3 proteinase domain and NS2B are required for cleavages at dibasic sites. *J Virol* 65:6042-6050.

25. Chambers, T. J., A. Nestorowicz, S. M. Amberg, and C. M. Rice. 1993. Mutagenesis of the yellow fever virus NS2B protein: effects on proteolytic processing, NS2B-NS3 complex formation, and viral replication. *J Virol* 67:6797-6807.

26. Clum, S., K. E. Ebner, and R. Padmanabhan. 1997. Cotranslational membrane insertion of the serine proteinase precursor NS2B-NS3(Pro) of dengue virus type 2 is required for efficient in vitro processing and is mediated through the hydrophobic regions of NS2B. *J Biol Chem* 272:30715-30723.

27. Yusof, R., S. Clum, M. Wetzel, H. M. Murthy, and R. Padmanabhan. 2000. Purified NS2B/NS3 serine protease of dengue virus type 2 exhibits cofactor NS2B dependence for cleavage of substrates with dibasic amino acids in vitro. *J Biol Chem* 275:9963-9969.

28. Wengler, G., T. Nowak, and E. Castle. 1990. Description of a procedure which allows isolation of viral nonstructural proteins from BHK vertebrate cells infected with the West Nile flavivirus in a state which allows their direct chemical characterization. *Virology* 177:795-801.

29. Yamshchikov, V. F., D. W. Trent, and R. W. Compans. 1997. Upregulation of signalase processing and induction of prM-E secretion by the flavivirus NS2B-NS3 protease: roles of protease components. *J Virol* 71:4364-4371.

30. Nall, T. A., K. J. Chappell, M. J. Stoermer, N. X. Fang, J. D. Tyndall, P. R. Young,

and D. P. Fairlie. 2004. Enzymatic characterization and homology model of a catalytically active recombinant West Nile virus NS3 protease. *J Biol Chem* 279:48535-48542.

31. Chappell, K. J., T. A. Nall, M. J. Stoermer, N. X. Fang, J. D. Tyndall, D. P. Fairlie, and P. R. Young. 2005. Site-directed mutagenesis and kinetic studies of the West Nile Virus NS3 protease identify key enzyme-substrate interactions. *J Biol Chem* 280:2896-2903.

32. Shiryaev, S. A., A. E. Aleshin, B. I. Ratnikov, J. W. Smith, R. C. Liddington, and A. Y. Strongin. 2007. Expression and purification of a two-component flaviviral proteinase resistant to autocleavage at the NS2B-NS3 junction region. *Protein Expr Purif* 52:334-339.

33. Schechter, I., and A. Berger. 1967. On the size of the active site in proteases. I. Papain. *Biochem Biophys Res Commun* 27:157-162.

34. Yamshchikov, V. F., and R. W. Compans. 1994. Processing of the intracellular form of the west Nile virus capsid protein by the viral NS2B-NS3 protease: an in vitro study. *J Virol* 68:5765-5771.

35. Chernov, A. V., S. A. Shiryaev, A. E. Aleshin, B. I. Ratnikov, J. W. Smith, R. C. Liddington, and A. Y. Strongin. 2008. The two-component NS2B-NS3 proteinase represses DNA unwinding activity of the West Nile virus NS3 helicase. *J Biol Chem* 283:17270-17278.

36. Uchil, P. D., and V. Satchidanandam. 2003. Architecture of the flaviviral replication complex. Protease, nuclease, and detergents reveal encasement within double-layered membrane compartments. *J Biol Chem* 278:24388-24398.

37. Chambers, T. J., C. S. Hahn, R. Galler, and C. M. Rice. 1990. Flavivirus genome organization, expression, and replication. *Annu Rev Microbiol* 44:649-688.

38. Bera, A. K., R. J. Kuhn, and J. L. Smith. 2007. Functional characterization of cis and trans activity of the Flavivirus NS2B-NS3 protease. *J Biol Chem* 282:12883-12892.

39. Grakoui, A., D. W. McCourt, C. Wychowski, S. M. Feinstone, and C. M. Rice. 1993. Characterization of the hepatitis C virus-encoded serine proteinase: determination of proteinase-dependent polyprotein cleavage sites. *J Virol* 67:2832-2843.

40. Shiryaev, S. A., I. A. Kozlov, B. I. Ratnikov, J. W. Smith, M. Lebl, and A. Y. Strongin. 2007. Cleavage preference distinguishes the two-component NS2B-NS3 serine proteinases of Dengue and West Nile viruses. *Biochem J* 401:743-752.

41. Hinson, E. R., and P. Cresswell. 2009. The antiviral protein, viperin, localizes to lipid droplets via its N-terminal amphipathic alpha-helix. *Proc Natl Acad Sci U S A* 106:20452-20457.

42. Chappell, K. J., M. J. Stoermer, D. P. Fairlie, and P. R. Young. 2006. Insights to substrate binding and processing by West Nile Virus NS3 protease through combined modeling, protease mutagenesis, and kinetic studies. *J Biol Chem* 281:38448-38458.

43. Shiryaev, S. A., B. I. Ratnikov, A. V. Chekanov, S. Sikora, D. V. Rozanov, A. Godzik, J. Wang, J. W. Smith, Z. Huang, I. Lindberg, M. A. Samuel, M. S. Diamond, and A. Y. Strongin. 2006. Cleavage targets and the D-arginine-based inhibitors of the West Nile virus NS3 processing proteinase. *Biochem J* 393:503-511.

44. Shiryaev, S. A., B. I. Ratnikov, A. E. Aleshin, I. A. Kozlov, N. A. Nelson, M. Lebl, J. W. Smith, R. C. Liddington, and A. Y. Strongin. 2007. Switching the substrate

specificity of the two-component NS2B-NS3 flavivirus proteinase by structure-based mutagenesis. *J Virol* 81:4501-4509.

45. Chappell, K. J., M. J. Stoermer, D. P. Fairlie, and P. R. Young. 2007. Generation and characterization of proteolytically active and highly stable truncated and full-length recombinant West Nile virus NS3. *Protein Expr Purif* 53:87-96.

46. Chappell, K. J., M. J. Stoermer, D. P. Fairlie, and P. R. Young. 2008. Mutagenesis of the West Nile virus NS2B cofactor domain reveals two regions essential for protease activity. *J Gen Virol* 89:1010-1014.

47. Chappell, K. J., M. J. Stoermer, D. P. Fairlie, and P. R. Young. 2008. West Nile Virus NS2B/NS3 protease as an antiviral target. *Curr Med Chem* 15:2771-2784.

48. Radichev, I., S. A. Shiryaev, A. E. Aleshin, B. I. Ratnikov, J. W. Smith, R. C. Liddington, and A. Y. Strongin. 2008. Structure-based mutagenesis identifies important novel determinants of the NS2B cofactor of the West Nile virus two-component NS2B-NS3 proteinase. *J Gen Virol* 89:636-641.

49. Ezgimen, M. D., N. H. Mueller, T. Teramoto, and R. Padmanabhan. 2009. Effects of detergents on the West Nile virus protease activity. *Bioorg Med Chem* 17:3278-3282.

50. Lin, C., T. J. Chambers, and C. M. Rice. 1993. Mutagenesis of conserved residues at the yellow fever virus 3/4A and 4B/5 dibasic cleavage sites: effects on cleavage efficiency and polyprotein processing. *Virology* 192:596-604.

51. Chambers, T. J., A. Nestorowicz, and C. M. Rice. 1995. Mutagenesis of the yellow fever virus NS2B/3 cleavage site: determinants of cleavage site specificity and effects on polyprotein processing and viral replication. *J Virol* 69:1600-1605.

Chapter 3

West Nile virus NS2B protein has a dual function in NS3 protease activity[2]

[2] **A version of this chapter will be submitted for publication:** Condotta, SA, MM Martin, M Boutin, F Jean. (2010) West Nile virus NS2B protein has a dual function in NS3 protease activity.

3.1. Introduction

West Nile virus (WNV) was first reported in the Western Hemisphere in New York State in 1999 (1). Since its introduction to North America, it has spread throughout the continent and has become a serious public health problem for which there are no vaccines or antiviral therapies currently available. WNV is a small (~50 nm) enveloped virus that contains a positive-sense, single-stranded RNA genome that is classified in the *Flaviviridae* family, genus *flavivirus* (2-5). The viral genome is translated following membrane fusion and nucleocapsid uncoating into a single polyprotein precursor (6). The polyprotein precursor is composed of ten viral proteins, three of which are structural (capsid (C), premembrane (prM), and envelope (E)) and seven that are nonstructural (NS1, NS2A, NS2B, NS3, NS4A, NS4B, NS5) arranged in the following order: 5′-UTR-C-prM-E-NS1-NS2A-NS2B-NS3-NS4A-NS4B-NS5-UTR-3′ (2, 3, 6-8). The polyprotein precursor is proteolytically processed by host proteases and the viral protease heterocomplex, NS2B/NS3 (9-12). These processing events are essential for virus life cycle (9), making the viral protease heterocomplex an attractive antiviral target.

The viral protease heterocomplex is composed of two viral proteins, NS2B and NS3. NS3 is a large protein (70 kDa) comprised of 619 amino acids (5, 6). It is a bifunctional enzyme that contains a serine protease domain in the N-terminus (amino acids 1-180; catalytic triad H51, D75, S135) and a helicase/ATPase domain in the C-terminus (10, 13-15). Hydrophobicity profiles of the full-length NS3 predict the protein to be cytoplasmic, and it has been proposed that NS3 is tethered to the endoplasmic reticulum (ER) membrane through its interaction with NS2B (5). NS2B is a small viral protein (15 kDa) comprised of 131 amino acids (5, 6). Hydrophobicity profiles of the full-length NS2B illustrate three

distinct regions, a hydrophobic region in the N-terminus (I), a central hydrophilic region (II) and a hydrophobic region in the C-terminus (III); the hydrophobic regions are thought to anchor NS2B to the ER membrane (5, 16-19). An autocatalytic cleavage event occurs at the NS2B↓NS3 protein junction within the NS2B/NS3 protease heterocomplex (20, 21).

The serine protease, NS3, from of the related Hepatitis C virus (HCV) (*Flaviviridae*: *hepacivirus)*, requires interactions with another HCV viral protein, NS4A, for enzymatic activity indicating that the NS4A protein acts as a cofactor to NS3 (22-25). It has been suggested that the WNV NS2B behaves in a similar manner acting as a cofactor for NS3 protease activity (17, 19, 26-28). While many *in vitro* studies have demonstrated that NS2B is required for protease activity its precise role remains controversial. Deletion studies have demonstrated that 40 amino acids from the central hydrophilic region of NS2B are sufficient for the proteolytic activity of the protease domain of NS3 (17, 19, 26-28). It is debated whether NS2B is truly a cofactor/activator of protease activity (i.e. NS2B must be present for NS3 to be active) or if NS2B functions as a prodomain (i.e. simply required for the proper folding of NS3 but not essential for final proteolytic activity) (29, 30). The possibility that the WNV NS2B protein may have a dual role has not been considered.

To address these issues, we conducted experiments to elucidate the role of the full-length NS2B on the protease activity of the full-length NS3. Using our recently described cell-based assay (31), we performed an alanine scanning analysis of conserved NS2B residues and assessed the proteolytic activity of the full-length NS2B/NS3 protease heterocomplex within host cells. Herein, we report several novel findings. Our data demonstrate that the NS2B/NS3 protease heterocomplex requires *cis* processing before acquiring *trans*-cleavage activity. Furthermore, we have identified several NS2B residues

critical for NS3 activity. Interestingly, we have also identified NS2B residues that appear to be required for proper folding of NS3. Taken together, this data represent the first experimental evidence that the WNV NS2B protein plays a dual role in the proteolytic activity of NS3, needed for both proper folding and enzymatic activity. These findings have important implications in the development of antiviral therapies targeted at the WNV NS2B/NS3 protease heterocomplex and suggest that targeting the interactions between NS2B and NS3 represent a potential therapeutic avenue.

3.2. Results

3.2.1. Identification of essential amino acid residues within NS2B

We hypothesized that there are essential residues within full-length NS2B that affect the protease activity of full-length NS3. To identify which amino acid residues within NS2B may be essential, we performed an amino acid sequence alignment of full-length NS2B protein using several *flavivirus* genus members that included WNV, Japanese Encephalitis virus (JEV), Dengue virus (DNV) type 1-4 and Yellow Fever virus (YFV). Fifteen completely conserved amino acid residues were identified from the amino acid alignment with eight residues in the N-terminus hydrophobic region I (residues P3, E6, A10, G12, L21, P32, G37, G47), five in the central hydrophilic region II (residues W62, A66, G70, S72, G83) and two in the C-terminus hydrophobic region III (residues P112, R131) (Figure 3.1). Each completely conserved amino acid residue was mutated to alanine with site-directed mutagenesis (excluding alanine residues) generating 13 different NS2B point mutants. The 13 NS2B point mutants generated were indicated as P3A, E6A, G12A, L21A, P32A, G37A, G47A, W62A, G70A, S72A, G83A, P112A and R131A.

3.2.2. Mutations within NS2B affect protease activity and protein stability of NS3

Next we wanted to test the effects of each of the NS2B point mutants on the protease activity of NS3. We assessed NS3 protease activity with two methods. First, we monitored the autocatalytic cleavage event (*cis*-cleavage) that occurs at the NS2B↓NS3 protein junction within the NS2B/NS3 protease heterocomplex. The intact full-length NS2B/NS3 protease heterocomplex is detected at 85 kDa and upon cleavage NS2B can be detected at 15 kDa and NS3 at 70 kDa with Western blot analysis.

Second, *trans*-cleavage activity was monitored using our recently described cell-based assay (31). Briefly, the substrate contains an ER membrane-anchoring domain, a WNV NS2B/NS3 protease-specific cleavage sequence corresponding to the NS4B/NS5 protein junction site and a DsRed fluorescent reporter group. Upon protease cleavage of the specific cleavage sequence the DsRed reporter group is released and the cleavage product can be detected with Western blot analysis. Intact substrate can be detected at 34 kDa and upon cleavage of the substrate a 29 kDa cleavage band can be detected with Western blot analysis. For these assays, we chose to measure the cleavage of the 4B5 substrate; we previously demonstrated this substrate to be significantly cleaved in our recently described cell-based assay (31).

In addition to the NS2B mutants we substituted the first residue of NS3 from glycine to alanine (GP1′A). The first residue of NS3 represents the P1′ residue that constitutes the cleavage sequence for the autocatalytic cleavage of the NS2B/NS3 heterocomplex. It has been shown *in vitro* that the preferred cleavage sequence for the WNV NS2B/NS3 protease is KR↓GG and that any substitution of the P1′ residue abrogates cleavage (32, 33). As a

control we used the catalytically inactive NS3 mutant (S135A) that we previously generated and described (31).

Huh7.5.1 cells were double-transfected with the 4B5 substrate and either wild-type WNV plasmid (pFLAG-NS2B/NS3-myc) or with each full-length pFLAG-NS2B/NS3-myc plasmid encoding NS2B point mutants of interest (P3A, E6A, G12A, L21A, P32A, G37A, G47A, W62A, G70A, S72A, G83A, P112A, R131A) or NS3 point mutants (GP1′A, S135A). Cells were harvested for Western blot analysis 24 h post-transfection and examined for the *cis*-cleavage of the NS2B/NS3 protease heterocomplex and *trans*-cleavage of the 4B5 substrate (Figure 3.2). While *cis*-cleavage activity was unaffected for the majority of the mutants tested, we observed that a substitution at residue G83 or R131 completely abrogates *cis*-cleavage (Figure 3.2A; G83A, R131A-85 kDa). Furthermore, we observed that substitution at residue G70 and the NS3 mutant GP1′A resulted in partial loss of *cis*-cleavage (Figure 3.2A; G70A, GP1′A-85 kDa and 70 kDa). Interestingly, a substitution at residues G47 or W62 resulted in no detectable NS3 protein suggesting that these residues may affect protein stability leading to misfolding and degradation (Figure 3.2A; G47A, W62A). These results demonstrate that NS2B influences the *cis*-cleavage activity of NS3.

Next, we examined the cleavage of the 4B5 substrate with our *trans*-cleavage cell-based assay by Western blot analysis. Some level of *trans*-cleavage was observed for all mutants expect for W62A, R131A, S135A (Figure 3.2B). Although a cleavage band was detectable in the majority of mutants, subsequent quantification revealed a statistically significant reduction in *trans*-cleavage activity for nine mutants (E6A, G12A, L21A, P32A, G47A, W62A, G70A, G83A, R131A) compared to wild-type WNV (Figure 3.2C). While

we observed a trend for reduced *trans*-cleavage activity by the GP1′A mutant, this reduction did not reach statistical significance.

Taken together, these results suggest that NS2B affects several aspects of NS3 activity. We demonstrate that NS2B influences both *cis* and *trans*-cleavage activity of NS3. Furthermore, our results suggest that *cis*-cleavage is a requirement for the activation for NS3 *trans*-cleavage activity, as *trans*-cleavage activity was significantly reduced in mutants lacking *cis*-cleavage activity. Finally, these results suggest that NS2B is involved in NS3 stability. As such, our results argue that NS2B fulfills a dual role, needed for proper folding and protease activity of NS3.

3.2.3. NS2B and NS3 localize to the ER membrane

Since NS2B has been suggested to anchor NS3 to the membrane, we investigated whether reduction in NS3 *trans*-cleavage activity was simply due to mislocalization. Subcellular localization of the NS2B mutants E6A, G12A, L21A, P32A, G70A, G83A and R131A was examined by confocal microscopy and their protein localization was compared to wild-type WNV. We observed a high degree of colocalization between the NS2B and NS3 proteins with no observable differences in localization among the mutants compared to wild-type WNV (Figure 3.3A; merge). Next, we investigated the subcellular localization of the NS2B and NS3 proteins using the ER membrane marker calnexin. Using confocal microscopy, we observed a high degree of colocalization between the NS2B and NS3 proteins with calnexin with no observable differences in localization compared to wild-type WNV (Figure 3.3B, 3.3C).

To confirm our microscopy observations, we further investigated the subcellular localization of the NS2B and NS3 proteins with a crude ER microsomal fraction preparation. In all sample preparations the ER membrane marker calnexin was detected in the membrane (M) fraction and not in the cytosol (C) fraction (Figure 3.3D; 90kDa). Similarly for wild-type WNV, the NS3 (70 kDa) and NS2B (15 kDa) proteins were detected in M fraction and not in C fraction (Figure 3.3D; WNV). This was also true for E6A, G12A and P32A. For L21A, only the NS3 70 kDa band was detectable in the M fraction, whereas no NS2B 15 kDa band was detectable in either the M or C fraction (Figure 3.3D; L21A). In G70A the NS2B/NS3 protease heterocomplex (85 kDa), NS3 (70 kDa) and NS2B (15 kDa) were detected in the M fraction (Figure 3.3D; G70A). For G83A and R131A only the NS2B/NS3 protease heterocomplex (85 kDa) was detected in the M fraction (Figure 3.3D; G83A, R131A). Taken together, these results demonstrate that mutations of NS2B conserved residues did not result in a reduction of NS3 activity due to mislocalization of the NS3 protein.

3.2.4. Residue G47 and W62 are important for the proper folding of NS3

A substitution at residues G47 or W62 resulted in no detectable NS3 in our Western blot analysis (Figure 3.2A; G47A, W62A). As such, we investigated whether these substitutions resulted in decreased NS3 stability and eventual degradation. To address this question, we transfected Huh7.5.1 cells with either G47A or W62A and 24 h post-transfection the proteasome inhibitor MG132 was added. Cells were harvested 24 h post-treatment and processed for Western blot analysis. The proteasome inhibitor MG132 reduces the degradation of ubiquitin-conjugated proteins in mammalian cells. Following

proteasome inhibitor treatment, NS3 (70 kDa) was detected in G47 and in W62A both the NS2B/NS3 protease heterocomplex (85 kDa) and NS3 (70 kDa) were detected (Figure 3.4). These results demonstrate that *cis*-cleavage of the NS2B/NS3 protease heterocomplex did occur. Following this event, the protein misfolded and subsequently was degraded by the proteasome. This provides evidence that NS2B is needed for the proper folding of NS3. Importantly, these results suggest that acquisition for *trans*-cleavage activity may be dependent on an NS3 conformational change following *cis*-cleavage and that NS2B is integral to this process.

3.3. Discussion

While *in vitro* studies have demonstrated an important role for NS2B in NS3 protease activity, its precise function remains debated. In particular, it has been argued that NS2B functions either as a cofocator or a prodomain (29, 30). Herein, we demonstrate that within the context of the full-length NS2B/NS3 protease heterocomplex, NS2B fulfills a dual role, needed for the enzymatic activity and proper folding of NS3. To our knowledge, this is the first study using the full-length WNV NS2B/NS3 protease heterocomplex to elucidate the role of NS2B on NS3 protease activity within host cells. In addition, we report the first analysis of the role of each completely conserved amino acid residue within NS2B on NS3 protease activity. We have identified several residues within NS2B that are critical for NS3 protease *cis*- and *trans*-cleavage activity (E6, G12, L21, P32, G70, G83, R131), as well as, for the proper folding of NS3 (G47, W62). Our data also demonstrates that *cis*-cleavage of the protease heterocomplex is required before NS3 acquires *trans*-cleavage

activity. Taken together, our results demonstrate that NS2B is an integral partner in the protease activity of NS3.

Cofactor-dependent protease activation has been demonstrated for other *Flaviviridae* such as HCV (22-25). Studies have shown that the protease domain of HCV NS3 requires interactions with the C-terminal NS4A protein to efficiently cleave substrates (22-25). Following intercalation of NS4A into the N-terminal region of NS3, a rearrangement of the protease active site occurs resulting in an induced-fit mechanism for the HCV NS3/NS4A protease heterocomplex (22, 23). Within the *flavivirus* genus many studies have shown that the NS2B protein facilitates the proteolytic activity of NS3. Deletion studies have demonstrated that 40 amino acids from the central hydrophilic region of NS2B are sufficient for NS3 protease activity, suggesting that NS2B acts as a cofactor for NS3 protease activity (17, 19, 26-28). We observed that mutations at residues E6, G12, L21 and P32 (which reside in the N-terminal hydrophobic region I) reduced the percent of substrate cleaved compared to wild-type activity indicating that these residues are important for NS3 *trans*-cleavage activity (Figure 3.2C). Since *cis*-cleavage of the NS2B/NS3 protease heterocomplex (Figure 3.2A) and localization of NS3 were not affected in these samples (Figure 3.3) we conclude from these results that NS2B act as a cofactor for NS3 protease activity. Chappell et al., (2007) observed *in vitro* a reduction in WNV NS3pro activity after $NS2B_{40}$ was autocatalytic cleaved from the $NS2B_{40}$-G_4SG_4-NS3pro recombinant protein. They concluded that $NS2B_{40}$ must be a cofactor/activator of NS3pro activity essential for the proteolytic activity of NS3 (30).

Conversely, Shiryaev et al., (2006) demonstrated *in vitro* that the truncated WNV NS3pro was still active after $NS2B_{40}$ was autocatalytically cleaved from the $NS2B_{40}$-G_4SG_4-

NS3pro recombinant protein. They argue that $NS2B_{40}$ functions as a prodomain that facilitates only the proper folding of NS3pro, rather than a cofactor/activator of NS3pro (29). We observed that mutations at residues G47 and W62 resulted in no detectable NS3 protein (Figure 3.2A) however, following proteasome inhibitor treatment NS3 was detectable by Western blot (Figure 3.4). This demonstrates that these residues are important for the proper folding of NS3 illustrating that NS2B is essential for this process. Mutation of W62 has been shown previously to reduce NS3 protease activity of the related DNV-2 and at the homologous residue W60 of Alkhurma virus (34, 35). The crystal structure of the $NS2B_{40}$-G_4SG_4-NS3pro recombinant protein illustrates that $NS2B_{40}$ wraps around NS3pro in a belt-like manner suggesting that $NS2B_{40}$ functions by stabilizing the protease (36, 37). The aromatic ring of W62 acts as an anchor, binding to a hydrophobic pocket within NS3 protease domain thus tethering NS2B to NS3 (37, 38), demonstrating the potential interactions between NS2B and NS3.

Taken together, our results demonstrate a dual role for NS2B, needed for proper folding and protease activity of NS3. But what remains unanswered is, does NS2B act as a prodomain? A prodomain or propeptide is typically an N-terminal extension of a mature protein (39). For example, furin, an extensively studied proprotein, is translated as an inactive zymogen with an N-terminal propeptide (39-41). The propeptide is autocatalytically cleaved however remains noncovalently bound to furin acting as an autoinhibitor (39, 40). The inactive furin•propeptide complex undergoes multi-step compartment-specific processing of the propeptide until the active furin enzyme remains. The propeptide region is dispensable and does not form a component of the active enzyme (39-41). We observed that a mutation at residues G83 or R131 resulted in an inactive NS2B/NS3 protease

heterocomplex unable to undergo *cis*-cleavage and subsequent *trans*-cleavage of substrate (Figure 3.2). Considering the furin activation pathway, this would suggest that the NS2B/NS3 protease heterocomplex is translated as an inactive zymogen, and then the N-terminal propeptide (in this case NS2B) is autocatalytically cleaved, discarded and the resulting protease (NS3) becomes active. However, the crystal structure illustrates that $NS2B_{40}$ wraps around NS3pro in a belt-like manner demonstrating that NS2B is a component of the active enzyme (36, 37), indicating that NS2B does not fulfill a prodomain role.

Alternatively, it has been suggested that NS2B of DNV-2 functions as a molecular chaperone assisting in the proper folding of NS3 to an active conformation (17, 42). Clum et al., (1997) demonstrated that the addition of microsomal membranes significantly enhanced the biological activity of DNV-2 NS2B in the activation of NS3 protease. They suggest that membrane-association of NS2B may influence the activity of the NS2B/NS3 protease heterocomplex by allowing the hydrophilic domain of NS2B to interact with the NS3 protease domain through a conformational change (17). We observed that residue G47 and W62 were important for the proper folding of NS3 (Figure 3.2A, Figure 3.4) suggesting that NS2B may function as a molecular chaperone. Our results suggest that following *cis*-cleavage of the NS2B/NS3 protease heterocomplex, NS3 undergoes a conformational change into an active conformation for *trans*-cleavage of substrates and that a mutation at either residue G47 or W62 resulted in protein misfolding and subsequent degradation by the proteasome. Importantly, these results also demonstrate that *cis*-cleavage of the heterocomplex precedes *trans*-cleavage activity suggesting a stepwise change in conformation. This stepwise model is also supported with our G83 and R131 results that

demonstrated that the NS2B/NS3 protease heterocomplex had a significant reduction of *trans*-cleavage of substrate.

Taken together, our results illustrate that NS2B has a dual role, functioning as a molecular chaperone and as a cofactor for NS3. Utilizing the full-length NS2B/NS3 protease heterocomplex allowed us to identified several residues within NS2B that are important for NS3 activity that lie outside the NS2B central hydrophilic region II. Although deletion studies of NS2B have elucidated regions that are of importance to NS3 activity the influence of specific residues are missed. Furthermore, our data demonstrates the robustness of our cell-based assay allowing for the biochemical characterization of the full-length NS2B/NS3 protease heterocomplex in a more physiologically relevant environment. Our data illustrates that NS2B is integral to NS3 activity and the information obtained will be useful for the design of inhibitors targeted at the interactions between NS2B and NS3.

3.4. Material and methods

3.4.1. Sequence alignments

Amino acid sequence alignment was performed on the full-length NS2B protein using sequences of several *flavivirus* genus members including WNV (Accession # AF196835), Dengue virus type 1-4 (Accession # FJ024472; Accession # FJ024461; Accession # FJ024471; Accession # FJ024476; respectively), Japanese Encephalitis virus (Accession # M18370) and Yellow Fever virus (Accession # X03700). Amino acid sequence alignment was performed in CLC Main Workbench version 5.5.

3.4.2. Plasmid constructs

Wild-type WNV plasmid: the full-length wild-type pFLAG-NS2B/NS3-myc plasmid has been previously described (31) and was indicated as wild-type WNV. NS2B mutants: using the wild-type WNV plasmid an alanine mutation was generated with site-directed mutagenesis (Stratagene, La Jolla, CA, USA) at each completely conserved amino acid residue generating 13 different point mutants. The 13 different NS2B point mutants were indicated as P3A, E6A, G12A, L21A, P32A, G37A, G47A, W62A, G70A, S72A, G83A, P112A and R131A. NS3 mutants: using the wild-type WNV plasmid the first amino acid residue of NS3 was mutated from glycine to alanine with site-directed mutagenesis (Stratagene) and was indicated as GP1′A. A catalytically inactive NS3 mutant has been previously described (31) and was indicated as S135A. 4B5 Substrate: the 4B5 substrate plasmid has been previously described (31) and was indicated as 4B5. All mutations were confirmed by automated sequencing (UBC DNA Sequencing Laboratory).

3.4.3. Cell culture

Human hepatocellular carcinoma cells (Huh7.5.1 cells a cell-line derivative of Huh7) were grown in complete Dulbecco's modified Eagle's medium [DMEM cat no. 11965-092, Gibco, Invitrogen (Burlington, ON, CA)] supplemented with heat-inactivated 10% v/v fetal bovine serum (Invitrogen), 50 units/ml penicillin, 50 µg/ml streptomycin, and 100 µM non-essential amino acids, 1% L-glutamine, 1% HEPES (Invitrogen). Cells were grown at 37ºC in the presence of 5% CO_2.

3.4.4. Transfections and Western blotting

Six well plates were seeded with Huh7.5.1 cells at 200,000 cells/well and grown to approximately 80% confluency. Huh7.5.1 cells were double-transfected with 2.5 μg of 4B5 substrate plasmid and 2.5 μg of wild-type WNV plasmid or with each mutant plasmid using *Trans*IT-LT1 Transfection Reagent (Mirus Bio, Madison, WI, USA). Controls included double-transfection of Huh7.5.1 cells with 2.5 μg of 4B5 substrate plasmid and 2.5 μg of inactive S135A protease or single-transfection with 2.5 μg of 4B5 substrate plasmid. 24 h post-transfection, cells were harvested for Western blot analysis as described previously (31) with the following modifications. Cell pellets were resuspended in 0.06 ml hypotonic lysis buffer containing 1x protease inhibitor cocktail (Roche, Laval., QC, Canada), 0.06 ml of 2x SDS-PAGE sample buffer was added and boiled. The membranes were probed according to Odyssey Infrared Imaging System Western blot analysis protocol (LI-COR Biosciences, Lincoln, NE, USA). Primary and secondary antibodies were diluted in Odyssey Blocking Buffer (LI-COR Biosciences) containing 0.1% v/v Tween-20 (Sigma-Aldrich Corp., St. Louis, MO, USA). Membranes were probed with primary anti-DsRed polyclonal antibody (1:1,000, Clontech Laboratories, Mountain View, CA, USA) and with primary anti-NS3 monoclonal antibody (2μg/ml, R&D Systems, Inc., Minneapolis, MN, USA) (60 min). Membranes were probed with secondary IRDye 680-conjugated goat anti-rabbit polyclonal antibody and with secondary IRDye 800-conjugated goat anti-mouse monoclonal antibody (1:10,000, LI-COR Biosciences) (30 min). Membranes were then imaged using an Odyssey Infrared Imaging System (LI-COR Biosciences).

3.4.5. Quantification and statistical analysis

Analysis and quantification of integrated band intensity were performed using the Odyssey Infrared Imaging System application software version 2.1.12 (LI-COR Biosciences). The percent of substrate cleaved was calculated by dividing the cleaved signal by the total signal (cleaved plus uncleaved) (normalizing the readout for each sample). Averages were calculated from three independent experiments run in duplicate. GraphPad Prism (GraphPad Software, Inc., La Jolla, CA, USA) was used for graphical representation and statistical analysis. P values were obtained for two-tailed, unpaired, student's *t*-test, and significance was noted when $p<0.05$.

3.4.6. Membrane fractionation

Six well plates were seeded with Huh7.5.1 cells at 200,000 cells/well, grown to approximately 80% confluency then transfected with 2.5 μg of wild-type WNV plasmid or with each statistically significant NS2B mutant. 24 h post-transfection cells were harvested as described previously (31). The six cell pellets were combined and were resuspended in 0.06 ml hypotonic lysis buffer (20 mM Tris pH 7.4, 10 mM $MgCl_2$, 10 mM $CaCl_2$) containing 1x protease inhibitor cocktail (Roche). Cells were placed on ice for 20 min then passed through a 28G syringe (10 times) to disrupt the cell membrane. Cells were centrifuged (600 *g*, 5 min, 4°C) and the supernatant was transferred to an ultracentrifuge tube (pellet contains nuclei and any unbroken cells) and ultracentrifuged (100,000 *g*, 30 min, 4°C). The supernatant was transferred to a new tube and the membrane pellet was resuspended in 0.06 ml hypotonic lysis buffer containing 1x protease inhibitor cocktail. Samples were prepared for Western blot analysis as described previously (31). Membranes were probed with the ER

membrane marker calnexin (primary anti-calnexin polyclonal antibody) (1:1000, Sigma-Aldrich Corp.), for NS2B detection, primary anti-FLAG polyclonal antibody (1:1000, Abcam Inc., Cambridge, MA, USA) and for NS3 detection, primary anti-NS3 monoclonal antibody (2μg/ml, R&D Systems, Inc.) (60 min). Membranes were probed with secondary IRDye 680-conjugated goat anti-mouse monoclonal antibody and with secondary IRDye 800-conjugated goat anti-rabbit polyclonal antibody (1:10,000, LI-COR Biosciences) (30 min). Membranes were then imaged using an Odyssey Infrared Imaging System (LI-COR Biosciences).

3.4.7. Proteasome inhibitor assay

Six well plates were seeded with Huh7.5.1 cells at 200,000 cells/well, grown to approximately 80% confluency then transfected with 2.5 μg of NS2B mutant G47A or W62A plasmid. 24 h post-transfection 5 μM of proteasome inhibitor MG132 (Calbiochem ®, EMD Chemicals Inc., Darmstadt, Germany) was added to cells. 24 h post-treatment cells were harvested and prepared for Western blot analysis as described previously (31). Membranes were probed with primary anti-NS3 monoclonal antibody (2μg/ml, R&D Systems, Inc.) (60 min) and with secondary IRDye 800-conjugated goat anti-mouse monoclonal antibody (1:10,000, LI-COR Biosciences) (30 min). Membranes were then imaged using an Odyssey Infrared Imaging System (LI-COR Biosciences).

3.4.8. Immunofluorescence microscopy

Huh7.5.1 cells were prepared as described previously (31). For the ER membrane marker, primary anti-calnexin polyclonal antibody was added to cells (1:100, Sigma-Aldrich

Corp.) (60 min). For NS2B detection, cells were probed with primary anti-FLAG polyclonal antibody (1:100, Abcam Inc.) or anti-FLAG monoclonal antibody (1:100, Sigma-Aldrich Corp.) (60 min). For NS3 detection, cells were probed with primary anti-myc monoclonal antibody (1:100, Stratagene) (60 min). Depending on the antibody combination cells were probed with secondary Alexa Fluor-568-conjugated donkey anti-mouse monoclonal antibody or anti-rabbit polyclonal antibody and secondary Alexa Fluor-488-conjugated donkey anti-rabbit polyclonal antibody or anti-mouse monoclonal antibody (1:100, Molecular Probes, Invitrogen) (60 min). Nuclei were stained with Hoechst stain (Invitrogen) (5 μg/ml, 15 min). Images were acquired using an Olympus Fluoview FV1000 laser scanning confocal microscope (Olympus Corporation, Markham, ON, Canada).

Figure 3.1

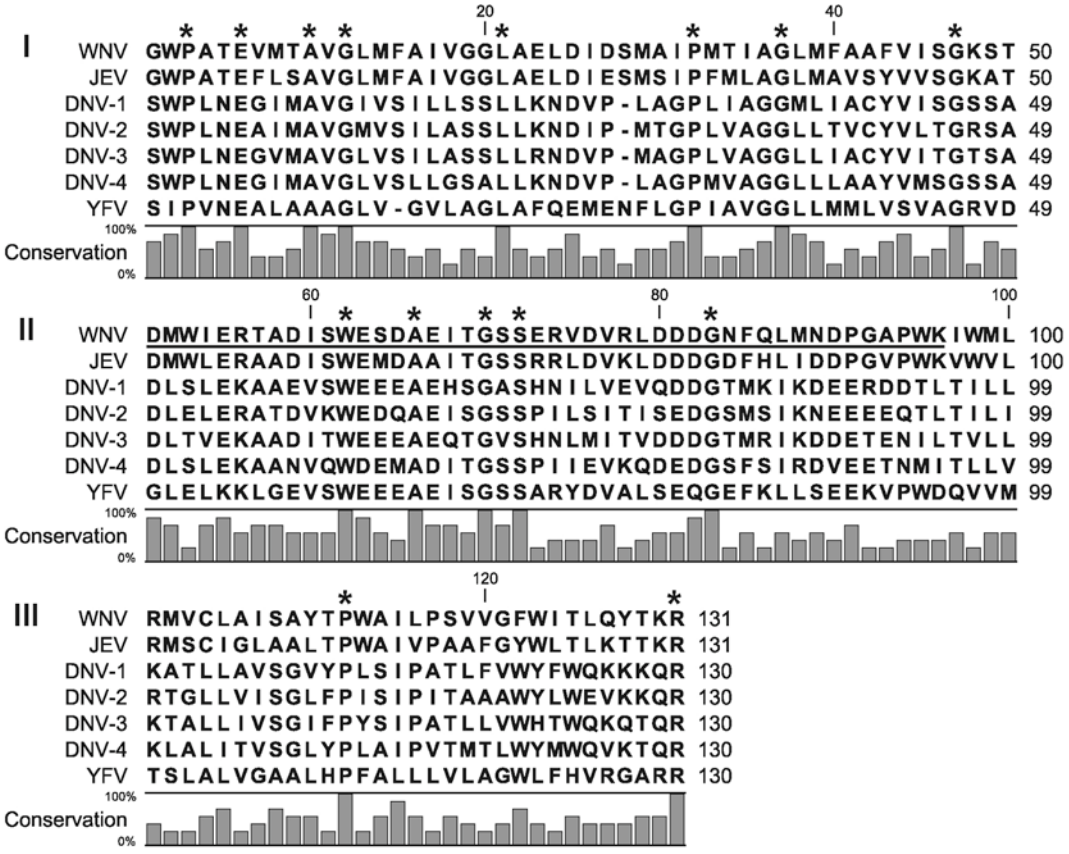

Figure 3.1. Amino acid sequence alignment of the full-length NS2B protein

Illustrated is an amino acid sequence alignment of the full-length NS2B from several *flavivirus* genus members including West Nile virus (WNV), Japanese Encephalitis virus (JEV), Dengue virus type 1-4 (DNV-1, DNV-2, DNV-3, DNV-4) and Yellow Fever virus (YFV). The NS2B regions are indicated, N-terminus hydrophobic region (I), central hydrophilic region (II) (underlined) and, C-terminus hydrophobic region (III). Conservation graph illustrating the percent of amino acid conservation is depicted below the alignment. Each completely conserved amino acid residue is indicated above with an asterisk (*). Alignment performed in CLC Main Workbench version 5.5.

Figure 3.2. NS2B mutations affect NS3 protease activity

(A) Effect on *cis*-cleavage activity. Depicted is a Western blot analysis of the effect of each mutant on the autocatalytic cleavage of the NS2B/NS3 protease heterocomplex. Membranes were probed with the anti-NS3 monoclonal antibody. Intact heterocomplex is detected at 85 kDa and the cleaved NS3 protein is detected at 70 kDa. First panel wild-type WNV and NS2B mutants; second panel NS3 mutants and 4B5 substrate. (B) Effect on *trans*-cleavage activity. Depicted is a Western blot analysis of the effect of each mutant on the *trans*-cleavage of the 4B5 substrate. Membranes were probed with the anti-DsRed polyclonal antibody. Intact 4B5 substrate is detected at 34 kDa and substrate cleavage product is detected at 29 kDa. First and second panel wild-type WNV and NS2B mutants; third panel NS3 mutants and 4B5 substrate. (C) Quantification of *trans*-cleavage activity of Western blot analysis. Depicted are the percent of 4B5 substrate cleaved (y-axis). Wild-type WNV (white bar), NS2B mutants (light gray bars), NS3 mutants (dark gray bars), 4B5 substrate only (black bar). Results shown are the average of three independent experiments run in duplicate. Asterisks denote statistically significant reduction in cleavage compared with wild-type WNV (*$p<0.05$, **$p<0.005$, ***$p<0.001$).

Figure 3.2

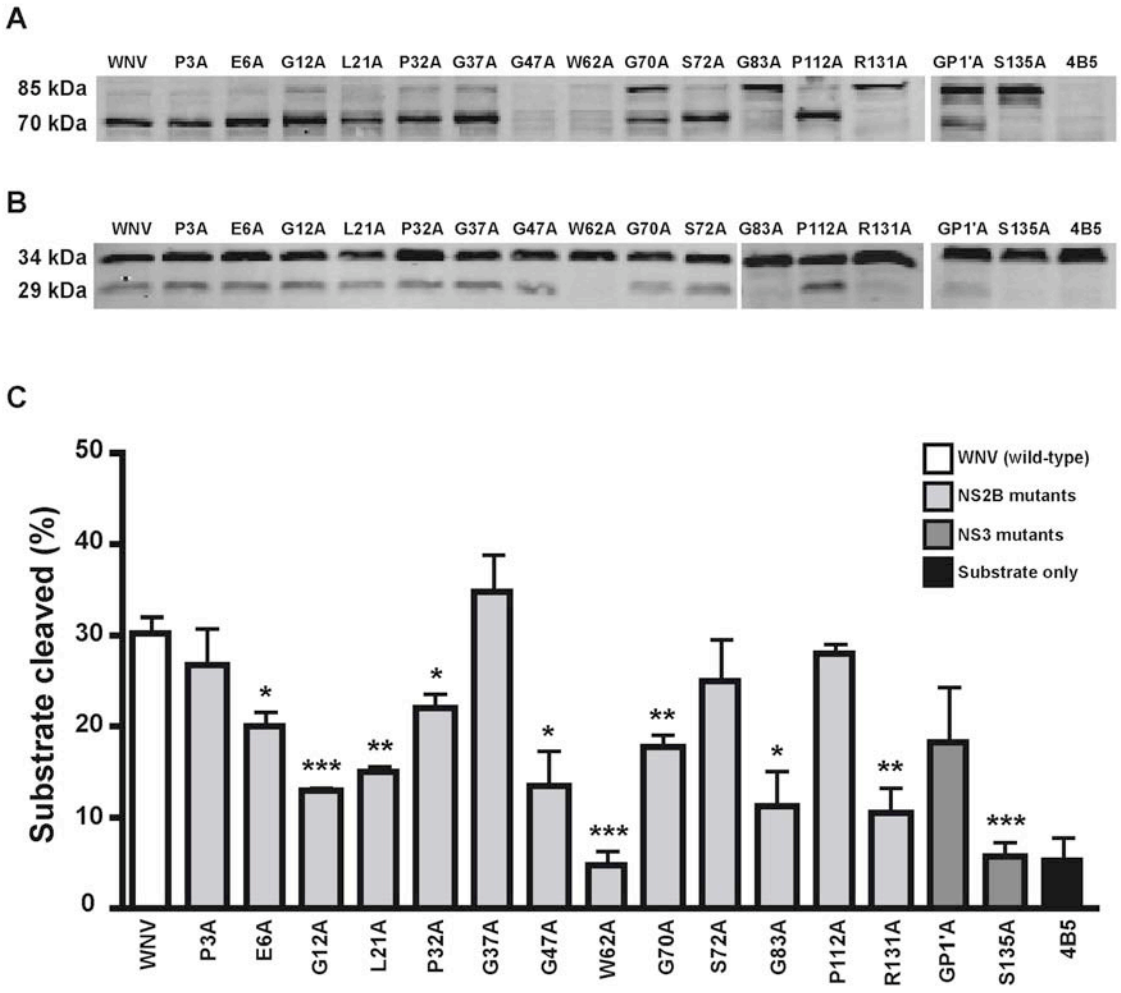
A
WNV P3A E6A G12A L21A P32A G37A G47A W62A G70A S72A G83A P112A R131A GP1'A S135A 4B5
85 kDa
70 kDa
B
WNV P3A E6A G12A L21A P32A G37A G47A W62A G70A S72A G83A P112A R131A GP1'A S135A 4B5
34 kDa
29 kDa
C
Substrate cleaved (%)
0
10
20
30
40
50
WNV (wild-type)
NS2B mutants
NS3 mutants
Substrate only
WNV P3A E6A G12A L21A P32A G37A G47A W62A G70A S72A G83A P112A R131A GP1'A S135A 4B5

Figure 3.3. Subcellular localization of mutants with reduced catalytic activity

Panels (A), (B), (C): Huh7.5.1 cells were transfected either with wild-type (WNV) or each significant mutant (E6A, G12A, L21A, P32A, G70A, G83A, R131A) and fixed 24 h post-transfection. Cells were probed for NS2B (anti-FLAG polyclonal or monoclonal antibody), NS3 (anti-myc monoclonal antibody) or for the ER membrane marker calnexin (anti-calnexin polyclonal antibody). Nuclei were visualized with Hoechst staining (shown in blue). Cells were imaged with an Olympus Fluoview scanning confocal microscope (Olympus Corporation). (A) Detection of NS2B (top row, FLAG) (shown in green) and NS3 (middle row, myc) (shown in red); merged NS2B and NS3 signal (bottom row). (B) Detection of NS2B (top row, FLAG) (shown in green) and the ER membrane marker calnexin (middle row, ER) (shown in red); merged NS2B and ER signal (bottom row). (C) Detection of NS3 (top row, myc) (shown in green) and the ER membrane marker calnexin (middle row, ER) (shown in red); merged NS3 and ER signal (bottom row). (D) Microsomal fraction preparation. Huh7.5.1 cells were transfected either with wild-type (WNV) or each significant mutant (E6A, G12A, L21A, P32A, G70A, G83A, R131A) and harvested 24 h post-transfection for microsomal fraction preparation as described in Material and methods. Western blots were probed for the ER membrane marker calnexin (anti-calnexin polyclonal antibody), NS3 (anti-NS3 monoclonal antibody) and NS2B (anti-FLAG polyclonal antibody). Cytosol fraction (C); membrane fraction (M); calnexin (90 kDa); intact NS2B/NS3 protease heterocomplex (85 kDa); NS3 protein (70 kDa); NS2B protein (15 kDa).

Figure 3.3

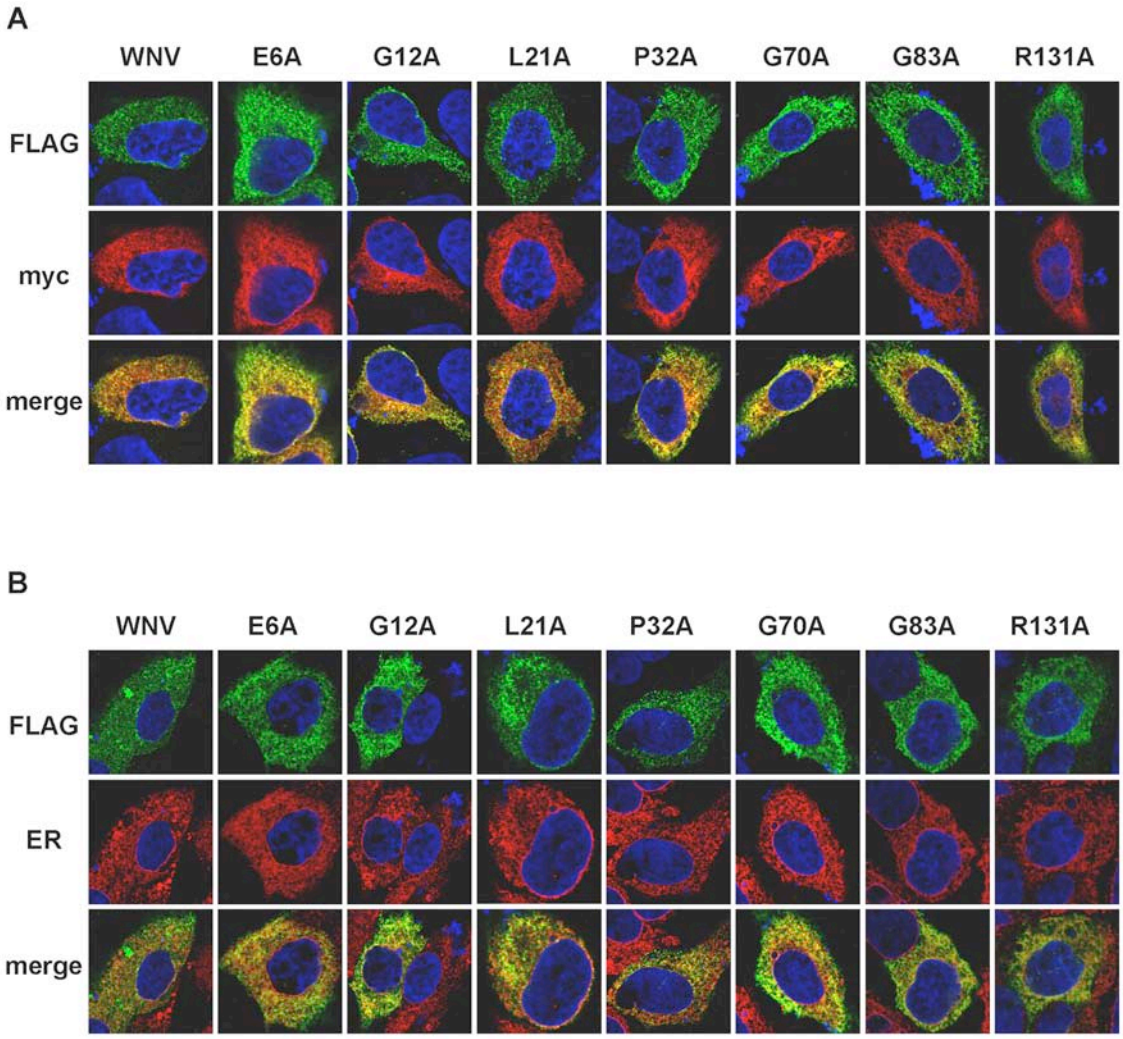
A
WNV
E6A
G12A
L21A
P32A
G70A
G83A
R131A
FLAG
myc
merge
B
WNV
E6A
G12A
L21A
P32A
G70A
G83A
R131A
FLAG
ER
merge

Figure 3.3

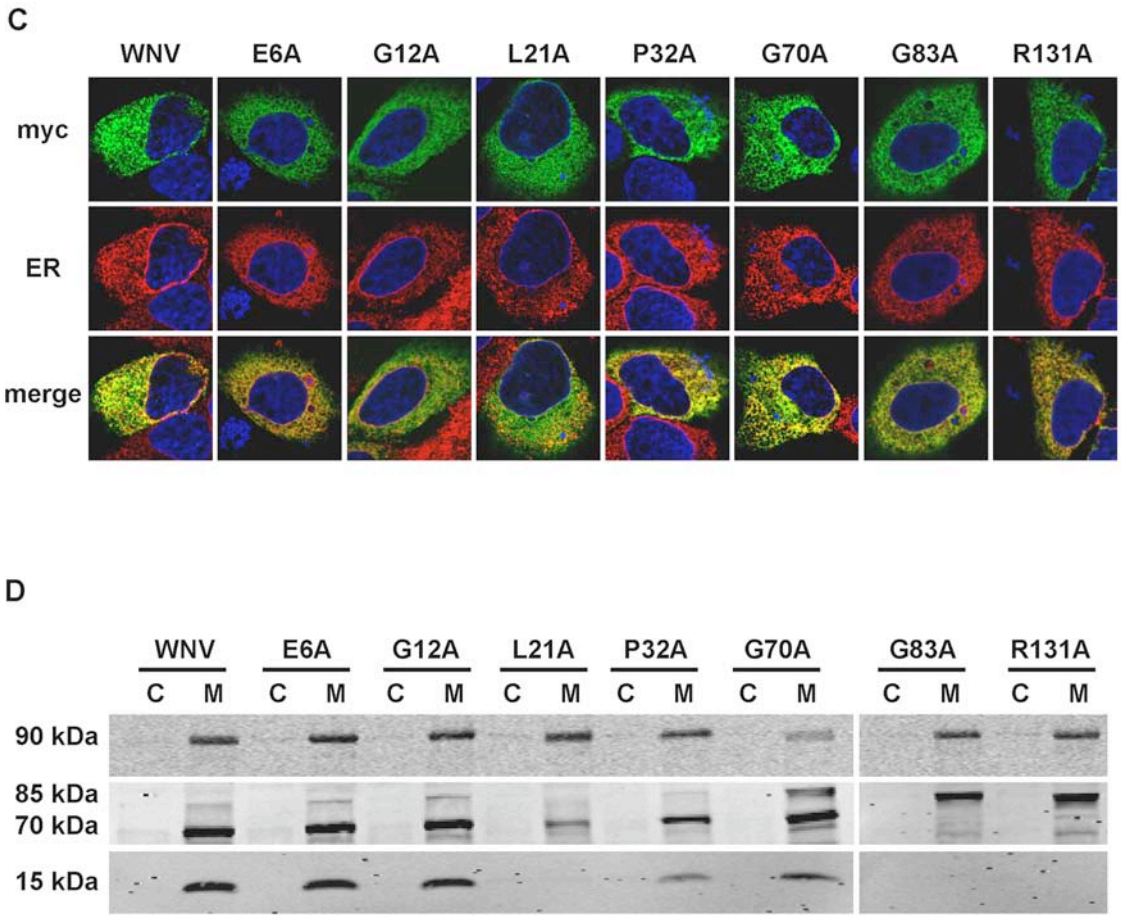
C
WNV
E6A
G12A
L21A
P32A
G70A
G83A
R131A
myc
ER
merge
D
WNV
E6A
G12A
L21A
P32A
G70A
G83A
R131A
C M C M C M C M C M C M C M C M
90 kDa
85 kDa
70 kDa
15 kDa

Figure 3.4

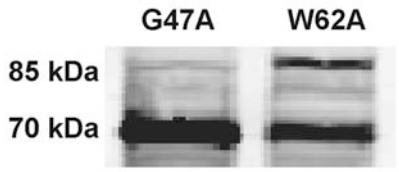

Figure 3.4. Mutations within NS2B affect NS3 protein stability

Huh7.5.1 cells were transfected either NS2B mutant G47A or W62A. 24 h post-transfection cells were treated with 5 μM of proteasome inhibitor MG132. 24 h post-treatment cells were harvested for Western blot analysis. Western blots were probed for NS3 (anti-NS3 monoclonal antibody). Intact NS2B/NS3 protease heterocomplex (85 kDa); NS3 protein (70 kDa).

3.5. References

1. (CDC), C. o. D. C. a. P. 1999. Outbreak of West Nile-like viral encephalitis--New York, 1999. *MMWR Morb Mortal Wkly Rep* 48:845-849.
2. Castle, E., T. Nowak, U. Leidner, and G. Wengler. 1985. Sequence analysis of the viral core protein and the membrane-associated proteins V1 and NV2 of the flavivirus West Nile virus and of the genome sequence for these proteins. *Virology* 145:227-236.
3. Castle, E., U. Leidner, T. Nowak, and G. Wengler. 1986. Primary structure of the West Nile flavivirus genome region coding for all nonstructural proteins. *Virology* 149:10-26.
4. Yamshchikov, V. F., and R. W. Compans. 1993. Regulation of the late events in flavivirus protein processing and maturation. *Virology* 192:38-51.
5. Lindenbach, B. D., H. Thiel, and C. M. Rice. 2007. Flaviviridae: The viruses and their replication. In *Fields Virology*, 5 ed. D. M. Knipe, and P. M. Howley, eds. Lippincott William and Wilkins, Philadelphia.
6. Brinton, M. A. 2002. The molecular biology of West Nile Virus: a new invader of the western hemisphere. *Annu Rev Microbiol* 56:371-402.
7. Rice, C. M., E. M. Lenches, S. R. Eddy, S. J. Shin, R. L. Sheets, and J. H. Strauss. 1985. Nucleotide sequence of yellow fever virus: implications for flavivirus gene expression and evolution. *Science* 229:726-733.
8. Castle, E., and G. Wengler. 1987. Nucleotide sequence of the 5'-terminal untranslated part of the genome of the flavivirus West Nile virus. *Arch Virol* 92:309-313.

9. Chambers, T. J., R. C. Weir, A. Grakoui, D. W. McCourt, J. F. Bazan, R. J. Fletterick, and C. M. Rice. 1990. Evidence that the N-terminal domain of nonstructural protein NS3 from yellow fever virus is a serine protease responsible for site-specific cleavages in the viral polyprotein. *Proc Natl Acad Sci U S A* 87:8898-8902.

10. Wengler, G. 1991. The carboxy-terminal part of the NS 3 protein of the West Nile flavivirus can be isolated as a soluble protein after proteolytic cleavage and represents an RNA-stimulated NTPase. *Virology* 184:707-715.

11. Cahour, A., B. Falgout, and C. J. Lai. 1992. Cleavage of the dengue virus polyprotein at the NS3/NS4A and NS4B/NS5 junctions is mediated by viral protease NS2B-NS3, whereas NS4A/NS4B may be processed by a cellular protease. *J Virol* 66:1535-1542.

12. Amberg, S. M., A. Nestorowicz, D. W. McCourt, and C. M. Rice. 1994. NS2B-3 proteinase-mediated processing in the yellow fever virus structural region: in vitro and in vivo studies. *J Virol* 68:3794-3802.

13. Bazan, J. F., and R. J. Fletterick. 1989. Detection of a trypsin-like serine protease domain in flaviviruses and pestiviruses. *Virology* 171:637-639.

14. Gorbalenya, A. E., A. P. Donchenko, E. V. Koonin, and V. M. Blinov. 1989. N-terminal domains of putative helicases of flavi- and pestiviruses may be serine proteases. *Nucleic Acids Res* 17:3889-3897.

15. Gorbalenya, A. E., E. V. Koonin, A. P. Donchenko, and V. M. Blinov. 1989. Two related superfamilies of putative helicases involved in replication, recombination, repair and expression of DNA and RNA genomes. *Nucleic Acids Res* 17:4713-4730.

16. Wengler, G., T. Nowak, and E. Castle. 1990. Description of a procedure which allows isolation of viral nonstructural proteins from BHK vertebrate cells infected with the West Nile flavivirus in a state which allows their direct chemical characterization. *Virology* 177:795-801.

17. Clum, S., K. E. Ebner, and R. Padmanabhan. 1997. Cotranslational membrane insertion of the serine proteinase precursor NS2B-NS3(Pro) of dengue virus type 2 is required for efficient in vitro processing and is mediated through the hydrophobic regions of NS2B. *J Biol Chem* 272:30715-30723.

18. Yamshchikov, V. F., D. W. Trent, and R. W. Compans. 1997. Upregulation of signalase processing and induction of prM-E secretion by the flavivirus NS2B-NS3 protease: roles of protease components. *J Virol* 71:4364-4371.

19. Brinkworth, R. I., D. P. Fairlie, D. Leung, and P. R. Young. 1999. Homology model of the dengue 2 virus NS3 protease: putative interactions with both substrate and NS2B cofactor. *J Gen Virol* 80 (Pt 5):1167-1177.

20. Chappell, K. J., T. A. Nall, M. J. Stoermer, N. X. Fang, J. D. Tyndall, D. P. Fairlie, and P. R. Young. 2005. Site-directed mutagenesis and kinetic studies of the West Nile Virus NS3 protease identify key enzyme-substrate interactions. *J Biol Chem* 280:2896-2903.

21. Bera, A. K., R. J. Kuhn, and J. L. Smith. 2007. Functional characterization of cis and trans activity of the Flavivirus NS2B-NS3 protease. *J Biol Chem* 282:12883-12892.

22. Failla, C., L. Tomei, and R. De Francesco. 1994. Both NS3 and NS4A are required for proteolytic processing of hepatitis C virus nonstructural proteins. *J Virol* 68:3753-3760.

23. Richer, M. J., L. Juliano, C. Hashimoto, and F. Jean. 2004. Serpin mechanism of hepatitis C virus nonstructural 3 (NS3) protease inhibition: induced fit as a mechanism for narrow specificity. *J Biol Chem* 279:10222-10227.

24. Hamill, P., and F. Jean. 2005. Enzymatic characterization of membrane-associated hepatitis C virus NS3-4A heterocomplex serine protease activity expressed in human cells. *Biochemistry* 44:6586-6596.

25. Martin, M. M., and F. Jean. 2006. Single-cell resolution imaging of membrane-anchored hepatitis C virus NS3/4A protease activity. *Biol Chem* 387:1075-1080.

26. Chambers, T. J., A. Grakoui, and C. M. Rice. 1991. Processing of the yellow fever virus nonstructural polyprotein: a catalytically active NS3 proteinase domain and NS2B are required for cleavages at dibasic sites. *J Virol* 65:6042-6050.

27. Chambers, T. J., A. Nestorowicz, S. M. Amberg, and C. M. Rice. 1993. Mutagenesis of the yellow fever virus NS2B protein: effects on proteolytic processing, NS2B-NS3 complex formation, and viral replication. *J Virol* 67:6797-6807.

28. Yusof, R., S. Clum, M. Wetzel, H. M. Murthy, and R. Padmanabhan. 2000. Purified NS2B/NS3 serine protease of dengue virus type 2 exhibits cofactor NS2B dependence for cleavage of substrates with dibasic amino acids in vitro. *J Biol Chem* 275:9963-9969.

29. Shiryaev, S. A., B. I. Ratnikov, A. V. Chekanov, S. Sikora, D. V. Rozanov, A. Godzik, J. Wang, J. W. Smith, Z. Huang, I. Lindberg, M. A. Samuel, M. S. Diamond, and A. Y. Strongin. 2006. Cleavage targets and the D-arginine-based inhibitors of the West Nile virus NS3 processing proteinase. *Biochem J* 393:503-511.

30. Chappell, K. J., M. J. Stoermer, D. P. Fairlie, and P. R. Young. 2007. Generation and characterization of proteolytically active and highly stable truncated and full-length recombinant West Nile virus NS3. *Protein Expr Purif* 53:87-96.

31. Condotta, S. A., M. M. Martin, M. Boutin, and F. Jean. 2010. Detection and in-cell selectivity profiling of the full-length West Nile virus NS2B/NS3 serine protease using membrane-anchored fluorescent substrates. *Biol Chem* 391:549-559.

32. Shiryaev, S. A., I. A. Kozlov, B. I. Ratnikov, J. W. Smith, M. Lebl, and A. Y. Strongin. 2007. Cleavage preference distinguishes the two-component NS2B-NS3 serine proteinases of Dengue and West Nile viruses. *Biochem J* 401:743-752.

33. Shiryaev, S. A., B. I. Ratnikov, A. E. Aleshin, I. A. Kozlov, N. A. Nelson, M. Lebl, J. W. Smith, R. C. Liddington, and A. Y. Strongin. 2007. Switching the substrate specificity of the two-component NS2B-NS3 flavivirus proteinase by structure-based mutagenesis. *J Virol* 81:4501-4509.

34. Niyomrattanakit, P., P. Winoyanuwattikun, S. Chanprapaph, C. Angsuthanasombat, S. Panyim, and G. Katzenmeier. 2004. Identification of residues in the dengue virus type 2 NS2B cofactor that are critical for NS3 protease activation. *J Virol* 78:13708-13716.

35. Pastorino, B. A., C. N. Peyrefitte, M. Grandadam, M. C. Thill, H. J. Tolou, and M. Bessaud. 2006. Mutagenesis analysis of the NS2B determinants of the Alkhurma virus NS2B-NS3 protease activation. *J Gen Virol* 87:3279-3283.

36. Erbel, P., N. Schiering, A. D'Arcy, M. Renatus, M. Kroemer, S. P. Lim, Z. Yin, T. H. Keller, S. G. Vasudevan, and U. Hommel. 2006. Structural basis for the activation of

flaviviral NS3 proteases from dengue and West Nile virus. *Nat Struct Mol Biol* 13:372-373.

37. Aleshin, A. E., S. A. Shiryaev, A. Y. Strongin, and R. C. Liddington. 2007. Structural evidence for regulation and specificity of flaviviral proteases and evolution of the Flaviviridae fold. *Protein Sci* 16:795-806.

38. Chappell, K. J., M. J. Stoermer, D. P. Fairlie, and P. R. Young. 2008. Mutagenesis of the West Nile virus NS2B cofactor domain reveals two regions essential for protease activity. *J Gen Virol* 89:1010-1014.

39. Anderson, E. D., J. K. VanSlyke, C. D. Thulin, F. Jean, and G. Thomas. 1997. Activation of the furin endoprotease is a multiple-step process: requirements for acidification and internal propeptide cleavage. *Embo J* 16:1508-1518.

40. Anderson, E. D., S. S. Molloy, F. Jean, H. Fei, S. Shimamura, and G. Thomas. 2002. The ordered and compartment-specfific autoproteolytic removal of the furin intramolecular chaperone is required for enzyme activation. *J Biol Chem* 277:12879-12890.

41. Thomas, G. 2002. Furin at the cutting edge: from protein traffic to embryogenesis and disease. *Nat Rev Mol Cell Biol* 3:753-766.

42. Leung, D., K. Schroder, H. White, N. X. Fang, M. J. Stoermer, G. Abbenante, J. L. Martin, P. R. Young, and D. P. Fairlie. 2001. Activity of recombinant dengue 2 virus NS3 protease in the presence of a truncated NS2B co-factor, small peptide substrates, and inhibitors. *J Biol Chem* 276:45762-45771.

Chapter 4

Development of a specific West Nile virus NS2B/NS3 serine protease inhibitor[3]

[3] **A version of this chapter will be submitted for publication:** Condotta, SA, C Lai, MM Martin, M Boutin, MJ Richer, H Tsao, F Jean. (2010) Development of a specific West Nile virus NS2B/NS3 serine protease inhibitor.

4.1. Introduction

The first cases of West Nile virus (WNV) in the Western Hemisphere were reported in 1999 in New York City (1). Since then, WNV has spread throughout North America and has become a serious public heath concern. There are currently no vaccines or antiviral therapies available. In the absence of prevention strategies, the development of an antiviral therapy becomes important for the treatment of human WNV infections. Understanding the virus life cycle is necessary for the rational design of an effective antiviral therapy.

WNV (*Flaviviridae*: *flavivirus*) is a small (~50 nm) enveloped virus that contains a single-stranded positive-sense RNA genome (2-5). Virions enter via receptor-mediated endocytosis, and the viral RNA is translated into a single polyprotein precursor, following membrane fusion and nucleocapsid uncoating (5, 6). The polyprotein precursor is composed of ten viral proteins, three of which are structural (capsid (C), premembrane (prM) and envelope (E)) and seven that are nonstructural (NS1, NS2A, NS2B, NS3, NS4A, NS4B, NS5) arranged in the following order N- to C-terminal: C-prM-E-NS1-NS2A-NS2B-NS3-NS4A-NS4B-NS5 (2, 3, 6-8). The polyprotein precursor is proteolytically processed by host proteases and the viral protease heterocomplex, NS2B/NS3 (9-12). Processing of the polyprotein precursor releases the component viral proteins, allowing the NS proteins to form a membrane-associated replication complex that facilitates viral RNA synthesis (6, 13). The processing of the polyprotein precursor is essential for the virus life cycle (9) making the viral protease heterocomplex, NS2B/NS3, an attractive target for rational drug design.

The WNV viral protease heterocomplex, NS2B/NS3, is comprised of two viral proteins, NS2B and NS3. The viral protein NS3 is a bi-functional enzyme that contains a serine protease domain (catalytic triad H51, D75, S135) in its N-terminus and a

helicase/ATPase domain in its C-terminus (10, 14-17). Hydrophobicity profiles of NS2B depict a central hydrophilic region flanked by hydrophobic regions. It is thought that NS3 is tethered to the endoplasmic reticulum (ER) membrane through its interaction with NS2B and that NS2B is associated to the ER membrane through its hydrophobic regions (5, 18-22). Deletion studies have demonstrated that the central hydrophilic region of NS2B (40 amino acids) is sufficient to activate the protease domain of NS3 (NS3pro) (19, 21, 23-25). As such, a recombinant truncated protein has been constructed ($NS2B_{40}$-G_4SG_4-NS3pro) and is typically used for *in vitro* assays (26-28).

In vitro studies have demonstrated that the $NS2B_{40}$-G_4SG_4-NS3pro recombinant protein has a preferred substrate specificity of KR↓GG (29, 30). Additionally, we have demonstrated with our novel cell-based fluorescent substrate assay that the ER membrane-associated full-length viral protease heterocomplex, NS2B/NS3, efficiently cleaved substrate corresponding to the NS4B/NS5 protein junction site sequence (KPGLKR↓GGAK) (22). Prior to virion release, the *flavivirus* virion undergoes a final maturation step that is mediated by the *trans*-Golgi network (TGN) host serine protease, furin (31) (minimum cleavage sequence: RXXR↓) (32). Several pathogens require processing by furin for cytotoxicity and for the generation of infectious virus particles. As such, furin represents a potential target for antiviral therapy (33-37). It has been demonstrated *in vitro* that the $NS2B_{40}$-G_4SG_4-NS3pro recombinant protein cleaved furin substrates suggesting that furin inhibitors could act against the WNV viral protease in a similar fashion (38).

An endogenous serine protease inhibitor (serpin), Spn4A, was identified from *Drosophila melanogaster*, to be a potent inhibitor of furin (K_i = 13pM) (32). Serpin architecture comprises of nine α-helices, three β-sheets and a reactive centre loop (RCL)

that typically contains 20 amino acid residues (39, 40). The RCL of the serpin contains a cleavage sequence that is recognized and processed by the target protease (40). Serpins operate as a suicide substrate inhibitor, that is, once the RCL is cleaved by the target protease the serpin undergoes a rapid and irreversible conformational change (40, 41). The RCL is incorporated into the core of the enzyme essentially trapping the target protease in an inactive configuration (41). The resulting protease•serpin complex is typically heat SDS-stable and a shift in protein mobility can be visualized by Western blot analysis (40, 41).

The RCL of Spn4A contains the cleavage sequence AVRRKR↓AIMS, which includes the consensus cleavage sequence of furin (RX(R/K)R↓) (32, 33). The similarity in cleavage sequence preference between furin and the WNV NS2B/NS3 protease heterocomplex, NS2B/NS3, suggests that Spn4A may have an inhibitory effect on the WNV NS2B/NS3 protease. Alternatively, the RCL of Spn4A could be altered to residues that are preferred by the WNV NS2B/NS3 protease allowing for the development of a selective inhibitor directed against the viral protease. To this effect, it has been demonstrated with a related *Drosophila* serpin, Spn6, that altering specific residues within the RCL of Spn6 produced a serpin with specific inhibitory properties towards the Hepatitis C virus (HCV) viral protease heterocomplex, NS3/NS4A (42). Based on this, it may be possible to alter the RCL of Spn4A creating a specific serpin directed against the WNV NS2B/NS3 protease. Herein, we describe our attempts to generate a serpin directed against the ER membrane-associated full-length WNV viral protease heterocomplex, NS2B/NS3.

4.2. Results

4.2.1. Designing a specific WNV NS2B/NS3 serpin

Our laboratory serpin, Spn4A (referred to as wild-type herein), contains a N-terminal secretory signal peptide (sp) sequence followed by two epitope tags (His-tag and FLAG-tag) (hf), a RCL that contains the cleavage sequence AVRRKR↓AIMS and a C-terminal ER retention motif that is comprised of the amino acids His-Asp-Glu-Leu (HDEL) (sp-hf-Spn4A-HDEL) (Figure 4.1) (32). The N-terminal signal peptide directs Spn4A to the secretory pathway where it transits through and is retained due to the C-terminal HDEL motif (32). As furin traffics through the secretory pathway, Spn4A would encounter furin and exhibit its inhibitory properties. The WNV viral protease heterocomplex, NS2B/NS3, is thought to be associated to the ER membrane facing towards the cytoplasm (5, 22). Since wild-type Spn4A traffics through the secretory pathway and is retained, it would not be predicted to encounter the viral protease heterocomplex NS2B/NS3 within the cytoplasm. As such, the N-terminal secretory signal peptide sequence was removed and a monomeric red fluorescent protein (mRFP) was added creating a red fluorescent cytoplasmic variant of Spn4A (mRFP-hf-Spn4A-HDEL) ($^{mRFP\text{-}C}$Spn4A) (Figure 4.1).

In vitro studies have demonstrated that the $NS2B_{40}$-G_4SG_4-NS3pro recombinant protein has a preferred substrate specificity of KR↓GG (29, 30). The minimum cleavage sequence of furin requires an arginine residue at P1 and P4 (RXXR↓) (33). Since the WNV NS2B/NS3 protease does not share the strict requirement of an arginine at P4, this restriction was exploited in attempt to modify the specificity of the serpin from furin to the WNV NS2B/NS3 protease. Three sequential rounds of site-directed mutagenesis were performed

on $^{mRFP\text{-}C}$Spn4A RCL to generate the RCL variants AVRRKR↓**G**IMS (P1′ variant), AVRRKR↓**GG**MS (P2′ variant) and AV**G**RKR↓**GG**MS (P4 variant) (Figure 4.1).

4.2.2. Testing the inhibitory properties of the RCL variants against recombinant furin

Complex formation is a hallmark of serpin-mediated inhibition that can be utilized to test the function of a serpin against a target protease (39-41). HEK 293A cells were singly-transfected with $^{mRFP\text{-}C}$Spn4A plasmid or with each RCL variant plasmid (P1′, P2′ or P4 variant) and harvested 48 h post-transfection. We utilized a recombinant furin complex assay, where crude cell lysates of each sample were incubated with recombinant furin for 30 min at 30°C then examined for a SDS-stable complex with Western blot analysis. A higher protein band, indicative of a SDS-stable furin•Spn4A complex, was observed in all samples except for the P4 variant demonstrating that the P4 variant lost its inhibitory properties towards furin (Figure 4.2).

4.2.3. Testing the inhibitory properties of the P4 variant against NS2B/NS3 protease

Next we wanted to test the inhibitory properties of the P4 variant directed against the ER membrane-associated full-length WNV viral protease heterocomplex, NS2B/NS3 within the intracellular microenvironment. HEK 293A cells were double-transfected with the WNV NS2B/NS3 protease plasmid and either $^{mRFP\text{-}C}$Spn4A plasmid or with P4 variant plasmid. Controls included single-transfections with either $^{mRFP\text{-}C}$Spn4A plasmid or with P4 variant plasmid. Cells were harvested 48 h post-transfection and examined for a SDS-stable complex with Western blot analysis (Figure 4.3A). No complex formation was observed

between the WNV NS2B/NS3 protease and the P4 variant suggesting that the serpin did not have inhibitory properties towards the viral protease.

Since no SDS-stable complex was detected, we hypothesized that the protein expression levels within the cell may have been too low to facilitate complex formation. We thought that incubating the crude cell lysates together might result in complex formation, demonstrating that the serpin was inhibitory towards the viral protease. HEK 293A cells were singly-transfected with either the P4 variant plasmid or with the WNV NS2B/NS3 protease plasmid and harvested 48 h post-transfection. The crude cell lysates were added together and either incubated overnight at room temperature or for 30 min at 30°C then examined for complex formation with Western blot analysis (Figure 4.3B). Controls included P4 variant alone-incubated overnight and no incubation. No complex formation was observed between the WNV NS2B/NS3 protease and the P4 variant suggesting that the serpin did not exhibit inhibitory properties towards the viral protease.

Given that no SDS-stable complex was observed with the crude cell lysate incubation experiment we hypothesized that using a highly transfectable cell-line (HEK 293T) would increase protein expression levels, thereby facilitating interaction and complex formation. The HEK 293T cell-line is a highly transfectable derivative of the HEK 293A cell-line. HEK 293T cells were double-transfected with the WNV NS2B/NS3 protease plasmid and the P4 variant plasmid or singly-transfected with P4 variant. Cells were harvested 48 h post-transfection and examined for a SDS-stable complex with Western blot analysis (Figure 4.3C). No complex formation was observed between the WNV NS2B/NS3 protease and the P4 variant. Taken together, these results demonstrate that the P4 variant does not form a SDS-stable complex with the WNV viral protease heterocomplex

NS2B/NS3, indicating that this Spn4A variant is not an effective serpin directed against the WNV NS2B/NS3 protease.

4.2.4. Testing the inhibitory properties of the P4 variant against recombinant NS3

Next we attempted to form a complex using a recombinant WNV NS3 protease complex assay. HEK 293T cells were transfected with the P4 variant plasmid and harvested 48 h post-transfection. Similar to the recombinant furin complex assay, the crude cell lysate was incubated with the recombinant WNV NS3 protease for 30 min at 37°C then examined for a SDS-stable complex with Western blot analysis (Figure 4.3D). No complex formation was observed between the recombinant WNV NS3 protease and the P4 variant indicating that the serpin did not exhibit inhibitory properties towards the recombinant NS3 protease.

4.2.5. Testing the effect of the P4 variant on NS2B/NS3 protease activity

Despite the lack of complex formation we hypothesized that the P4 variant might still inhibit the ability of the NS2B/NS3 protease to cleave substrate. To test this, we used our cell-based fluorescent substrate assay to evaluate the serpin's effect on protease activity. Our cell-based fluorescent assay has been described previously (22). Briefly, the assay consists of an ER membrane-anchored red fluorescent (DsRed) substrate that is specific for the ER membrane-associated full-length WNV viral protease heterocomplex, NS2B/NS3. As the WNV NS2B/NS3 protease recognizes the specific sequence, the substrate is proteolytically cleaved, releasing the DsRed fluorescent reporter group from the ER membrane into the cytoplasm. The substrate cleavage products can be detected with Western

blot analysis and the change in DsRed protein location from the ER membrane to the cytoplasm can be visualized with fluorescent microscopy (22).

We triple-transfected Huh7 cells with the WNV NS2B/NS3 protease plasmid, the P4 variant plasmid and the KRG substrate plasmid. Controls included double-transfection with the WNV NS2B/NS3 protease plasmid and the KRG substrate plasmid or single-transfection with the KRG substrate plasmid. Cells were harvested 24 h post-transfection and examined for substrate cleavage products with Western blot analysis (Figure 4.4A). No significant reduction in substrate cleavage by the NS2B/NS3 protease was observed indicating that the P4 variant had no effect on protease activity (Figure 4.4B). These results confirm that the P4 variant of Spn4A is unable to inhibit NS2B/NS3 protease activity.

4.2.6. Redesigning a specific WNV NS2B/NS3 serpin

Given that the $^{mRFP\text{-}C}$Spn4A P4 variant did not exhibit inhibitory properties towards the NS2B/NS3 protease we decided to generate a new serpin variant. In order to be able to use our cell-based fluorescent substrate assay to evaluate the serpin's effect on protease activity with fluorescent microscopy, we needed to create another serpin that lacked a red fluorescent group. Since our cell-based fluorescent assay consists of red fluorescent substrates (22), it would not be feasible to utilize any $^{mRFP\text{-}C}$Spn4A variants, as the red fluorescent protein patterns produced by the substrate or the serpin would be indistinguishable with fluorescent microscopy. As such, a new cytoplasmic Spn4A variant lacking the red fluorescent protein was created. Starting from the wild-type Spn4A (sp-hf-Spn4A-HDEL) the N-terminal secretory signal peptide and the C-terminal ER retention

motif were removed creating a new cytoplasmic Spn4A variant (hf-Spn4A) ($Spn4A^C$) (Figure 4.5).

We hypothesized that the lack of inhibition of the serpin might be due to the RCL sequence. We had demonstrated with our cell-based fluorescent substrate assay that the full-length viral protease heterocomplex, NS2B/NS3, efficiently processed substrate corresponding to the NS4B/NS5 protein junction site sequence (KPGLKR↓GGAK) whereas substrate corresponding to the NS2B/NS3 protein junction site sequence (LQYTKR↓GGVL) was poorly processed (22), despite the presence of the preferred KR↓GG minimal site in both sequences (29, 30). These results strongly suggested that the other residues present within the cleavage sequence contribute to protease specificity (22). As serpin inhibition is intrinsically dependant on the cleavage of the RCL (40, 41), we hypothesized that mutating other residues within the RCL would generate a specific inhibitor. Based on this, residues within the RCL of $Spn4A^C$ were modified via four sequential rounds of site-directed mutagenesis (AVRRKR↓AIMS → AVRRKR↓AI**AK** → AVRRKR↓**GGAK** → **KP**R**L**KR↓**GGAK** → **KPGL**KR↓**GGAK**) generating the resultant $Spn4A^C$ RCL 4B5 variant (4B5 variant) (Figure 4.5).

4.2.7. Testing the inhibitory properties of the 4B5 variant against NS2B/NS3 protease

We tested the inhibitory properties of the 4B5 variant against the WNV NS2B/NS3 protease by double-transfecting Huh7.5.1 cells with the WNV NS2B/NS3 protease plasmid and the 4B5 variant plasmid. Cells were harvested 24 h post-transfection and examined for a SDS-stable complex with Western blot analysis (Figure 4.6A). No complex formation was observed between the WNV NS2B/NS3 protease and the 4B5 variant.

Due to the lack of complex formation, we hypothesized that the expression of one protein had to occur prior to the expression of the other in order to facilitate complex formation. To test this, Huh7.5.1 cells were singly-transfected with the WNV NS2B/NS3 protease plasmid or the 4B5 variant plasmid. 24 h post-first transfection cells were singly-transfected with the opposite plasmid ($4B5_1 \rightarrow WNV_2$; $WNV_1 \rightarrow 4B5_2$). Cells were harvested 24 h post-second transfection and examined for a SDS-stable complex with Western blot analysis (Figure 4.6B). No complex formation was observed between the WNV NS2B/NS3 protease and the 4B5 variant. Taken together, these results demonstrate that the 4B5 variant does not form a complex with the WNV viral protease heterocomplex NS2B/NS3, indicating that this Spn4A variant is not an effective inhibitor of the WNV NS2B/NS3 protease.

4.3. Discussion

Based on previous reports of successful serpin-based inhibition (33-36, 42), we attempted to rationally design a serpin directed against the ER membrane-associated full-length WNV viral protease heterocomplex, NS2B/NS3, within the cell. Mutation of specific RCL residues results in a change in specificity of a serpin (33, 42, 43). For example, a naturally occurring mutation within the RCL of $alpha_1$-antitrypsin at residue P1 (AIPM↓ → AIP**R**↓) changed the serpin's specificity from elastase to thrombin ($alpha_1$-antitrypsin Pittsburg) (α_1-PIT), which had been identified in a patient who had a severe thrombin deficiency (43).

Furin mediates the processing of several proteins that pathogens require for cytotoxicity or for the generation of infectious virus particles. As such serpin-based inhibitors directed against furin have been produced (32, 33, 37). One such inhibitor was

engineered from α_1-PIT by mutating the P4 residue within the RCL from A → R (AIPR↓ → **R**IPR↓) (alpha$_1$-antitrypsin Portland) (α_1-PDX), resulting in the minimum cleavage sequence of furin (RXXR↓) present within the RCL (33). Alpha$_1$-PDX has been shown to be a potent furin inhibitor (K_i = 600pM) and has been used to prevent furin activity, blocking the processing of HIV-1 gp160, measles virus F protein, *Pseudomonas* exotoxin A protein and human cytomegalovirus glycoprotein B (33-36). Furthermore, our laboratory has previously characterized a potent endogenous furin inhibitor from *Drosophila melanogaster*, Spn4A (32). Richer et al., (2004) demonstrated *in vitro* that Spn4A inhibits furin with a K_i of 13pM and exhibited a 1:1 stoichiometry with furin, indicating that Spn4A is the most potent furin inhibitor currently described (32). As many pathogens require furin for activation, inhibiting its activity by Spn4A represents a potentially promising therapeutic approach.

While, the inhibition of furin demonstrates a potential therapeutic avenue, targeting the viral protease provides an alternative approach, which could be used in combination with furin inhibitors. To this effect, Richer et al., (2004) previously demonstrated that modifying specific residues within RCL of a related *Drosophila* serpin, Spn6, changed its specificity from trypsin to the HCV NS3/NS4A protease, generating a specific HCV NS3/NS4A serpin (42). The similarity in cleavage sequence preference between furin and the WNV NS2B/NS3 protease, suggested that altering specific residues within the RCL of Spn4A would generate a serpin with specific inhibitory properties towards the WNV NS2B/NS3 protease. We had previously demonstrated with our cell-based fluorescent substrate assay that the ER membrane-associated full-length WNV NS2B/NS3 protease, efficiently cleaves substrate corresponding to the NS4B/NS5 protein junction site sequence

(KPGLKR↓GGAK) (22). We hypothesized that modifying only a few residues within the RCL of Spn4A or altering the residues to correspond to the NS4B/NS5 protein junction site sequence would produce the specificity needed for the formation of a NS2B/NS3 protease•Spn4A complex. However, we were unsuccessful in creating a specific serpin directed against the ER membrane-associated full-length WNV viral protease heterocomplex, NS2B/NS3.

Since the full-length WNV NS2B/NS3 protease is associated to the ER membrane facing towards the cytoplasm (5, 22), we rationally designed Spn4A to be located within the cytosol of the cell. While, we hypothesized that the cytoplasmic Spn4A would encounter the WNV NS2B/NS3 protease at the ER membrane resulting in a NS2B/NS3 protease•Spn4A complex, our results demonstrate that complex formation and inhibition did not occur. A possible explanation might actually be related to the cytoplasmic location of Spn4A. Targeting Spn4A to the ER membrane may potentially result in a NS2B/NS3 protease•Spn4A complex and resultant protease inhibition. However, this approach raises several further questions such as: Can Spn4A maintain its inhibitory properties if targeted at the ER membrane? Can Spn4A complex with ER membrane-associated proteases? As the mechanism of action of serpins involves target protease translocation to the bottom of the serpin (40, 41), membrane-association of a protease may prevent the capacity of a serpin to properly form the inhibitory complex. Specifically, the target protease membrane-association or its interaction with other proteins at the membrane might be too strong for the serpin's mechanism of action to overcome. These questions warrant further investigation for the rational drug design of ER membrane-associated viral proteases.

Protein Z-dependent protease inhibitor (ZPI), a member of the serpin superfamily, inhibits factor Xa, a serine protease responsible for the generation of thrombin in the coagulation cascade (44, 45). ZPI is an unusual serpin, in that, it requires protein Z, anionic phospholipids and calcium as cofactors to inhibit factor Xa (46). Moreover, ZPI inhibition of factor Xa is only transient and does not result in the formation of a SDS-stable complex (47). Additionally, it was observed that the factor Xa•ZPI complex is less stable under physiologic conditions and is only detected in acidic conditions. The tendency of the complex to dissociate at physiologic pH most likely explains the inability to observe a SDS-stable complex (45). Considering that serpins are able to inhibit membrane-associated proteases under certain conditions, suggests that utilizing Spn4A directed against the WNV NS2B/NS3 protease remains a valid approach and requires further optimization.

Despite our unsuccessful attempts to generate a serpin directed against the ER membrane-associated full-length WNV viral protease heterocomplex, NS2B/NS3, our results highlight the importance of studying viral proteases within the intracellular microenvironment. Based on the *in vitro* data from our group, demonstrating the inhibition of the HCV NS3/NS4A protease by Spn6 (42), theoretically, altering the RCL of Spn4A should have produced a serpin directed against the WNV NS2B/NS3 protease. Similarly to the WNV NS2B/NS3 protease, the HCV NS3/NS4A protease associates with membranes within the cell (5). As such, it would be interesting to test the inhibitory properties of Spn6 against the HCV NS3/NS4A protease within the intracellular microenvironment to evaluate whether protease inhibition is still observed. Our results emphasize the need for cell-based assays to study viral proteases within a physiologically relevant environment, the

information gathered will provide insight into the rational drug design to membrane-associated viral proteases.

4.4. Material and methods

4.4.1. Plasmid constructs

WNV NS2B/NS3 protease plasmid: the full-length WNV viral protease heterocomplex, NS2B/NS3, was cloned into a dual-labeled mammalian expression vector (pFLAG-NS2B/NS3-myc) and has been previously described (22) (indicated as WNV NS2B/NS3 protease). KRG substrate plasmid: the KRG substrate plasmid has been previously described (22) (indicated as KRG). Wild-type laboratory Spn4A serpin plasmid: the wild-type laboratory Spn4A plasmid (sp-hf-Spn4A-HDEL) has been previously described (32). Spn4A cytoplasmic red fluorescent variant: hf-Spn4A-HDEL was PCR amplified from the wild-type laboratory Spn4A plasmid construct and cloned into the pDsRed-Monomer-C1 expression vector (Clontech Laboratories, Inc., Mountain View, CA, USA) using the SacI and EcoRI restriction sites (Forward primer: 5'-CCGAGCTCTCGACTACAAAGACGACG-3'; Reverse primer: 5'-GGAATTCTCACAGCTCATCATGC-3'; SacI and EcoRI restriction sites underlined, respectively), creating a red fluorescent cytoplasmic variant of Spn4A (mRFP-hf-Spn4A-HDEL) (indicated as $^{mRFP\text{-}C}$Spn4A) (Figure 4.1). $^{mRFP\text{-}C}$Spn4A RCL variants: using the $^{mRFP\text{-}C}$Spn4A plasmid the RCL was mutated with three sequential rounds of site-directed mutagenesis (Stratagene, La Jolla, CA, USA) to generate three RCL variants AVRRKR↓**G**IMS (P1′ variant), AVRRKR↓**GG**MS (P2′ variant) and AV**G**RKR↓**GG**MS (P4 variant) (Figure 4.1); sequential RCL mutations are highlighted in bold. All mutations

were confirmed by automated sequencing (UBC DNA Sequencing Laboratory). Spn4A cytoplasmic variant: hf-Spn4A was PCR amplified from the wild-type laboratory Spn4A plasmid construct and cloned into the pcDNA3.1(+) expression vector (Invitrogen, Burlington, ON, CA) using the KpnI and NotI restriction sites (Forward primer: 5'-ATCGGGTACCATGCACCACCACCACCACCACGAC-3'; Reverse primer: 5'-ATCGGCGGCCGCTCACTCGCTGGAGGCGAAGGTATTTTC-3'; KpnI and NotI restriction sites underlined, respectively) creating a cytoplasmic variant of Spn4A (hf-Spn4A) (indicated as $Spn4A^{C}$) (Figure 4.5). $Spn4A^{C}$ RCL 4B5 variant: using the $Spn4A^{C}$ plasmid the RCL was mutated with four sequential rounds of site-directed mutagenesis (Stratagene, La Jolla, CA, USA) to generate the 4B5 variant (AVRRKR↓AIMS → AVRRKR↓AI**AK** → AVRRKR↓**GGAK** → **KP**R**L**KR↓**GGAK** → **KPGL**KR↓**GGAK**) (Figure 4.5); sequential RCL mutations are highlighted in bold. All mutations were confirmed by automated sequencing (UBC DNA Sequencing Laboratory, BC, CA).

4.4.2. Cell culture

Human embryonic kidney cells (HEK 293A cells and HEK 293T cells) (HEK 293T cells are a highly transfectable cell-line derivative of HEK 293A cells) were grown in complete Dulbecco's modified Eagle's medium (DMEM cat no. 11965-092, Invitrogen) supplemented with heat-inactivated 10% v/v fetal bovine serum (Invitrogen), 50 units/ml penicillin, 50 µg/ml streptomycin (Invitrogen). Cells were grown at 37ºC in the presence of 5% CO_2. Human hepatocellular carcinoma cells (Huh7 cells and Huh7.5.1 cells) (Huh7.5.1 cells are a cell-line derivative of Huh7) were grown in complete DMEM (cat no. 11965-092) (Invitrogen) supplemented with heat-inactivated 10% v/v fetal bovine serum (Invitrogen), 50

units/ml penicillin, 50 μg/ml streptomycin, and 100 μM non-essential amino acids (Invitrogen). Cells were grown at 37ºC in the presence of 5% CO_2. WNV has a broad tissue tropism thus experimentation in varying cell lines is justifiable.

4.4.3. Transfections

Transfections of each cell-line (HEK 293A, HEK 293T, Huh7, Huh7.5.1) were performed in the same manner. Six well plates were seeded with cells at 200,000 cells/well and grown to approximately 80% confluency. Cells (HEK 293A; HEK 293T; Huh7.5.1) were either double-transfected with 2.5 μg of WNV NS2B/NS3 protease plasmid and 2.5 μg of corresponding Spn4A plasmid ($^{mRFP\text{-}C}$Spn4A; P4 variant; 4B5 variant) using *Trans*IT-LT1 Transfection Reagent (Mirus Bio, Madison, WI, USA) or cells (HEK 293A; HEK 293T) were singly-transfected with 2.5 μg of WNV NS2B/NS3 protease plasmid or 2.5 μg of corresponding Spn4A plasmid ($^{mRFP\text{-}C}$Spn4A; P1′ variant; P2′ variant; P4 variant). For cell-based substrate assays, Huh7 cells were triple-transfected with 2.5 μg of WNV NS2B/NS3 protease plasmid and 2.5 μg of P4 variant plasmid and 2.5 μg of KRG substrate plasmid. Controls included double-transfection of cells (Huh7) with 2.5 μg of WNV NS2B/NS3 protease plasmid and 2.5 μg of KRG substrate plasmid. Cells were harvested for Western blot analysis at 24 h or 48 h post-transfection.

4.4.4. Recombinant furin complex assay

Ten microliters of crude cell lysates (48 h post single-transfection of HEK 293A cells with either $^{mRFP\text{-}C}$Spn4A; P1′ variant; P2′ variant; P4 variant plasmids) was added to 0.01475 ml of furin reaction buffer (100 mM HEPES pH 7.5, 1 mM $CaCl_2$, 0.5% v/v Triton

X-100, 1x protease inhibitor cocktail (Roche, Laval, QC, Canada)). Recombinant human furin (R&D Systems, Inc., Minneapolis, MN, USA) was added (final concentration 1.73 μg/ml) and incubated (30 min, 30°C) (total reaction volume 0.025 ml). Five microliters of 50 mM EDTA was added to stop the reaction. Thirty microliters of 2x SDS-PAGE sample buffer (0.1 M Tris pH 6.8, 20% v/v glycerol, 4% w/v SDS, 0.002% w/v bromophenol blue, 0.7 M 2-mercaptoethanol) was added and samples were boiled (10 min, 95°C) prior to Western blot analysis.

4.4.5. Recombinant WNV NS3 protease complex assay

Ten microliters of crude cell lysates (48 h post single-transfection of HEK 293T cells with either $^{mRFP\text{-}C}$Spn4A; P4 variant plasmid) was added to 0.01475 ml of WNV NS3 reaction buffer (50 mM HEPES pH 7.5, 0.1% v/v Triton X-100). Recombinant WNV NS3 protease ($NS2B_{40}$-G_4SG_4-NS3pro) (R&D Systems Inc.) was added (final concentration 2.0 μg/ml or 12.0 μg/ml) and incubated (30 min, 37°C) (total reaction volume 0.025 ml). Five microliters of 50 mM EDTA was added to stop the reaction. Thirty microliters of 2x SDS-PAGE sample buffer (0.1 M Tris pH 6.8, 20% v/v glycerol, 4% w/v SDS, 0.002% w/v bromophenol blue, 0.7 M 2-mercaptoethanol) was added and samples were boiled (10 min, 95°C) prior to Western blot analysis.

4.4.6. Western blot analysis

Western blot analysis has been described previously (22) with the following modifications. Cell pellets from HEK 293A and HEK 293T transfections were resuspended in 0.1 ml hypotonic lysis buffer containing 1x protease inhibitor cocktail (Roche). Cell

pellets from Huh7 transfections were resuspended in 0.2 ml hypotonic lysis buffer containing 1x protease inhibitor cocktail (Roche). Cell pellets from Huh7.5.1 transfections were resuspended in 0.06 ml hypotonic lysis buffer containing 1x protease inhibitor cocktail (Roche). The membranes were probed according to Odyssey Infrared Imaging System Western blot analysis protocol (LI-COR Biosciences, Lincoln, NE, USA). Primary and secondary antibodies were diluted in Odyssey Blocking Buffer (LI-COR Biosciences) containing 0.1% v/v Tween-20 (Sigma-Aldrich Corp., St. Louis, MO, USA). For complex formation with $^{mRFP\text{-}C}$Spn4A variants, membranes were probed with primary anti-FLAG polyclonal antibody (1:1000, Abcam Inc., Cambridge, MA, USA) (60 min) and with secondary IRDye 800-conjugated goat anti-rabbit polyclonal antibody (1:10,000, LI-COR Biosciences) (30 min) or with secondary IRDye 680-conjugated goat anti-rabbit polyclonal antibody (1:10,000, LI-COR Biosciences) (30 min). For cell-based KRG substrate assay, membrane was probed with primary antibodies anti-DsRed polyclonal antibody (1:1,000, Clontech Laboratories, Mountain View, CA, USA) and anti-FLAG polyclonal antibody (1:1000, Sigma-Aldrich Corp) (60 min). Secondary antibody was IRDye 680-conjugated goat anti-rabbit polyclonal antibody (1:10,000, LI-COR Biosciences) (30 min). For complex formation with Spn4A^{C} RCL 4B5 variant, membranes were probed with primary anti-NS3 monoclonal antibody (2 μg/ml, R&D Systems Inc.) (60 min). Secondary antibody was IRDye 800-conjugated goat anti-mouse monoclonal antibody (1:10,000, LI-COR Biosciences) (30 min). Membranes were then imaged using an Odyssey Infrared Imaging System (LI-COR Biosciences).

4.4.7. Quantification and statistical analysis

Analysis and quantification of integrated band intensity were performed using the Odyssey Infrared Imaging System application software version 2.1.12 (LI-COR Biosciences). The percent of substrate cleaved was calculated by dividing the cleaved signal by the total signal (cleaved plus intact), thereby normalizing the readout for each sample. Averages were calculated from two independent experiments run in duplicate. GraphPad Prism (GraphPad Software, Inc., La Jolla, CA, USA) was used for graphical representation and statistical analysis. P values were obtained for two-tailed, unpaired, student's *t*-test, and significance was noted when $p<0.05$.

Figure 4.1

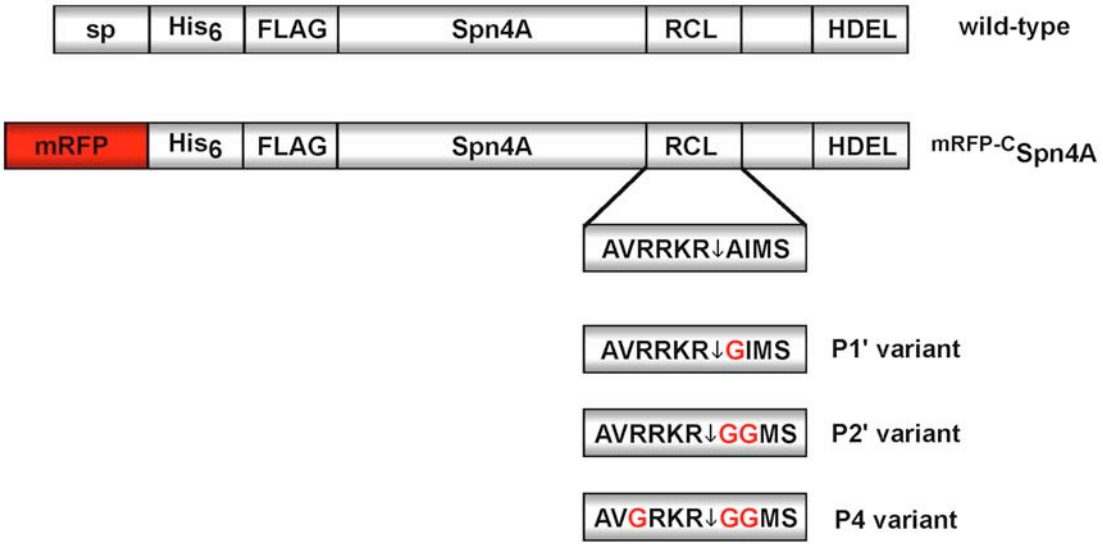

Figure 4.1. Designing a specific WNV NS2B/NS3 serpin

Wild-type laboratory serpin, Spn4A, contains a N-terminal secretory signal peptide (sp) sequence, two epitope tags (His-tag and FLAG-tag), a reactive centre loop (RCL) that contains the cleavage sequence AVRRKR↓AIMS and a C-terminal ER retention motif that is comprised of the amino acids His-Asp-Glu-Leu (HDEL) (32). The signal peptide was removed and a monomeric red fluorescent protein (mRFP) was added N-terminal, to create a cytoplasmic variant of Spn4A ($^{mRFP\text{-}C}$Spn4A). The $^{mRFP\text{-}C}$Spn4A RCL was modified with three sequential rounds of site-directed mutagenesis to generate the RCL variants AVRRKR↓**G**IMS (P1′ variant), AVRRKR↓**GG**MS (P2′ variant) and AV**G**RKR↓**GG**MS (P4 variant). Mutations indicated in red font.

Figure 4.2

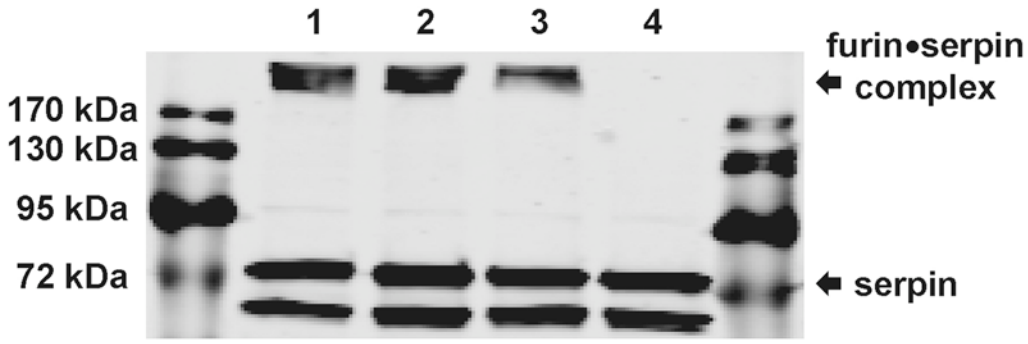

Figure 4.2. Inhibitory properties of the RCL variants against recombinant furin

HEK 293A cells were singly-transfected with $^{mRFP\text{-}C}$Spn4A plasmid or with each RCL variant plasmid (P1′, P2′ or P4 variant) and harvested 48 h post-transfection. Crude cell lysates of each sample were incubated with recombinant furin (rfurin = 1.73 μg/ml) for 30 min at 30°C then examined for a SDS-stable complex. Membranes were probed with anti-FLAG polyclonal antibody. A higher protein band (>170 kDa), indicative of a SDS-stable furin•serpin complex, was observed in all samples except for the P4 variant. Non-complex serpin detected approximately at 74 kDa and 70 kDa. (1 = $^{mRFP\text{-}C}$Spn4A + rfurin; 2 = P1′ variant + rfurin; 3 = P2′ variant + rfurin; 4 = P4 variant + rfurin).

Figure 4.3. Inhibitory properties of the P4 variant against NS2B/NS3 protease

(A) HEK 293A cells were double-transfected with the NS2B/NS3 protease plasmid (WNV) and either $^{mRFP\text{-}C}$Spn4A plasmid or with P4 variant plasmid (P4). Controls included single-transfections with either $^{mRFP\text{-}C}$Spn4A plasmid or with P4 variant plasmid. Cells were harvested 48 h post-transfection and examined for a SDS-stable complex. (B) HEK 293A cells were singly-transfected with either the P4 variant plasmid (P4) or with the NS2B/NS3 protease plasmid (WNV) then harvested at 48 h post-transfection. Crude cell lysates were added together and incubated overnight (O/N) at room temperature or for 30 min at 30°C then examined for a SDS-stable complex. Controls included P4 variant only incubated overnight (O/N) and no incubation (time = 0 min). (C) HEK 293T cells were double-transfected with the NS2B/NS3 protease plasmid (WNV) and the P4 variant plasmid (P4) or single-transfection with P4 variant. Cells were harvested 48 h post-transfection and examined for a SDS-stable complex. (D) P4 variant inhibitory properties were tested against recombinant NS3. HEK 293T cells were singly-transfected with the P4 variant plasmid (P4) and harvested 48 h post-transfection. Crude cell lysate was incubated with recombinant WNV NS3 protease (rWNV = 2 μg/ml or 12 μg/ml) for 30 min at 37°C then examined for a SDS-stable complex. Non-complex serpin detected at 74 kDa and 70 kDa. Membranes were probed with anti-FLAG polyclonal antibody.

Figure 4.3

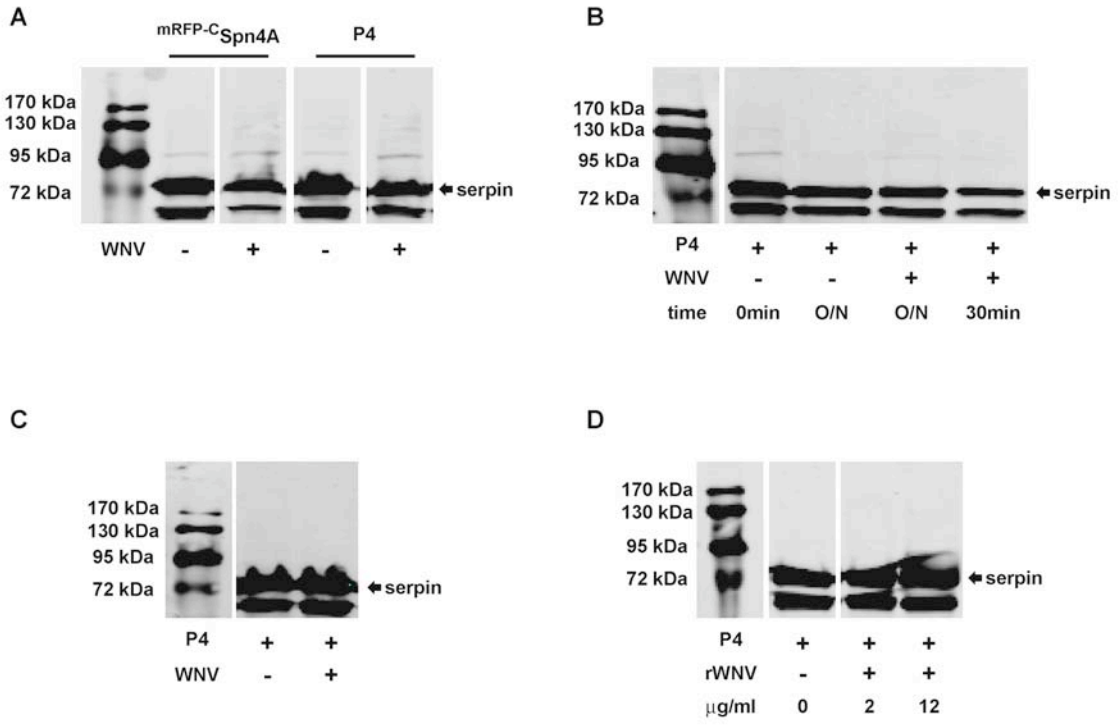
A
mRFP-CSpn4A
P4
170 kDa
130 kDa
95 kDa
72 kDa
serpin
WNV - + - +
B
170 kDa
130 kDa
95 kDa
72 kDa
serpin
P4 + + + +
WNV - - + +
time 0min O/N O/N 30min
C
170 kDa
130 kDa
95 kDa
72 kDa
serpin
P4 + +
WNV - +
D
170 kDa
130 kDa
95 kDa
72 kDa
serpin
P4 + + +
rWNV - + +
μg/ml 0 2 12

Figure 4.4. Testing the effects of the P4 variant on NS2B/NS3 protease activity

(A) Huh7 cells were either singly-transfected with the KRG substrate plasmid (KRG), or double-transfected with KRG and the NS2B/NS3 protease plasmid (WNV), or triple-transfected with KRG and WNV and the P4 variant plasmid (P4). Cells were harvested 24 h post-transfection and examined for KRG substrate cleavage products and an SDS-stable complex. Membranes were probed with anti-DsRed polyclonal antibody (for substrate detection) and anti-FLAG polyclonal antibody (for complex detection). Intact KRG substrate detected at ~34 kDa, cleaved KRG substrate detected at ~29 kDa and non-complex serpin detected at 74 kDa and 70 kDa. (B) The percent of substrate cleaved was quantified from the above Western blot analysis. No significant differences were observed between KRG + WNV and KRG + WNV + P4 ($p = 0.6$).

Figure 4.4

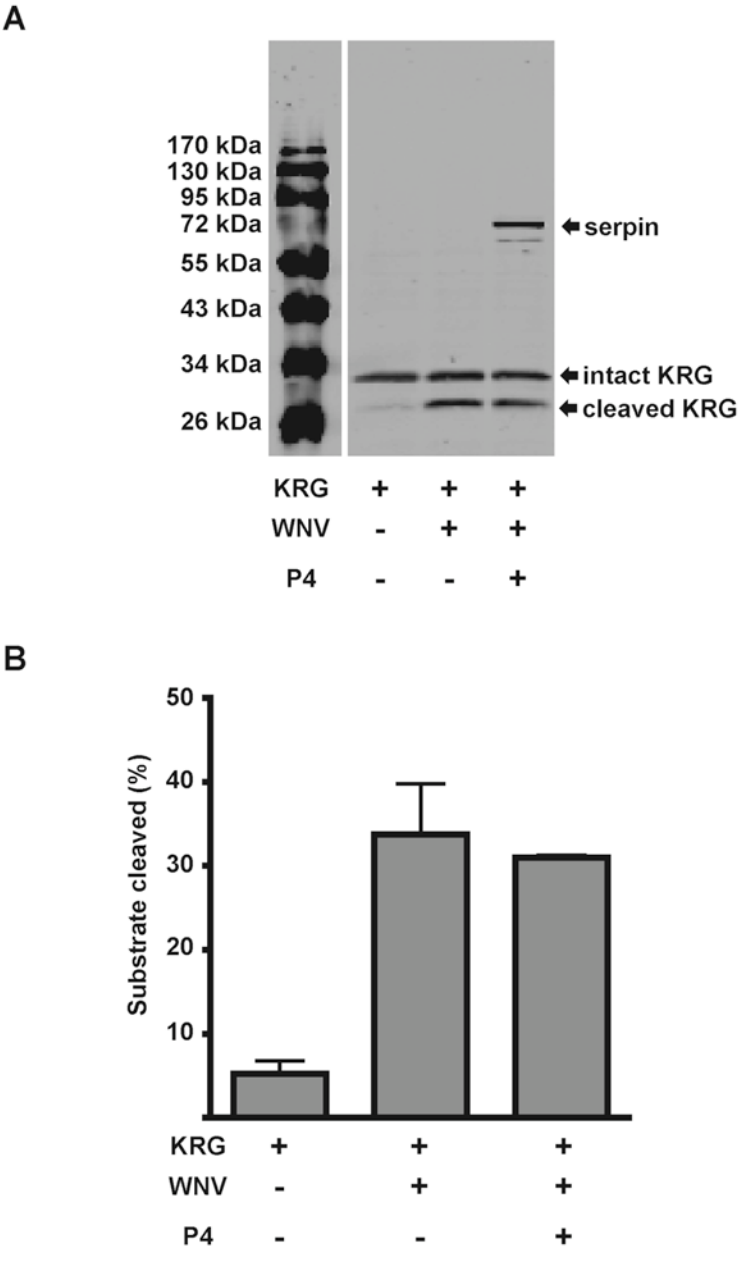
A
170 kDa
130 kDa
95 kDa
72 kDa
55 kDa
43 kDa
34 kDa
26 kDa
serpin
intact KRG
cleaved KRG
KRG + + +
WNV - + +
P4 - - +
B
Substrate cleaved (%)
50
40
30
20
10
KRG + + +
WNV - + +
P4 - - +

Figure 4.5

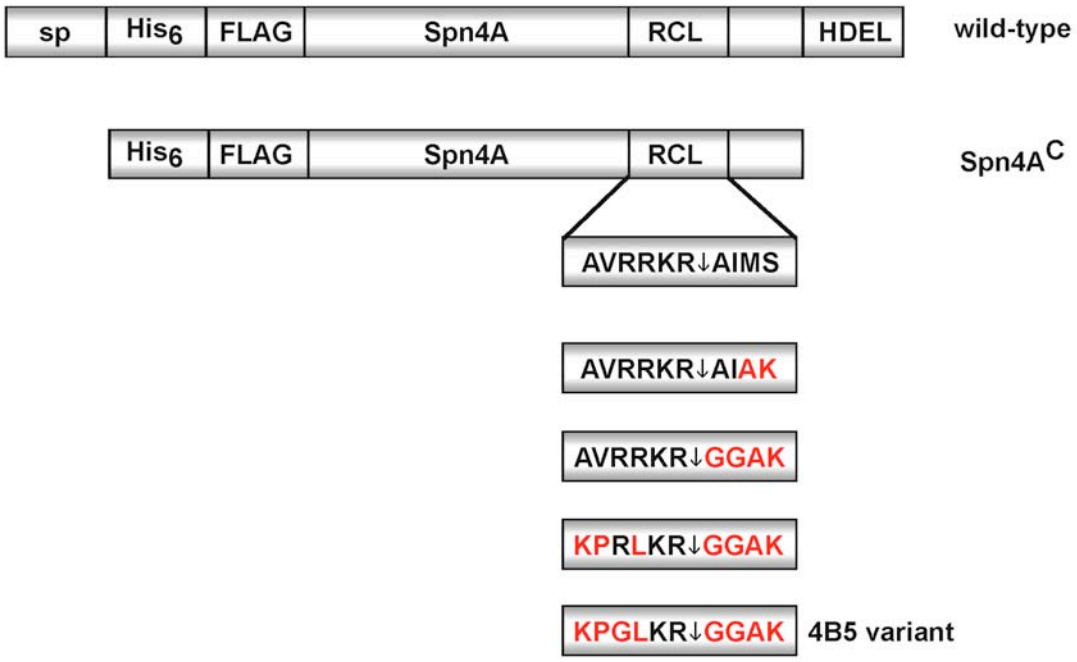

Figure 4.5. Redesigning a specific WNV NS2B/NS3 serpin

The generation of a cytoplasmic Spn4A variant, created from the wild-type laboratory Spn4A, which lacks the N-terminal signal peptide and C-terminal ER retention motif ($Spn4A^{C}$). The $Spn4A^{C}$ RCL was modified with four sequential rounds of site-directed mutagenesis (AVRRKR↓AIMS → AVRRKR↓AI**AK** → AVRRKR↓**GGAK** → **KP**R**L**KR↓**GGAK** → **KPGL**KR↓**GGAK**) generating the resultant $Spn4A^{C}$ RCL 4B5 variant (4B5 variant). Mutations indicated in red font.

Figure 4.6

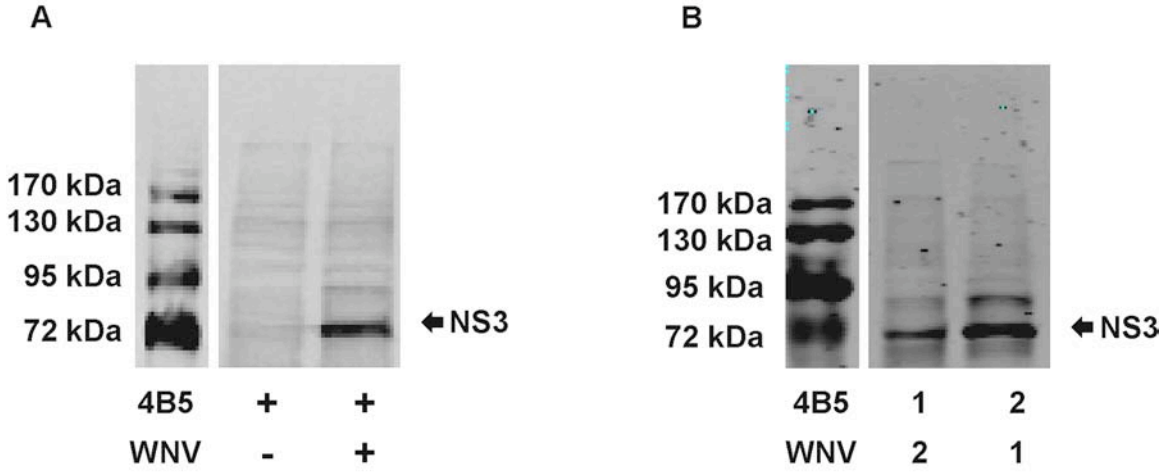

Figure 4.6. Inhibitory properties of the 4B5 variant against NS2B/NS3 protease

(A) Huh7.5.1 cells were double-transfected with the NS2B/NS3 protease plasmid (WNV) and the 4B5 variant plasmid (4B5). Cells were harvested 24 h post-transfection and examined for a SDS-stable complex. (B) Huh7.5.1 cells were singly-transfected with the NS2B/NS3 protease plasmid (WNV) or the 4B5 variant plasmid (4B5) then 24 h post-first transfection, cells were singly-transfected with the opposite plasmid ($4B5_1 \rightarrow WNV_2$; $WNV_1 \rightarrow 4B5_2$). Cells were harvested 24 h post-second transfection and examined for a SDS-stable complex. Membranes were probed with anti-NS3 monoclonal antibody. NS3 detected at 70 kDa and NS2B/NS3 heterocomplex detected at 85 kDa.

4.5. References

1. (CDC), C. o. D. C. a. P. 1999. Outbreak of West Nile-like viral encephalitis--New York, 1999. *MMWR Morb Mortal Wkly Rep* 48:845-849.
2. Castle, E., T. Nowak, U. Leidner, and G. Wengler. 1985. Sequence analysis of the viral core protein and the membrane-associated proteins V1 and NV2 of the flavivirus West Nile virus and of the genome sequence for these proteins. *Virology* 145:227-236.
3. Castle, E., U. Leidner, T. Nowak, and G. Wengler. 1986. Primary structure of the West Nile flavivirus genome region coding for all nonstructural proteins. *Virology* 149:10-26.
4. Yamshchikov, V. F., and R. W. Compans. 1993. Regulation of the late events in flavivirus protein processing and maturation. *Virology* 192:38-51.
5. Lindenbach, B. D., H. Thiel, and C. M. Rice. 2007. Flaviviridae: The viruses and their replication. In *Fields Virology*, 5 ed. D. M. Knipe, and P. M. Howley, eds. Lippincott William and Wilkins, Philadelphia.
6. Brinton, M. A. 2002. The molecular biology of West Nile Virus: a new invader of the western hemisphere. *Annu Rev Microbiol* 56:371-402.
7. Rice, C. M., E. M. Lenches, S. R. Eddy, S. J. Shin, R. L. Sheets, and J. H. Strauss. 1985. Nucleotide sequence of yellow fever virus: implications for flavivirus gene expression and evolution. *Science* 229:726-733.
8. Castle, E., and G. Wengler. 1987. Nucleotide sequence of the 5'-terminal untranslated part of the genome of the flavivirus West Nile virus. *Arch Virol* 92:309-313.

9. Chambers, T. J., R. C. Weir, A. Grakoui, D. W. McCourt, J. F. Bazan, R. J. Fletterick, and C. M. Rice. 1990. Evidence that the N-terminal domain of nonstructural protein NS3 from yellow fever virus is a serine protease responsible for site-specific cleavages in the viral polyprotein. *Proc Natl Acad Sci U S A* 87:8898-8902.

10. Wengler, G., G. Czaya, P. M. Farber, and J. H. Hegemann. 1991. In vitro synthesis of West Nile virus proteins indicates that the amino-terminal segment of the NS3 protein contains the active centre of the protease which cleaves the viral polyprotein after multiple basic amino acids. *J Gen Virol* 72 (Pt 4):851-858.

11. Cahour, A., B. Falgout, and C. J. Lai. 1992. Cleavage of the dengue virus polyprotein at the NS3/NS4A and NS4B/NS5 junctions is mediated by viral protease NS2B-NS3, whereas NS4A/NS4B may be processed by a cellular protease. *J Virol* 66:1535-1542.

12. Amberg, S. M., A. Nestorowicz, D. W. McCourt, and C. M. Rice. 1994. NS2B-3 proteinase-mediated processing in the yellow fever virus structural region: in vitro and in vivo studies. *J Virol* 68:3794-3802.

13. Uchil, P. D., and V. Satchidanandam. 2003. Architecture of the flaviviral replication complex. Protease, nuclease, and detergents reveal encasement within double-layered membrane compartments. *J Biol Chem* 278:24388-24398.

14. Bazan, J. F., and R. J. Fletterick. 1989. Detection of a trypsin-like serine protease domain in flaviviruses and pestiviruses. *Virology* 171:637-639.

15. Gorbalenya, A. E., A. P. Donchenko, E. V. Koonin, and V. M. Blinov. 1989. N-terminal domains of putative helicases of flavi- and pestiviruses may be serine proteases. *Nucleic Acids Res* 17:3889-3897.

16. Gorbalenya, A. E., E. V. Koonin, A. P. Donchenko, and V. M. Blinov. 1989. Two related superfamilies of putative helicases involved in replication, recombination, repair and expression of DNA and RNA genomes. *Nucleic Acids Res* 17:4713-4730.

17. Wengler, G. 1991. The carboxy-terminal part of the NS 3 protein of the West Nile flavivirus can be isolated as a soluble protein after proteolytic cleavage and represents an RNA-stimulated NTPase. *Virology* 184:707-715.

18. Wengler, G., T. Nowak, and E. Castle. 1990. Description of a procedure which allows isolation of viral nonstructural proteins from BHK vertebrate cells infected with the West Nile flavivirus in a state which allows their direct chemical characterization. *Virology* 177:795-801.

19. Clum, S., K. E. Ebner, and R. Padmanabhan. 1997. Cotranslational membrane insertion of the serine proteinase precursor NS2B-NS3(Pro) of dengue virus type 2 is required for efficient in vitro processing and is mediated through the hydrophobic regions of NS2B. *J Biol Chem* 272:30715-30723.

20. Yamshchikov, V. F., D. W. Trent, and R. W. Compans. 1997. Upregulation of signalase processing and induction of prM-E secretion by the flavivirus NS2B-NS3 protease: roles of protease components. *J Virol* 71:4364-4371.

21. Brinkworth, R. I., D. P. Fairlie, D. Leung, and P. R. Young. 1999. Homology model of the dengue 2 virus NS3 protease: putative interactions with both substrate and NS2B cofactor. *J Gen Virol* 80 (Pt 5):1167-1177.

22. Condotta, S. A., M. M. Martin, M. Boutin, and F. Jean. Detection and in-cell selectivity profiling of the full-length West Nile virus NS2B/NS3 serine protease using membrane-anchored fluorescent substrates. *Biol Chem* 391:549-559.

23. Chambers, T. J., A. Grakoui, and C. M. Rice. 1991. Processing of the yellow fever virus nonstructural polyprotein: a catalytically active NS3 proteinase domain and NS2B are required for cleavages at dibasic sites. *J Virol* 65:6042-6050.

24. Chambers, T. J., A. Nestorowicz, S. M. Amberg, and C. M. Rice. 1993. Mutagenesis of the yellow fever virus NS2B protein: effects on proteolytic processing, NS2B-NS3 complex formation, and viral replication. *J Virol* 67:6797-6807.

25. Yusof, R., S. Clum, M. Wetzel, H. M. Murthy, and R. Padmanabhan. 2000. Purified NS2B/NS3 serine protease of dengue virus type 2 exhibits cofactor NS2B dependence for cleavage of substrates with dibasic amino acids in vitro. *J Biol Chem* 275:9963-9969.

26. Nall, T. A., K. J. Chappell, M. J. Stoermer, N. X. Fang, J. D. Tyndall, P. R. Young, and D. P. Fairlie. 2004. Enzymatic characterization and homology model of a catalytically active recombinant West Nile virus NS3 protease. *J Biol Chem* 279:48535-48542.

27. Chappell, K. J., T. A. Nall, M. J. Stoermer, N. X. Fang, J. D. Tyndall, D. P. Fairlie, and P. R. Young. 2005. Site-directed mutagenesis and kinetic studies of the West Nile Virus NS3 protease identify key enzyme-substrate interactions. *J Biol Chem* 280:2896-2903.

28. Shiryaev, S. A., A. E. Aleshin, B. I. Ratnikov, J. W. Smith, R. C. Liddington, and A. Y. Strongin. 2007. Expression and purification of a two-component flaviviral

proteinase resistant to autocleavage at the NS2B-NS3 junction region. *Protein Expr Purif* 52:334-339.

29. Shiryaev, S. A., I. A. Kozlov, B. I. Ratnikov, J. W. Smith, M. Lebl, and A. Y. Strongin. 2007. Cleavage preference distinguishes the two-component NS2B-NS3 serine proteinases of Dengue and West Nile viruses. *Biochem J* 401:743-752.

30. Shiryaev, S. A., B. I. Ratnikov, A. E. Aleshin, I. A. Kozlov, N. A. Nelson, M. Lebl, J. W. Smith, R. C. Liddington, and A. Y. Strongin. 2007. Switching the substrate specificity of the two-component NS2B-NS3 flavivirus proteinase by structure-based mutagenesis. *J Virol* 81:4501-4509.

31. Yu, I. M., W. Zhang, H. A. Holdaway, L. Li, V. A. Kostyuchenko, P. R. Chipman, R. J. Kuhn, M. G. Rossmann, and J. Chen. 2008. Structure of the immature dengue virus at low pH primes proteolytic maturation. *Science* 319:1834-1837.

32. Richer, M. J., C. A. Keays, J. Waterhouse, J. Minhas, C. Hashimoto, and F. Jean. 2004. The Spn4 gene of Drosophila encodes a potent furin-directed secretory pathway serpin. *Proc Natl Acad Sci U S A* 101:10560-10565.

33. Anderson, E. D., L. Thomas, J. S. Hayflick, and G. Thomas. 1993. Inhibition of HIV-1 gp160-dependent membrane fusion by a furin-directed alpha 1-antitrypsin variant. *J Biol Chem* 268:24887-24891.

34. Watanabe, M., A. Hirano, S. Stenglein, J. Nelson, G. Thomas, and T. C. Wong. 1995. Engineered serine protease inhibitor prevents furin-catalyzed activation of the fusion glycoprotein and production of infectious measles virus. *J Virol* 69:3206-3210.

35. Jean, F., K. Stella, L. Thomas, G. Liu, Y. Xiang, A. J. Reason, and G. Thomas. 1998. alpha1-Antitrypsin Portland, a bioengineered serpin highly selective for furin: application as an antipathogenic agent. *Proc Natl Acad Sci U S A* 95:7293-7298.

36. Jean, F., L. Thomas, S. S. Molloy, G. Liu, M. A. Jarvis, J. A. Nelson, and G. Thomas. 2000. A protein-based therapeutic for human cytomegalovirus infection. *Proc Natl Acad Sci U S A* 97:2864-2869.

37. Thomas, G. 2002. Furin at the cutting edge: from protein traffic to embryogenesis and disease. *Nat Rev Mol Cell Biol* 3:753-766.

38. Shiryaev, S. A., B. I. Ratnikov, A. V. Chekanov, S. Sikora, D. V. Rozanov, A. Godzik, J. Wang, J. W. Smith, Z. Huang, I. Lindberg, M. A. Samuel, M. S. Diamond, and A. Y. Strongin. 2006. Cleavage targets and the D-arginine-based inhibitors of the West Nile virus NS3 processing proteinase. *Biochem J* 393:503-511.

39. Huntington, J. A., R. J. Read, and R. W. Carrell. 2000. Structure of a serpin-protease complex shows inhibition by deformation. *Nature* 407:923-926.

40. Huntington, J. A. 2006. Shape-shifting serpins--advantages of a mobile mechanism. *Trends Biochem Sci* 31:427-435.

41. Gettins, P. G. 2002. Serpin structure, mechanism, and function. *Chem Rev* 102:4751-4804.

42. Richer, M. J., L. Juliano, C. Hashimoto, and F. Jean. 2004. Serpin mechanism of hepatitis C virus nonstructural 3 (NS3) protease inhibition: induced fit as a mechanism for narrow specificity. *J Biol Chem* 279:10222-10227.

43. Brennan, S. O., M. C. Owen, D. R. Boswell, J. H. Lewis, and R. W. Carrell. 1984. Circulating proalbumin associated with a variant proteinase inhibitor. *Biochim Biophys Acta* 802:24-28.

44. Rezaie, A. R., C. Manithody, and L. Yang. 2005. Identification of factor Xa residues critical for interaction with protein Z-dependent protease inhibitor: both active site and exosite interactions are required for inhibition. *J Biol Chem* 280:32722-32728.

45. Huang, X., R. Swanson, G. J. Broze, Jr., and S. T. Olson. 2008. Kinetic characterization of the protein Z-dependent protease inhibitor reaction with blood coagulation factor Xa. *J Biol Chem* 283:29770-29783.

46. Han, X., Z. F. Huang, R. Fiehler, and G. J. Broze, Jr. 1999. The protein Z-dependent protease inhibitor is a serpin. *Biochemistry* 38:11073-11078.

47. Han, X., R. Fiehler, and G. J. Broze, Jr. 2000. Characterization of the protein Z-dependent protease inhibitor. *Blood* 96:3049-3055.

Chapter 5

Conclusions and future directions

5.1. Discussion

The overall goal of this thesis was to gain a better understanding into the function of the full-length WNV NS2B/NS3 protease within the intracellular microenvironment. My results demonstrate that protease activity is tightly regulated through various mechanisms. I demonstrated that regulation occurs at the level of polyprotein processing, with the cleavage of the protein junction sites regulated by the *cis*- and *trans*-cleavage activity of the protease. Furthermore, my results suggest that the *cis*- and *trans*-cleavage activity of the protease is regulated by a conformational change in NS3, which is facilitated by the NS2B protein. Finally, my results indicate that NS2B plays a critical role in this regulation, needed for the proper function of the full-length NS2B/NS3 protease within the intracellular microenvironment.

Processing of the polyprotein precursor is important for the virus life cycle (1) and the regulation of cleavage events mediated by the NS2B/NS3 protease, makes the viral protease an attractive target for antiviral therapy. Understanding NS2B/NS3 protease function within the intracellular microenvironment is critical for the rational design of inhibitors directed towards this membrane-associated viral protease. My results demonstrated that the protein regions present within the full-length protease (i.e. NS2B hydrophobic and hydrophilic regions and NS3 protease and helicase domain), the amino acid residues included in the substrate cleavage sequence (P6-P4′) and the complexity of the intracellular microenvironment (membrane-anchoring) all contribute to protease specificity and/or selectivity (Chapter 2). Together, these contributions have important implications on understanding protease function and will ultimately influence drug design. Currently, the majority of studies attempt to assess WNV protease activity utilizing a truncated

recombinant form of the protease ($NS2B_{40}$-G_4SG_4-NS3pro) within *in vitro* assay conditions that generally include, non-physiological pH, addition of glycerol and detergents (2-13). Furthermore, these assays are typically conducted in the absence of intracellular membranes and, as such, do not take into account the effect of membrane-anchoring on protease activity. Ezgimen et al., (2009) demonstrated that the detergents commonly used in *in vitro* assays, lead to enhanced WNV protease activity. This suggests that *in vitro* assays conducted in the presence of these detergents would not be ideal for the screening of potential drug candidates (14). Furthermore, Clum et al., (1997) demonstrated that the addition of microsomal membranes *in vitro* enhanced the endoproteolytic activity of the DNV protease, suggesting that NS2B membrane-association influences NS3 protease activity (15). While, *in vitro* assays provide a rapid assessment of protease activity and inhibitor screening, the influence of the complex intracellular microenvironment and the other protein regions within the full-length protease are not taken into account, which ultimately will have an impact on understanding protease function and on the development of effective protease inhibitors. Our cell-based assay allows for the assessment of the full-length protease in a more physiologically relevant environment and has the potential to be developed as an important tool to validate candidate WNV protease inhibitors.

My results highlight the importance of utilizing cell-based assays to assess viral protease activity within the cell. I demonstrated that membrane-anchored substrate corresponding to the NS4B/NS5 protein junction site sequence was efficiently processed in *trans* by the membrane-associated NS2B/NS3 protease, whereas substrate corresponding to the other protein junction site sequences (NS2A/NS2B, NS2B/NS3, NS3/NS4A) were poorly processed in *trans* (Chapter 2). This is contrary to *in vitro* results (2, 9), suggesting

that within the context of the cell, the NS2B/NS3 protease behaves differently than previously demonstrated. The majority of *in vitro* assay inhibitor screens utilize substrate corresponding to the NS2B/NS3 protein junction site (4-13), which appears to be poorly processed by the full-length protease within the cell (Chapter 2) (16). This suggests that the *in vitro* results may not translate once applied to a cell-based system. As such, our cell-based assay, permitting the analysis of the full-length protease, represents a great complement to the *in vitro* assay systems. This will allow for further understanding of viral protease function and provides a tool for the validation of potential inhibitors in a more physiologically relevant environment.

A discrepancy in substrate specificity has also been previously observed with the related YFV (17). Chambers et al., (1991) demonstrated in a cellular expression system of YFV that the NS4B/NS5 junction site was efficiently cleaved in *trans* whereas the other junction sites examined were inefficiently processed. They suggested that perhaps *cis*-cleavage is preferred at these other junction sites (17). Similarly, my results demonstrated that the NS2B/NS3 heterocomplex undergoes an autocatalytic cleavage event, indicating that the NS2B/NS3 protein junction site is efficiently processed in *cis* (Chapter 3). Additionally, Chambers et al., (1995) observed that substitutions at the NS2B/NS3 junction site of the YFV polyprotein precursor could either positively or negatively modulate endoproteolytic efficiency, suggesting that the wild-type residues present are not always optimal for cleavage by the protease (18). These results suggest that the regulated processing of the polyprotein precursor may, in turn, have an effect on the resultant viral protein molarity, thus controlling the viral protein products generated during virus replication. Taken together, the results suggest that processing of the polyprotein precursor is regulated

by the *cis*-cleavage and *trans*-cleavage activity of the protease. To this effect, my results suggest that the NS2B/NS3 protease requires different conformations to perform *cis* or *trans* proteolytic activity (Chapter 3). I demonstrated that *cis*-cleavage of the NS2B/NS3 heterocomplex precedes the *trans*-cleavage activity of the NS2B/NS3 protease (Chapter 3). Further, my results suggest that NS3 undergoes a conformational change before attaining its *trans*-cleavage activity and that the NS2B protein facilitates this refolding process (Chapter 3). While, *in vitro* studies have demonstrated an important role for NS2B in NS3 protease activity, its precise function has remained debated. It has been proposed that NS2B acts a cofactor (needed for enzymatic activity) or as a prodomain (only needed for folding but not final activity) (5, 8). My results demonstrate that NS2B fulfills a dual role, needed for the proteolytic activity and proper folding of NS3, suggesting cofactor and chaperone-like roles for NS2B (Chapter 3). Interestingly, it has been proposed that the NS2B protein from DNV may also play a chaperone-like role for NS3, assisting in the proper folding of NS3 into an active conformation (15). These results are intriguing, and demonstrate that NS2B is an integral partner for the proper function of the NS2B/NS3 protease heterocomplex within the intracellular microenvironment. This suggests that targeting the interactions between NS2B and NS3 represents an alternative therapeutic approach for WNV antiviral therapy.

Based on the *in vitro* data generated previously from our group (19), I attempted to rationally design a specific serpin-based inhibitor directed against the membrane-associated full-length WNV NS2B/NS3 protease heterocomplex within the cell (Chapter 4). My results highlight that *in vitro* assay strategies do not always translate within the complexity of the intracellular microenvironment, emphasizing the need for cell-based assays to assess protease activity and for inhibitor screening (Chapter 4). Our cell-based fluorescent substrate

assay could be used to complement *in vitro* inhibitor screening assays by validating the identified drug candidates in a more physiologically relevant environment. As my results have shown that the enzymatic activity of the NS2B/NS3 protease is a regulated process, this indicates that each regulatory step also represents a potential target for inhibition. Viral protease inhibitors have been used to treat HIV-1 infections (20) and Phase-III clinical trials are underway for inhibitors of the HCV protease (21, 22), indicating that targeting the WNV protease remains a valid approach however, drug resistance is always a concern. As such, it is critical to investigate new potential drug targets. I identified several NS2B residues that are critical for NS3 proteolytic activity and protein stability (E6, G12, L21, P32, G47, W62, G70, G83, R131) (Chapter 3) (Figure 5.1). A mutation at residue R131 abrogates *cis*-cleavage resulting in a significant reduction in *trans*-cleavage of substrate. This residue resides within the C-terminal hydrophobic region III of NS2B and constitutes the P1 residue of the NS2B↓NS3 protein junction site. Following *cis*-cleavage at this protein junction the C-terminal hydrophobic region III might insert into the ER membrane, which may facilitate the association of NS3 with the central hydrophilic region II of NS2B (Figure 5.1). A mutation at residues G47 (which lies just outside the central hydrophilic region II) and W62 (resides within the central hydrophilic region II) affected NS3 protein stability perhaps due to a disruption of association of NS2B with NS3 resulting in NS3 misfolding and eventually degradation. Mutations within the N-terminal hydrophobic region I (residues E6, G12, L21, P32) did not have an affect on *cis*-cleavage or protein localization suggesting that this region may be involved in NS2B membrane anchoring. A significant reduction in *trans*-cleavage was observed suggesting that a mutation in this region affects the proteolytic activity of NS3 perhaps due to the proper association of the NS2B with the membrane and NS2B with NS3.

A more detailed study examining the protein-membrane interaction might reveal that slight differences in the membrane microenvironment may be enough to affect NS3 proteolytic activity. These essential residues are strongly conserved among several *flavivirus* genus members. As such, they represent potential targets for drug discovery that could be extended to several *flavivirus* genus members, thus having the potential to be developed as a broad-based inhibitor directed towards several flaviviruses. Targeting the interactions between NS2B and NS3 represents alternative therapeutic option and warrants further investigation.

Taken together, my results highlight the importance of studying full-length viral proteases and emphasize the need to develop cell-based assays for investigating the activity of membrane-associated viral proteases. In addition, the strength of our cell-based assay is that it can be adapted to other membrane-associated viral proteases, allowing for customization, which can be extended to other *flavivirus* genus members. The information gathered furthers our understanding of protease function within the cell and can be used to rationally design drugs targeting the membrane-associated full-length WNV NS2B/NS3 protease heterocomplex within the complex intracellular microenvironment.

5.2. Future directions

5.2.1. Development of a stable fluorescent substrate reporter cell-line for WNV

Our current cell-based fluorescent substrate assay utilizes a transient transfection system for protein expression (Chapter 2) (16), which is not ideal for high-throughput-screening (HTS). Generating a stable cell-line expressing the ER membrane-anchored NS4B/NS5 substrate would facilitate HTS and could be utilized for numerous applications. For instance, the system could be used for WNV diagnostic testing and for inhibitor

screening assays. Currently, a number of procedures are used for WNV diagnostic testing including virus isolation, serological assays and the detection of WNV nucleic acids (23). However, these procedures are complex and often time consuming. A stable cell-line expressing a WNV protease specific substrate could be used as a diagnostic test of WNV infectivity. WNV samples could be added to the stable substrate expressing cell-line and the change in fluorescent protein localization would indicate a positive sample. Detection would only take the time that is needed for the first round of infection, typically less than 24 h. This system could also be used to screen for inhibitors against WNV. The change in fluorescent protein localization, or lack thereof, would indicate the inhibitory properties of the potential drug candidate. This system could also be extended to other *flavivirus* genus members, customized to the specific viral protease substrate specificity.

Before generating the stable cell-line, our current fluorescent substrate plasmid construct, pTm-4B5-DsRed, should be modified. Recently, Jones et al., (2010) reported on a similar fluorescent cell-based system for HCV (24). The substrate is tethered to the mitochondria and, upon cleavage the fluorescent reporter group is released from the mitochondria and is directed into the nucleus, due to a nuclear localization signal (NLS) sequence added to the reporter group (24). This allows for easier identification of cleavage and for HTS. While, within our current fluorescent cell-based substrate assay, the protease specific substrate is targeted to the ER membrane. Upon processing of the protease specific substrate cleavage sequence the fluorescent reporter group, DsRed, is released from the ER membrane into the cytoplasm (16, 25). Our current pTm-4B5-DsRed substrate plasmid construct could be modified to include the NLS sequence (PKKKRKV), as this would facilitate HTS (24).

The Thermo Scientific Cellomics® ArrayScan® system allows for HTS using high-capacity automated fluorescence imaging and quantitative analysis for fixed and live cells. The systems software can be customized for particular algorithms, which could be used to detect the change in fluorescent protein pattern location. The disadvantage associated with our current system lies with the Cellomics® software, as it would be difficult for the software to distinguish between DsRed protein patterns in cells of varying sizes. That is, the algorithm would not be able to distinguish between a cytoplasmic DsRed protein pattern in a small sized cell from a ER perinuclear DsRed protein pattern in a large sized cell. Modifying our current system to include the NLS would facilitate this distinction, as the algorithm could be programmed to detect either an ER perinuclear DsRed protein pattern versus a DsRed protein pattern within the nucleus.

Additionally, placing the NLS sequence (PKKKRKV) C-terminal to the DsRed reporter group would not interfere with the 4B5-substrate cleavage sequence (KPGLKR↓GGAK) that is N-terminal to the DsRed reporter group within our current system. The NLS can be added C-terminal to the DsRed reporter group with site-directed mutagenesis within the current pTm-4B5-DsRed substrate plasmid generating the pTm-4B5-DsRed-NLS substrate plasmid. The current plasmid contains a neomycin-resistance cassette that allows for the stable transfection into eukaryotic cells using G418 for selection. The resultant stable transformants will constitutively express the DsRed 4B5-substrate at the ER membrane. Alternatively, protein expression of the DsRed 4B5-substrate within the stable transformants could be regulated with an inducible promoter. In order to do this, the Tm-4B5-DsRed-NLS regions would have to be cloned into another mammalian expression vector that allows for regulation, such as, a tetracycline inducible promoter expression

system. This would allow for the regulation of the substrate to be expressed or repressed during different stages of WNV infection or at different time points. The generation of a stable DsRed 4B5-substrate reporter cell-line would allow for real-time imaging of WNV infections. In addition, the DsRed 4B5-substrate reporter cell-line could be used to screen for WNV inhibitors and has the potential to be used for related flaviviruses such as DNV.

5.2.2. What are the effects of NS2B mutations on the WNV life cycle?

I identified several residues within NS2B (E6, G12, L21, P32, G47, W62, G70, G83, R131) (Figure 5.1) that were critical for the proper function of the NS2B/NS3 protease heterocomplex within the cell (Chapter 3). It would be interesting to investigate the effect of these NS2B mutations on the virus life cycle. Several questions arise such as: Will a mutation of any of the essential NS2B residues identified have an effect on the WNV life cycle? Will the effect be deleterious? Or, will the virus become attenuated? It would be of particular interest, if the virus does become attenuated, as this would suggest a potential strategy for vaccine development.

Using the DNA-infectious molecular clone of WNV developed by Pierson and colleagues, we could directly test the effects of NS2B mutations on virus life cycle (26). The advantage of this WNV DNA-infectious molecular clone is that it encodes a GFP reporter gene (pWNII-GFP) (26). Pierson et al., (2005) demonstrated that upon transfection of host cells with the plasmid encoding for the recombinant virus, pWNII-GFP, infectious WNV particles are produced (WNII-GFP) capable of expressing GFP. Infection with the resultant WNII-GFP virus was shown to result in expression of GFP in infected cells that was detectable as early as 14 h post-infection. Stability of the WNII-GFP genome was

maintained for approximately four rounds of replication based on a 24 h replication cycle (26). Mutations within the NS2B protein can be introduced into the pWNII-GFP plasmid with site-directed mutagenesis and expression of GFP can be used to evaluate the effect of the mutations on virus fitness.

Several point mutant viruses can be generated, based on the essential NS2B residue that I identified, and the effects on virus fitness evaluated. Additionally, multiple mutations could also be introduced into NS2B and the effects of these mutations on virus fitness could also be investigated. Once the mutations are introduced by site-directed mutagenesis the resultant pWNII-GFP_{mutant} plasmids would then be transfected into host cells. WNV has a broad tissue tropism indicating that multiple cell-lines can be utilized. Once the pWNII-GFP_{mutant} plasmid is transfected, virus replication and assembly should occur and infectious virus progeny (WNII-GFP) should be released into the supernatant. If the mutation is deleterious to the virus, no infectious WNII-GFP_{mutant} virus will be released into the supernatant following the initial transfection of the pWNII-GFP_{mutant} plasmid. Alternatively, if the mutation attenuates the virus, WNII-GFP_{mutant} virus should still be released into the supernatant following transfection and, the collected virus particles can then be used for subsequent infection. Upon infection of host cells with the nascent WNII-GFP_{mutant} virus, the effects of the NS2B mutations on virus fitness can be evaluated with the expression of GFP. GFP expression should be reduced in the attenuated WNII-GFP_{mutant} virus compared to WNII-$GFP_{wild\text{-}type}$ virus. GFP protein expression can be visualized with fluorescent microscopy and evaluated with Western blot analysis and flow cytometry. Additionally, our stable DsRed 4B5-substrate reporter cell-line could also be used to evaluate the effects on NS2B/NS3 protease activity relative to WNV infectivity. The information gathered would

further our understanding into the role of NS2B on the function of the NS2B/NS3 protease heterocomplex within the context of the virus life cycle. The generation of an attenuated virus, resulting from the NS2B mutations, could also be extended to other flaviviruses as these residues are strongly conserved among several *flavivirus* genus members.

5.2.3. Optimization of a specific NS2B/NS3 serine protease inhibitor

I attempted to rationally design a specific serpin directed against the membrane-associated full-length WNV NS2B/NS3 protease heterocomplex within the cell. My results highlighted that *in vitro* assay strategies may not always translate within the complexity of the intracellular microenvironment (Chapter 4). However, *in vitro* assays do provide a rapid screen for the assessment of protease activity for which multiple conditions can be evaluated in a relatively short period of time. Taking into account that serpins are able to inhibit membrane-associated proteases under certain conditions (27), indicates that serpins remain a valid approach for being developed as an inhibitor directed against the WNV NS2B/NS3 protease. Optimization of the serpin could be conducted first *in vitro*, and then our stable DsRed 4B5-substrate reporter cell-line could be utilized to validate the *in vitro* results. Utilizing both systems will facilitate the development of a specific WNV NS2B/NS3 serpin. Furthermore, once the serpin is validated in our stable DsRed 4B5-substrate reporter cell-line, its inhibitory properties could then be tested on the WNII-GFP virus (26). The serpin and the WNII-GFP virus could be added onto the stable DsRed 4B5-substrate reporter cell-line and GFP expression and DsRed nuclei localization could be monitored. Reduction in GFP expression and the absence of DsRed within the nucleus would indicate the inhibitory

properties of the serpin directed against the NS2B/NS3 protease within the context of the WNV life cycle.

5.3. Conclusions

In conclusion, the work presented in this thesis furthers our understanding into the activity of the full-length WNV NS2B/NS3 protease heterocomplex within the complex intracellular microenvironment. The hypothesis was confirmed, in that there are critical residues essential for the interaction between NS2B and NS3 that affect protease activity and protein stability. Together with the data I have presented in this thesis, the future work proposed would significantly increase our understanding of the protease's role in the WNV life cycle. In particular, we would gain a better understanding of the regulation of protease activity and how this, in turn, regulates the production of progeny virions. Understanding the mechanism of protease function within the context of the virus life cycle provides important insight and potentially reveals new therapeutic targets. This would ultimately allow for the development of targeted therapies aimed at the viral protease thus providing a treatment to reduce the morbidity and mortality associated with human WNV infections.

Figure 5.1. Schematic representation of NS2B residues that are critical for NS3 proteolytic activity and protein stability

(A) Illustrated are the identified NS2B residues that are critical for NS3 protease activity and protein stability (Chapter 3). The NS2B regions are indicated with the identified NS2B residues noted below, N-terminus hydrophobic region (I) (E6, G12, L21, P32, G47), central hydrophilic region (II) (W62, G70, G83) and C-terminus hydrophobic region (III) (R131). The effects that each mutation had on *cis*-cleavage and *trans*-cleavage activity of NS3 are also indicated. *Cis*-cleavage detected (✓), partial loss of *cis*-cleavage (✓), no *cis*-cleavage detected (✖). *Cis*-cleavage of G47 (✓*) and W62 (✓*) was only observed following MG132 proteasome inhibitor treatment. All mutations caused a significant reduction in *trans*-cleavage of substrate (⬇). (B) (C) Depicted are the amino acid sequence secondary structure predictions of the full-length NS2B/NS3 (B) and the full-length NS2B protein alone (C). The identified NS2B residues that are critical for NS3 protease activity are indicated (*). The NS2B regions are separated by dashed lines, hydrophobic region I (residue G1-T50), central hydrophilic region II (D51-K96) and hydrophobic region III (residue I97-R131). The first and last residues of NS2B are also indicated (G1-R131). The NS2B/NS3 protein junction cleavage site (↓) is indicated, followed by the first residue of NS3 (G1) (in B only). Predictions were generated with SOSUI (Classification and Secondary Structure Prediction of Membrane Proteins) (available at: http://bp.nuap.nagoya-u.ac.jp/sosui/).

Figure 5.1

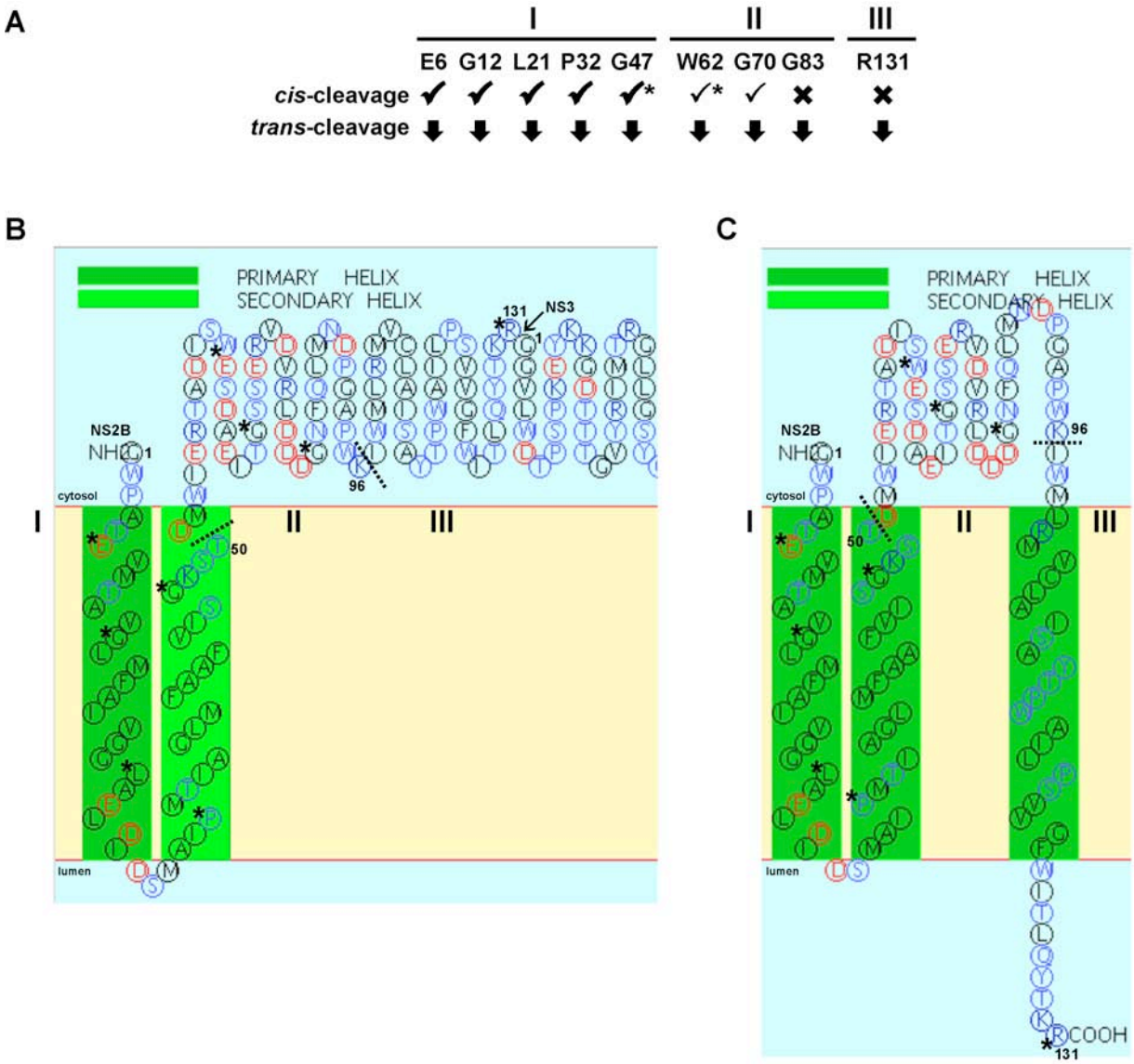
A
I
II
III
E6 G12 L21 P32 G47 W62 G70 G83 R131
cis-cleavage
trans-cleavage
B
C
PRIMARY HELIX
SECONDARY HELIX
NS2B
NS3
131
96
50
cytosol
lumen
I
II
III
COOH

5.4. References

1. Chambers, T. J., R. C. Weir, A. Grakoui, D. W. McCourt, J. F. Bazan, R. J. Fletterick, and C. M. Rice. 1990. Evidence that the N-terminal domain of nonstructural protein NS3 from yellow fever virus is a serine protease responsible for site-specific cleavages in the viral polyprotein. *Proc Natl Acad Sci U S A* 87:8898-8902.
2. Nall, T. A., K. J. Chappell, M. J. Stoermer, N. X. Fang, J. D. Tyndall, P. R. Young, and D. P. Fairlie. 2004. Enzymatic characterization and homology model of a catalytically active recombinant West Nile virus NS3 protease. *J Biol Chem* 279:48535-48542.
3. Chappell, K. J., T. A. Nall, M. J. Stoermer, N. X. Fang, J. D. Tyndall, D. P. Fairlie, and P. R. Young. 2005. Site-directed mutagenesis and kinetic studies of the West Nile Virus NS3 protease identify key enzyme-substrate interactions. *J Biol Chem* 280:2896-2903.
4. Chappell, K. J., M. J. Stoermer, D. P. Fairlie, and P. R. Young. 2006. Insights to substrate binding and processing by West Nile Virus NS3 protease through combined modeling, protease mutagenesis, and kinetic studies. *J Biol Chem* 281:38448-38458.
5. Chappell, K. J., M. J. Stoermer, D. P. Fairlie, and P. R. Young. 2007. Generation and characterization of proteolytically active and highly stable truncated and full-length recombinant West Nile virus NS3. *Protein Expr Purif* 53:87-96.

6. Chappell, K. J., M. J. Stoermer, D. P. Fairlie, and P. R. Young. 2008. Mutagenesis of the West Nile virus NS2B cofactor domain reveals two regions essential for protease activity. *J Gen Virol* 89:1010-1014.

7. Chappell, K. J., M. J. Stoermer, D. P. Fairlie, and P. R. Young. 2008. West Nile Virus NS2B/NS3 protease as an antiviral target. *Curr Med Chem* 15:2771-2784.

8. Shiryaev, S. A., B. I. Ratnikov, A. V. Chekanov, S. Sikora, D. V. Rozanov, A. Godzik, J. Wang, J. W. Smith, Z. Huang, I. Lindberg, M. A. Samuel, M. S. Diamond, and A. Y. Strongin. 2006. Cleavage targets and the D-arginine-based inhibitors of the West Nile virus NS3 processing proteinase. *Biochem J* 393:503-511.

9. Shiryaev, S. A., I. A. Kozlov, B. I. Ratnikov, J. W. Smith, M. Lebl, and A. Y. Strongin. 2007. Cleavage preference distinguishes the two-component NS2B-NS3 serine proteinases of Dengue and West Nile viruses. *Biochem J* 401:743-752.

10. Shiryaev, S. A., B. I. Ratnikov, A. E. Aleshin, I. A. Kozlov, N. A. Nelson, M. Lebl, J. W. Smith, R. C. Liddington, and A. Y. Strongin. 2007. Switching the substrate specificity of the two-component NS2B-NS3 flavivirus proteinase by structure-based mutagenesis. *J Virol* 81:4501-4509.

11. Shiryaev, S. A., A. E. Aleshin, B. I. Ratnikov, J. W. Smith, R. C. Liddington, and A. Y. Strongin. 2007. Expression and purification of a two-component flaviviral proteinase resistant to autocleavage at the NS2B-NS3 junction region. *Protein Expr Purif* 52:334-339.

12. Bera, A. K., R. J. Kuhn, and J. L. Smith. 2007. Functional characterization of cis and trans activity of the Flavivirus NS2B-NS3 protease. *J Biol Chem* 282:12883-12892.

13. Radichev, I., S. A. Shiryaev, A. E. Aleshin, B. I. Ratnikov, J. W. Smith, R. C. Liddington, and A. Y. Strongin. 2008. Structure-based mutagenesis identifies important novel determinants of the NS2B cofactor of the West Nile virus two-component NS2B-NS3 proteinase. *J Gen Virol* 89:636-641.

14. Ezgimen, M. D., N. H. Mueller, T. Teramoto, and R. Padmanabhan. 2009. Effects of detergents on the West Nile virus protease activity. *Bioorg Med Chem* 17:3278-3282.

15. Clum, S., K. E. Ebner, and R. Padmanabhan. 1997. Cotranslational membrane insertion of the serine proteinase precursor NS2B-NS3(Pro) of dengue virus type 2 is required for efficient in vitro processing and is mediated through the hydrophobic regions of NS2B. *J Biol Chem* 272:30715-30723.

16. Condotta, S. A., M. M. Martin, M. Boutin, and F. Jean. 2010. Detection and in-cell selectivity profiling of the full-length West Nile virus NS2B/NS3 serine protease using membrane-anchored fluorescent substrates. *Biol Chem* 391:549-559.

17. Chambers, T. J., A. Grakoui, and C. M. Rice. 1991. Processing of the yellow fever virus nonstructural polyprotein: a catalytically active NS3 proteinase domain and NS2B are required for cleavages at dibasic sites. *J Virol* 65:6042-6050.

18. Chambers, T. J., A. Nestorowicz, and C. M. Rice. 1995. Mutagenesis of the yellow fever virus NS2B/3 cleavage site: determinants of cleavage site specificity and effects on polyprotein processing and viral replication. *J Virol* 69:1600-1605.

19. Richer, M. J., L. Juliano, C. Hashimoto, and F. Jean. 2004. Serpin mechanism of hepatitis C virus nonstructural 3 (NS3) protease inhibition: induced fit as a mechanism for narrow specificity. *J Biol Chem* 279:10222-10227.

20. Anderson, J., C. Schiffer, S. K. Lee, and R. Swanstrom. 2009. Viral protease inhibitors. *Handb Exp Pharmacol*:85-110.

21. Merck. Merck February Combined Pipeline. Available at: http://www.merck.com/research/pipeline/home.html (Last modified: March 1, 2010).

22. Vertex. Development Pipeline. Available at: http://www.vrtx.com/current-projects.html (Last modified: February 22, 2010).

23. Drebot, M. A., R. Lindsay, I. K. Barker, P. A. Buck, M. Fearon, F. Hunter, P. Sockett, and H. Artsob. 2003. West Nile virus surveillance and diagnostics: A Canadian perspective. *Can J Infect Dis* 14:105-114.

24. Jones, C. T., M. T. Catanese, L. M. Law, S. R. Khetani, A. J. Syder, A. Ploss, T. S. Oh, J. W. Schoggins, M. R. MacDonald, S. N. Bhatia, and C. M. Rice. 2010. Real-time imaging of hepatitis C virus infection using a fluorescent cell-based reporter system. *Nat Biotechnol* 28:167-171.

25. Martin, M. M., and F. Jean. 2006. Single-cell resolution imaging of membrane-anchored hepatitis C virus NS3/4A protease activity. *Biol Chem* 387:1075-1080.

26. Pierson, T. C., M. S. Diamond, A. A. Ahmed, L. E. Valentine, C. W. Davis, M. A. Samuel, S. L. Hanna, B. A. Puffer, and R. W. Doms. 2005. An infectious West Nile virus that expresses a GFP reporter gene. *Virology* 334:28-40.

27. Han, X., Z. F. Huang, R. Fiehler, and G. J. Broze, Jr. 1999. The protein Z-dependent protease inhibitor is a serpin. *Biochemistry* 38:11073-11078.

Appendix

A.1. Chapter 2 site-directed mutagenesis primers

A.1.1. Substrate plasmids

KRG substrate

Round 1: 5′-cgactcctcaactccccgctcaggatcctggctac-3′

Round 2: 5′-cgactcctcaactaaacgctcaggatcctggctaccg-3′

Round 3: 5′-cgactcctcaactaaacgcggaggatcctggctac-3′

NS2B/NS2A substrate

Round 1: 5′-ctcaactaaacgcggatggcccgcgctaccggtcgccacc-3′

Round 2: 5′-cgattgccggaattcgaccccaaccgtaaacgcggatggcccgcg-3′

NS2B/NS3 substrate

Round 1: 5′-ttcgactcctacactaaacgcggaggagtcttgctaccggtcgcc-3′

Round 2: 5′-ccgcgattgccggaattcctccaatacactaaacgcggaggagtc-3′

NS3/NS4A substrate

Round 1: 5′-ccgcgattgccggaattcttcgcctcaggtaaacgcggaggatcc-3′

Round 2: 5′-gcctcaggtaaacgctcacaatcctggctaccggtcgcc-3′

Round 3: 5′-ggtaaacgctcacaaatcgggctaccggtcgccacc-3′

NS4B/NS5 substrate

Round 1: 5′-ccgcgattgccggaattcaaacccggaactaaacgcggaggatcc-3′

Round 2: 5′-caaacccggacttaaacgcggaggagccaagctaccggtcgccac-3′

A.1.2. NS3 mutant

NS3 S135A

5′-cttccccactggaaccgcgggctcaccaatagtg-3′

A.2. Chapter 3 site-directed mutagenesis primers

A.2.1. NS2B mutants

NS2B P3A

5′-gcgaattcaggatgggccgcaactgaagtg-3′

NS2B E6A

5′-ggatggcccgcaactgcagtgatgacagct-3′

NS2B G12A

5′-gtgatgacagctgtcgccctaatgtttgccatc-3′

NS2B L21A

5′-ccatcgtcggaggggcggcagagcttgacatt-3′

NS2B P32A

5′-gactccatggccattgcaatgactatcgcgg-3′

NS2B G37A

5′-ccaatgactatcgcggcgctcatgtttgctg-3′

NS2B G47A

5′-gctgctttcgtgatttctgcgaaatcaacagatatgtgg-3′

NS2B G70A

5′-gtgatgcagaaattacagcctcgagcgaaagagttgatg-3′

NS2B S72A

5′-gaaattacaggctcggccgaaagagttgatgtgcgg-3′

NS2B G83A

5′-cggcttgatgatgatgccaacttccagctcatg-3′

NS2B P112A

5′-gattagtgcgtacaccgcctgggcaatctgg-3′

NS2B R131A

5′-ctccaatacacaaaggcaggaggcgtgttgtggg-3′

A.2.2. NS3 mutant

NS3 GP1′A

5′-ctccaatacacaaagagagcaggcgtgttgtgggac-3′

A.3. Chapter 4 site-directed mutagenesis primers

A.3.1. $^{mRFP\text{-}C}$Spn4A RCL variants

Round 1 (P1′ variant): 5′-gtgcgtaggaagcgcggtattatgtcgcctg-3′

Round 2 (P2′ variant): 5′-cgtaggaagcgcggtggtatgtcgcctgagg-3′

Round 3 (P4 variant): 5′-ggcatggcggtgggtaggaagcgcggtg-3′

A.3.2. Spn4A^{C} RCL 4B5 variant

Round 1: 5′-cgtaggaagcgcgctattgcgaagcctgaggaaccaattgag-3′

Round 2: 5′-gtgcgtaggaagcgcggtggtgcgaagcctgaggaacc-3′

Round 3: 5′-gctgctacgggcatgaagccgcgtctgaagcgcggtggtgcg-3′

Round 4: 5′-gggcatgaagccgggtctgaagcgcggtg-3′

Figure A.1

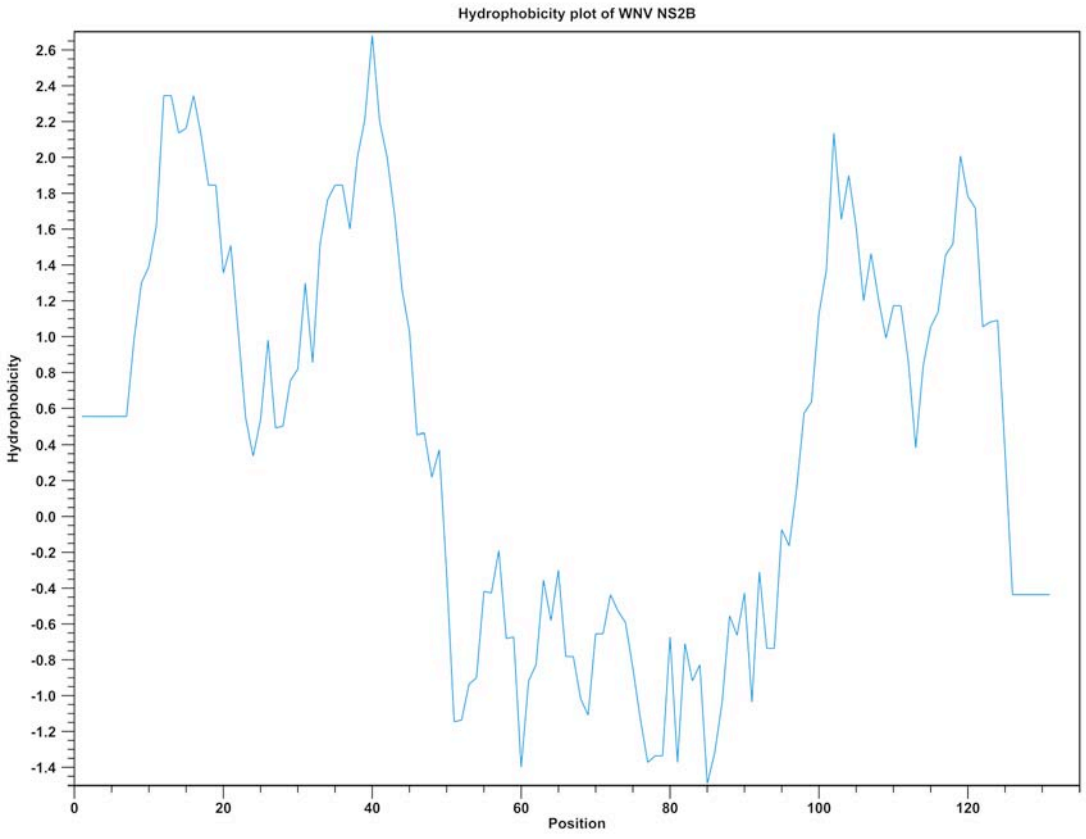

Figure A.1. West Nile virus full-length NS2B protein hydrophobicity profile

Depicted is the hydrophobicity plot (Kyte-Doolittle scale) of the full-length NS2B protein. Hydrophobicity values (y-axis) and amino acid position (x-axis). Positive hydrophobicity values represent hydrophobic regions. Negative hydrophobicity values represent hydrophilic regions. Profile was generated in CLC Main Workbench version 5.5.

Figure A.2

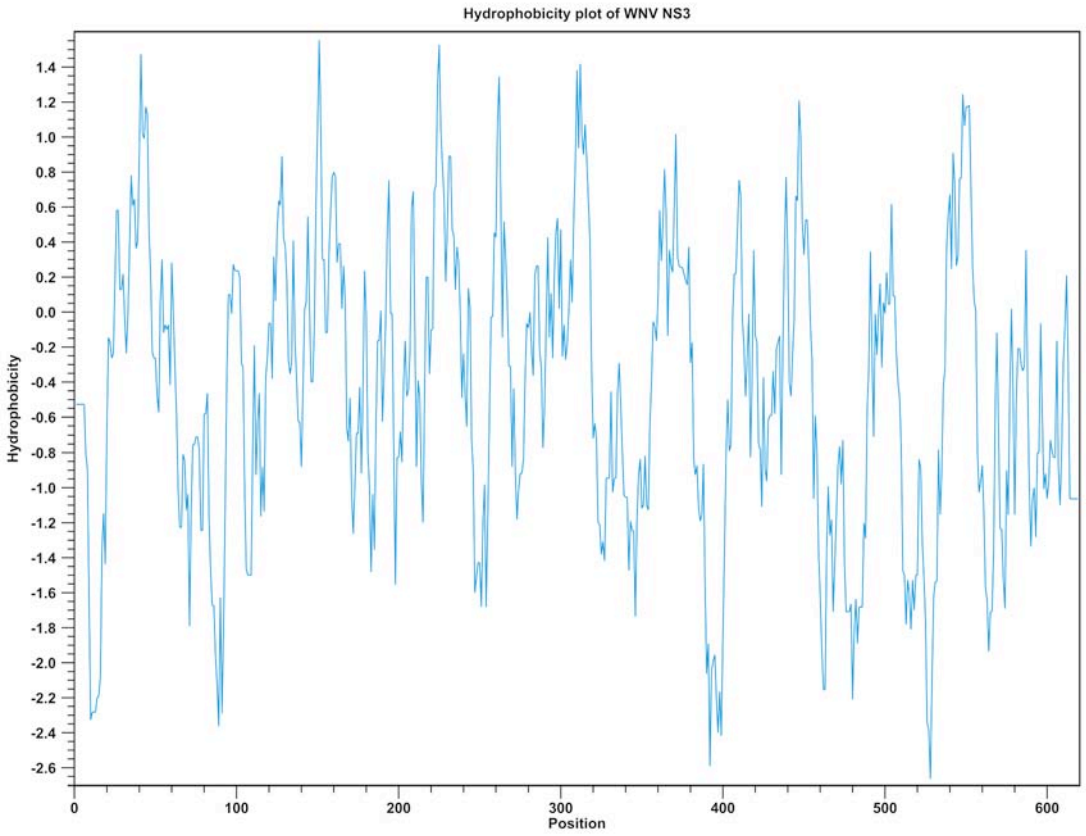

Figure A.2. West Nile virus full-length NS3 protein hydrophobicity profile

Depicted is the hydrophobicity plot (Kyte-Doolittle scale) of the full-length NS3 protein. Hydrophobicity values (y-axis) and amino acid position (x-axis). Positive hydrophobicity values represent hydrophobic regions. Negative hydrophobicity values represent hydrophilic regions. Profile was generated in CLC Main Workbench version 5.5.

Figure A.3

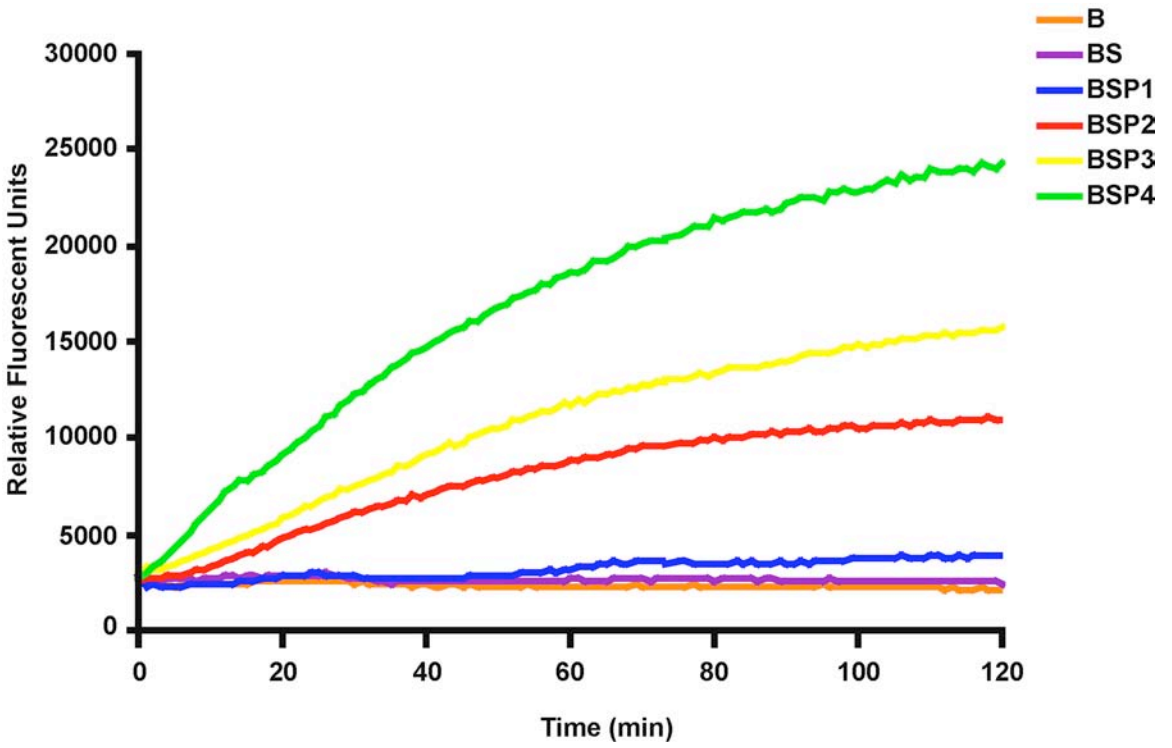

Figure A.3. Recombinant WNV NS3 protease activity

Depicted are the kinetics data for the recombinant WNV NS3 protease (rWNV) (Chapter 4). Relative fluorescent units (y-axis) and reaction time (min) (x-axis). Reaction buffer (B) (50 mM HEPES pH 7.5, 0.1% Triton X-100), substrate (S) 20 μM (Cal Red-GKRS-(K-BHQ-1) amide) (Biosearch Technologies, Inc., Navato, CA) and rWNV (P) ($NS2B_{40}$-G_4SG_4-NS3pro) (R&D Systems Inc., Minneapolis, MN). Varying concentrations of rWNV were tested: BSP1 (rWNV = 0.5 μg/ml), BSP2 (rWNV = 3.0 μg/ml), BSP3 (rWNV = 5.0 μg/ml) and BSP4 (rWNV = 10.0 μg/ml). BS was pre-incubated at room temperature for 5 min then P (rWNV) was added; reaction was performed at 37°C for 120 min.